Ecohydrology and self-organization of black ash wetlands

Jacob Sullivan Diamond

Dissertation submitted to the faculty of the Virginia Polytechnic Institute and State University in partial fulfillment of the requirements for the degree of

Doctor of Philosophy
In
Forest Resources and Environmental Conservation

Daniel L. McLaughlin, Co-Chair
Robert A. Slesak, Co-Chair
Brian Strahm
John Seiler

March 28, 2019
Blacksburg, Virgina

Keywords: ecohydrology, black ash, *Fraxinus nigra*, microtopography, biogeochemistry

Ecohydrology and self-organization of black ash wetlands

Jacob Sullivan Diamond

ABSTRACT

Wetlands self-organize through reciprocal controls between vegetation and hydrology, but external disturbance may disrupt these feedbacks with consequent changes to ecosystem state. Imminent and widespread emerald ash borer (EAB) infestation throughout North America has raised concern over possible ecosystem state shifts in forested wetlands (i.e., to wetter, more herbaceous systems) and loss of forest function, calling for informed landscape-scale management strategies. In this dissertation, I use black ash wetlands as a model system to understand complex ecohydrological dynamics, and I use these dynamics to explain the self-organization of observed patterns in vegetation, hydrology, and microtopographic structure. The combined inferences from the three research chapters strongly implicate black ash trees as autogenic ecosystem engineers, who, through the process of improving their local growing conditions, cause a cascade of environmental changes that result in a unique ecosystem structure. This unique ecosystem structure is under existential threat from the invasive EAB. Through experiment, I show that loss of black ash trees to EAB induces persistent shifts in hydrology that result from reduced evapotranspiration and subsequent changes to water table regime (Chapter 2). These results suggest the potential for catastrophic shifts of black ash wetlands from forested to non-forested, marsh-like states under a do-nothing EAB management scenario. However, research presented here suggests that preemptive management of black ash wetlands can potentially mitigate loss of desirable forested conditions. Forest management to replace black ash with other wetland canopy species may be a slow and steady path towards forest maintenance, and harvesting may facilitate establishment of alternative species. In the case of preemptive harvesting of black ash, I posit that maintenance of microtopographic structure, either through leaving downed woody debris or through physical creation, is paramount to forest recovery. Microtopography in these ecosystems provides crucial relief from anaerobic stress generated by higher water tables, allowing woody species to persist on elevated microsites (e.g., 30 cm above base soil elevation). Moreover, I show that microtopography in black ash wetlands has clear structure and pattern and that its presence arises from self-organizing processes, driven by feedbacks among hydrology, biota, and soils (Chapter 3). I further show that this structured and non-random microtopography has profound influence on biogeochemical processes in black ash wetlands, controlling plant richness and biomass, and soil chemistry gradients (Chapter 4). Based on this work, I propose that structured wetland microtopography is a diagnostic feature of strongly coupled plant-water interactions, and these interactions may be important for ecosystem resilience to disturbance.

Ecohydrology and self-organization of black ash wetlands

Jacob Sullivan Diamond

GENERAL AUDIENCE ABSTRACT

Plants need water, but not too much nor too little. In wetland ecosystems, plants influence water levels through both water use and their effect on soil surfaces. When wetland plants use water, they take it from the soil, which leads to lowering of water levels and drier soil conditions. In many wetlands, the amount of water that plants take from the soil is a fine-tuned process. Therefore, when disturbances happen to wetland ecosystems, like large-scale tree mortality, major changes can occur to the amount of water in the soil and soils typically become wetter. This change to a wetter ecosystem can persist for long periods, and can affect the types of plants that can live in the wetland. However, plants also affect wetland water levels by engineering the soil around them, essentially lifting themselves to drier conditions. Through this engineering, plants create a mosaic of different habitat types that are important for many organisms and ecological processes. Exactly how plants engineer their environment is still not well understood, but we know that ecosystem engineering by plants is critical to the structure and function of wetlands around the world. Understanding how plants create and maintain their own environmental structures provides a deeper insight into the development of vegetated landscapes and their response to change. This dissertation aims to improve our understanding of ecosystem engineering by plants in forested wetlands so that we may more effectively manage these important natural resources and in turn more accurately predict their response to global change.

Dedication

I dedicate this dissertation to my mother, my father, my brother, and my sister.

Acknowledgments

This dissertation is the result of countless intellectual and emotional contributions from colleagues, mentors, friends, family, and community members. I am grateful to those who inspire me to ask important and interesting questions about the world around us, and am further indebted to those who motivate me to go about the hard task of actually answering them. Naturally, I acknowledge my committee chair, Dr. Daniel L. McLaughlin, whose persistent positive attitude, encouragement, and unwavering support saved me in many moments of self-doubt and struggle. His practical perspective on science and rational clarity has been a guiding light for me over these past four years. My committee co-chair, Dr. Robert A. Slesak, has additionally provided me with valuable scientific mentorship and much-needed levity in otherwise difficult situations. Thanks also to my two committee members, Dr. Brian Strahm and Dr .John Seiler for a critical eye and valuable feedback throughout the research process. I would like to thank Dr. Atticus Stovall in particular for his magnanimity in helping with the terrestrial laser scanning fieldwork and analysis, and for his consistent, quick, and helpful responses to a multitude of questions. I would also like to thank David Mitchem for his patience, practicality, and assistance in helping to develop a procedure for soil chemistry analysis. Work in this dissertation was made possible by the Virginia Tech Forest Resources and Environmental Conservation department, the Virginia Tech Institute for Critical Technology and Applied Science, and the Virginia Tech William J. Dann Fellowship. Additional funding and support came from the Minnesota Environmental and Natural Resources Trust Fund, the USDA Forest Service Northern Research Station, and the Minnesota Forest Resources Council. I am ingratiated to Mitch Slater, Alan Toczydlowksi, and Hannah Friesen for crucial help during fieldwork and data collection, and to Breanna Anderson and Kelly Peeler for assistance with sample processing.
I would finally like to thank Hannah G. Lee for countless hours of support, love, and friendship.

Table of Contents

List of Figures

List of Tables

List of Abbreviations

AIC	Akaike information criterion
BA	Basal area
BIC	Bayesian information criterion
CSR	Complete spatial randomness
DBH	Diameter at breast height
EAB	Emerald ash borer
ET	Evapotranspiration
GLMM	Generalized linear mixed effects model
GPP	Gross primary productivity
IV	Indicator value
LAI	Leaf area index
LiDAR	Light detection and ranging
NMDS	Nonmetric multi-dimensional scaling
PET	Potential evapotranspiration
RMSE	Root mean square error
S_y	Specific yield
TLS	Terrestrial laser scanning

Attribution

Chapter 2

Chapter 2 was published in the Journal of Environmental Management in 2018.

Daniel L. McLaughlin, Ph.D, (Virginia Tech, Forest Resources and Environmental Conservation and Virginia Water Resources Research Center) helped with the editing of the manuscript.

Robert A. Slesak, Ph.D., (Minnesota Forest Resources Council and University of Minnesota, Department of Forest Resources) helped with the editing of the manuscript was part of initial project conception.

Anthony D'Amato, Ph.D (University of Vermont) helped with editing of the manuscript and was part of initial project conception.

Brian Palik, Ph.D., (United States Forest Service, Northern Research Station) helped with editing of the manuscript and was part of initial project conception.

Chapter 3

Chapter 3 is in preparation for submission to Ecology.

Daniel L. McLaughlin, Ph.D, (Virginia Tech, Forest Resources and Environmental Conservation and Virginia Water Resources Research Center) helped with the editing of the manuscript.

Robert A. Slesak, Ph.D., (Minnesota Forest Resources Council and University of Minnesota, Department of Forest Resources) helped with the editing of the manuscript.

Chapter 4

Chapter 4 is in preparation for submission to Biogeosciences.

Daniel L. McLaughlin, Ph.D, (Virginia Tech, Forest Resources and Environmental Conservation and Virginia Water Resources Research Center) helped with the editing of the manuscript.

Robert A. Slesak, Ph.D., (Minnesota Forest Resources Council and University of Minnesota, Department of Forest Resources) helped with the editing of the manuscript.

CHAPTER 1: INTRODUCTION

This introduction is organized to lead the reader to the eventual questions and hypotheses that structure this dissertation. I first explain what I mean by "ecohydrology and self-organization of black ash wetlands", the focus of this dissertation, and then justify why this focus represents an important and fundamental knowledge gap in our scientific understanding of ecosystem ecology. I next present the context for why I studied black ash wetlands in particular. Finally, I present the specific objectives of this dissertation and describe how I met these objectives in research presented in Chapters 2-4.

1.1 Theoretical background

Despite a growing understanding of the influence that plants can have on their environment, many open question remain regarding the extent and magnitude of this influence. This is not to say that we do not understand many plant behaviors, which we do (Darwin 1880, Karban 2010), or that we do not understand how environmental factors affect where plants live, which we also certainly do (Von Humboldt 1807, Holdridge 1967). What we lack, however, is a coherent understanding of how these directional influences are interlinked (Callaway et al. 2003). One can summarize the current paradigm for plant behavior with the following analogy: plants are actors on a stage set by greater forces, and their roles are limited to simply exploring this stage. That is, we still do not have a complete answer to a deeper, more interesting question about the agency of plants: how do plants modify their environment? This unanswered question is the fundamental inquiry of this dissertation.

Recent efforts in the research community have started to focus on vegetation-environment feedbacks and the co-evolution of plants and landscapes (Pawlik et al. 2016, Brantley et al. 2017). In particular, the natural intersection of vegetation with the water cycle has spurred numerous research efforts investigating the feedbacks that develop among vegetation, hydrology, and landscape structure (e.g., Troch et al. 2015). Such efforts have led to the delineation of a new scientific discipline termed "ecohydrology", whose stated purpose is to probe directly such vegetation-water-environment feedbacks (Rodriguez-Iturbe 2000). Since its conception, the preponderance of ecohydrological evidence suggests that plants are readily capable of modifying their environment in a

diverse array of ways, with a correspondingly diverse array of reciprocal influences on hydrology and landscape form (Corenblit et al. 2011 and references therein). However, many open questions remain regarding the commonality of vegetation-environment feedbacks and their implications for ecosystem stability and resilience to change.

Wetlands are candidate ecosystems for investigating feedbacks between vegetation and hydrology (Rodriguez-Iturbe et al. 2007). Wetlands are biomes that support biota adapted to regular inundation and/or saturation and the associated anaerobic soil conditions. In these systems, in contrast to uplands, hydrologic controls on vegetation are generally the result of too much rather than too little water (Jackson and Colmer 2005). Too much water results in inadequate oxygen supply (Armstrong and Drew 2002) and accumulation of ethylene and anaerobic metabolism byproducts (Ponnamperuma 1984), limiting primary production. At the same time, wetland vegetation can also control local hydrology through evapotranspiration and interception, which lower water tables and reduce soil moisture (e.g., Dubé et al., 1995).

Direct feedbacks between vegetation and water in wetlands can result in larger feedback loops that include biogeochemical controls on primary productivity. Soil moisture is a dominant control on soil oxygen content and soil reduction-oxidation (redox) potentials in wetland soils, regulating biogeochemical processes such as decomposition (Skopp et al. 1990), nitrogen mineralization (Sleutel et al. 2008), and nitrification/denitrification (Porporato et al., 2003). As such, excess soil moisture in wetlands not only directly impacts primary production through anaerobic stress and vegetation selection (Kozlowski 2002), but also indirectly by influencing redoximorphic pathways that constrain biogeochemical cycling of nutrients (Faulwetter et al. 2009). It then stands to reason that within wetlands, vegetation can alleviate biogeochemical stresses by affecting the soil moisture regime, where zones of lower soil moisture would be more favorable to primary production than zones of higher soil moisture.

These ecohydrologic feedback loops between vegetation, hydrology, soils, and biogeochemical cycling induce ecosystem stability, a process termed “self-organization”. However, the complexity of such self-organizing systems leads to situations where more than one ecosystem configuration may be possible at the same location in space (AKA “alternative stable states”; Scheffer et al. 2001). Alternative stable states can arise when

vegetation forms positive feedbacks with its environment that promote favorable growth conditions (Ridolfi et al. 2006). But, some positive feedbacks may be limited to a certain range of environmental conditions, outside of which new positive feedbacks may take over, promoting an alternative stable state (Kéfi et al. 2016 and references therein). For wetland systems, simulation models suggest that, by lowering the water table through ET, wetland plant communities may act as ecosystem engineers (*sensu* Jones et al. 1994) and affect their physical environment creating conditions that promote their own success (Rodríguez-Iturbe et al. 2007). The vegetation-water table feedback suggests the emergence of at least two alternative stable states with a wetland system dominated either by water intolerant species thriving on deep(er) water tables, or water tolerant species thriving on shallow(er) water tables (e.g., Chambers and Linnerooth, 2001).

Importantly, ecosystem resilience to disturbance depends on the positive feedbacks that maintain and promote stable ecosystem states. For example, feedbacks between vegetation and water table depth are the putative mechanisms for the ‘‘watering-up’’ process that is observed following clearcuts of wetland forests (Dubé et al. 1995). In this situation, too much water table rise following vegetation loss (and subsequent reduction in ET) prevents or delays tree-species seedling establishment, which may favor the invasion of non-tree species (i.e., a different, non-forested ecosystem state). Over time though, early successional non-tree species could potentially lower water tables enough to promote reestablishment of tree-species seedlings, thereby leading to dynamic ecohydrologically controlled succession following disturbance (Ridolfi et al., 2007).

The strength of species-specific ecohydrological feedbacks in wetlands is likely an important control on the stability of a given ecosystem state. Species richness has been shown to improve resilience of wetland ecosystems to disturbance (e.g., Carvalho et al. 2013), suggesting wetlands with low species richness may be prone to catastrophic shifts in ecosystem state (*sensu* Scheffer et al. 2001). However, because most vascular plants are not adapted to flooded soils, species diversity is limited under shallow water table conditions. Evidence suggests that species richness decreases with increasing levels of inundation, where many hydric ecosystems tend to be dominated by relatively few tree species (e.g., cypress domes or tupelo swamps; McKnight et al. 1981). Therefore, the feedbacks that maintain wetland ecosystems may be highly species-specific, and species-

specific disturbances may result in catastrophic shifts in ecosystem state. Black ash (*Fraxinus nigra* Marshall) wetlands across North American are highly vulnerable to the invasive emerald ash borer (*Agrilus planipennis*, EAB) raising concern for such catastrophic shifts in ecosystem state, a focus of this dissertation (Chapter 2).

The feedbacks loops that develop from biota-water interactions may also induce the development of self-organized wetland topographic structure, another primary focus of this dissertation (Chapters 3 and 4). Inputs of organic matter from primary production vary spatially throughout a wetland because of local scale variability in soil moisture (e.g., zones of relatively lower soil moisture may be associated with relatively greater primary production). Spatially variable decomposition rates that also depend on soil moisture couple to inputs and lead to the development of structure in the form of microtopography in wetland systems (*sensu* Belyea and Clymo 2001). Microtopography, or the small-scale (10^{-2}–10^{0} m) variation in ground surface height, is dynamic throughout time, and likely a function of local hydrology (Wolf et al. 2011) and its influence on production inputs and respiratory losses (Jones et al. 2000). Because microtopography is pervasive throughout wetland systems, it may be a general emergent physical property of wetland ecohydrologic feedbacks.

Wetland microtopographic structure modulates vegetation-water interactions that control primary productivity and community composition. The difference in elevation on the order of centimeters can provide enough aeration to limit anaerobic stress to vegetation, promoting higher primary production (Rodríguez-Iturbe et al. 2007). Simply put, hummocks, or the high points in a wetland, effectively lower the water table that vegetation experiences, thereby reducing local soil moisture. Consequently, microtopography has also been shown to increase species richness and abundance in wetland systems (Bruland and Richardson 2005; Moser et al. 2007). Species richness may increase with microtopography due to differential germination of species growth forms (e.g., tree vs. forb) (Huenneke and Sharitz 1986; Titus 1990), with woody perennials favoring hummocks (Vivian-Smith 1997). By simply changing the relative water table, microtopography inherently affects vegetative growth and composition in wetlands.

Elevated microsites also promote increased primary production through their indirect controls on nutrient cycling. Throughout wetland systems, hummocks are consistently found to be zones of greater nutrient concentrations and nutrient cycling rates than hollows (Bruland and Richardson 2005; Wolf et al. 2011). In fact, in an arctic fen, Sullivan et al. (2008) found four times more N, C, and root mass in hummocks compared to hollows, leading to similar increases (i.e., a factor of four increase) in gross primary production. Similarly, Jones et al (1996) found five times greater Bray-extractable P and significantly more root mass in hummocks than in hollows in a floodplain wetland forest. By providing less saturation and better rooting zone aeration, hummocks promote greater growth rates and survival probabilities compared to hollows (Roy et al. 1999). Moreover, microtopography influences greenhouse gas (GHG) emissions via its control on decomposition pathways (Bubier et al. 1993; Bubier et al. 1995; Lai 2009). Hence, through indirect controls on nutrient cycling, microtopography has a clear capacity to regulate ecosystem processes.

Despite the many recent efforts to elucidate plant-soil-water interactions in wetlands, many questions remain. What are the types of feedbacks that can develop in coupled plant-water systems, and how do these feedbacks affect ecosystem processes and landscape evolution over space and time? Are there common diagnostics we can test across ecosystems to assess the strength of ecohydrologic feedbacks? How resilient are wetland ecosystems to disturbance? How can we use our understanding of ecohydrology and self-organization of ecosystems to manage our natural resources? These unanswered questions motivate the research presented in this dissertation.

1.2 Relevance and justification

While understanding vegetation-environment feedbacks is interesting and worthwhile in-and-of-itself, looming global change imparts an additional need to improve our understanding of the ecosystems that sustain us. Large-scale disturbance to ecosystems, such as loss of vegetation or dramatic shifts in environmental conditions, is having profound effects on ecosystem processes and structure across the globe (Vitousek 1994, Brook et al. 2008). Biological invasions are an obvious and pernicious agent of global change around the world, yet we rarely anticipate or preemptively manage for their impacts to ecosystems (Vitousek et al. 2017).

EAB an invasive beetle, has already caused widespread-loss of ash trees (*Fraxinus spp*.) throughout the U.S. and Canada (Klooster et al. 2014), with some comparing ash extirpation rates to that of elm trees from Dutch Elm disease (Poland and McCullough 2006). Since initial reports of ash loss in North America in 2002, EAB has killed tens of millions of ash trees with no discernible preferences for tree health, size, or ecological setting (Herms and McCullough 2014). Moreover, ash species have a nearly 100% mortality rate when infected with EAB (Klooster et al. 2014). These observations have led to a surge in research and publications on ash trees and EAB with focus on EAB biology (Cappaert et al. 2005, Lelito et al. 2007), economic impacts of EAB (Kovacs et al. 2010), EAB prevention and eradication (Crook et al. 2008, Herms et al. 2009), susceptibility mapping and modeling (Muirhead et al. 2006), and ecologic impacts (Herms and McCullough 2014). However, EAB has yet to invade black ash wetlands throughout northern North America, allowing a unique opportunity to prepare and manage for potential ecosystem shifts from EAB's expected arrival. Indeed, recently, teams in Michigan and Minnesota have begun investigating these black ash wetlands, with hopes to mitigate consequences of EAB infestation.

Black ash in the U.S. Lake States (MN, WI, MI) and provinces in Canada is unique among ash species because it often occurs in nearly pure stands (i.e., over 90% canopy cover) in wetland conditions with very little regeneration of other tree species (Palik et al. 2012 and personal observations). These observations are characteristic of a system with positive feedbacks between black ash and its environment, possibly coupled with negative feedbacks to other woody species' growth (*sensu* Wilson and Agnew 1992). Because systems with self-reinforcing feedbacks are particularly subject to instability in the event of catastrophic change, there is concern that the loss of black ash in forested wetlands will lead to a non-forested alternative stable state characterized by shrubs (Palik et al. 2012), invasive herbaceous plants, and an elevated water table (Slesak et al. 2014). Therefore, black ash wetlands represent an ideal study system to explore ecohydrological feedbacks and ecosystem self-organization, with important and pressing management implications. This dissertation focuses on the internal ecosystem processes of black ash wetlands to develop a more comprehensive and predictive understanding of their response to environmental change.

1.3 Objectives and organization

The primary objective of this dissertation is to investigate ecosystem self-organization through analysis of vegetation-soil-hydrology dynamics in wetlands. I address this primary research objective through a portfolio of research efforts. In these efforts, I employ an array of techniques including time-series analysis of water tables, geospatial analysis of wetland microtopography, and field surveys of wetland vegetation and soils. This dissertation represents a collection of these research efforts in the form of three manuscripts, bounded by an Introduction (Chapter 1) and a Conclusion (Chapter 5). The three research manuscripts (Chapters 2–4) link studies that collectively seek to address the primary research objective. Briefly, this dissertation is organized as follows:

In Chapter 2, I use a large-scale experimental design in 24 black ash wetland plots to assess ecohydrologic effects of simulated EAB disturbance and the possibility for management intervention. In field simulations of EAB-disturbed systems, I found clear and persistent changes in hydrologic regime defined by shallower water tables and lower ET rates. These hydrologic changes coupled with community shifts to an herbaceous-dominated system indicate ecosystem state change driven by vegetation-water table interactions. However, results also indicate that preemptive management strategies have high potential to preserve desired forested wetland habitat if periodically executed over time before EAB infestation.

In Chapter 3, I evaluated the hypothesis that microtopography in black ash wetlands results from scale-dependent ecohydrologic feedbacks. Using a high spatial resolution dataset generated by terrestrial laser scanning, a three-year hydrology dataset, and information from a synoptic field sampling campaign, I showed that microtopography in black ash wetlands is likely a plant-induced response to shallow water tables. To support this, I demonstrated regular patterning and structure of black ash wetland microtopography, whose properties are best explained through feedbacks between vegetation and their environment.

In Chapter 4, I used a suite of information gathered from field surveys to test the influence of microtopography on vegetation and soils, and to further test predicted feedback mechanisms in black ash wetlands that maintain and reinforce structured microtopography. I found that microtopography in black ash wetlands strongly controls

spatial patterns of vegetation communities and soil chemistry, and that these patterns are effectively explained by two vegetation-environment feedback loops. These feedback loops further explain the structure and persistence of microtopography that I observed in Chapter 3.

In Chapter 5, the Conclusion, I integrate the findings of the three research studies (Chapters 2–4) to summarize the dissertation contributions to the study of vegetation-environment feedbacks, with attention paid to practical implications.

1.4 References

Armstrong, W., & Drew, M. C. (2002). Root growth and metabolism under oxygen deficiency. Plant roots: the hidden half, 3, 729-761.

Belyea, L. R., & Clymo, R. S. (2001). Feedback control of the rate of peat formation. Proceedings of the Royal Society of London B: Biological Sciences, 268(1473), 1315-1321.

Brantley, S. L., Eissenstat, D. M., Marshall, J. A., Godsey, S. E., Balogh-Brunstad, Z., Karwan, D. L., ... & Chadwick, O. (2017). Reviews and syntheses: on the roles trees play in building and plumbing the critical zone. Biogeosciences (Online), 14(22).

Brook, B. W., Sodhi, N. S., & Bradshaw, C. J. (2008). Synergies among extinction drivers under global change. Trends in ecology & evolution, 23(8), 453-460.

Bubier, J., Costello, A., Moore, T. R., Roulet, N. T., & Savage, K. (1993). Microtopography and methane flux in boreal peatlands, northern Ontario, Canada. Canadian Journal of Botany, 71(8), 1056-1063.

Bubier, J. L., Moore, T. R., Bellisario, L., Comer, N. T., & Crill, P. M. (1995). Ecological controls on methane emissions from a northern peatland complex in the zone of discontinuous permafrost, Manitoba, Canada. Global Biogeochemical Cycles, 9(4), 455-470.

Bruland, G. L. and C. J. Richardson. 2005. Hydrologic, edaphic, and vegetative responses to microtopographic reestablishment in a restored wetland. Restoration Ecology 13:515-523.

Callaway, R. M., Pennings, S. C., & Richards, C. L. (2003). Phenotypic plasticity and interactions among plants. Ecology, 84(5), 1115-1128.

Cappaert, D., McCullough, D.G., Poland T.M., & Siegert N.W. (2005). Emerald ash borer in North America: a research and regulatory challenge. American Entomologist, 51:152–63.

Carvalho, P., Thomaz S., Kobayashi, J. T., & Bini, L. (2013). Species richness increases the resilience of wetland plant communities in a tropical floodplain. Austral Ecology, 38(5), 592-598.

Chambers, J. C., & Linnerooth, A. R. (2001). Restoring riparian meadows currently dominated by Artemisia using alternative state concepts-the establishment component. Applied Vegetation Science, 4(2), 157-166.

Corenblit, D., Baas, A. C., Bornette, G., Darrozes, J., Delmotte, S., Francis, R. A., ... & Steiger, J. (2011). Feedbacks between geomorphology and biota controlling Earth surface processes and landforms: a review of foundation concepts and current understandings. Earth-Science Reviews, 106(3-4), 307-331.

Crook, D. J., Khrimian, A., Francese, J. A., Fraser, I., Poland, T. M., Sawyer, A. J., & Mastro, V. C. (2008). Development of a host-based semiochemical lure for trapping emerald ash borer Agrilus planipennis (Coleoptera: Buprestidae). Environmental Entomology, 37(2), 356-365

Darwin, C. (1880). The Power of Movement in Plants. John Murray, London.

Diamond, J.S., McLaughlin, D.M., Slesak, R.A., & Stovall, A. (in prep). A microtopographic signature of life.

Dubé, S., Plamondon, A. P., & Rothwell, R. L. (1995). Watering up after clear-cutting on forested wetlands of the St. Lawrence lowland. Water Resources Research, 31(7), 1741-1750.

Faulwetter, J. L., Gagnon, V., Sundberg, C., Chazarenc, F., Burr, M. D., Brisson, J., ... & Stein, O. R. (2009). Microbial processes influencing performance of treatment wetlands: a review. Ecological engineering, 35(6), 987-1004.

Herms, D. A., McCullough, D. G., Smitley, D. R., Sadof, C., Williamson, R. C., & Nixon, P. L. (2009). Insecticide options for protecting ash trees from emerald ash borer. Urbana, 51, 61801.

Herms, D. A., & McCullough, D. G. (2014). Emerald ash borer invasion of North America: history, biology, ecology, impacts, and management. Annual Review of Entomology, 59, 13-30.

Holdridge, L. R. (1967). Life zone ecology. Life zone ecology., (rev. ed.)).

Huenneke, L. F. and R. R. Sharitz. 1986. Microsite abundance and distribution of woody seedlings in a South Carolina cypress-tupelo swamp. American Midland Naturalist 115:328-335.

Jackson, M. B., & Colmer, T. D. (2005). Response and adaptation by plants to flooding stress. Annals of Botany, 96(4), 501-505.

Jones, C. G., Lawton, J. H., & Shachak, M. (1994). Organisms as ecosystem engineers. In Ecosystem management (pp. 130-147). Springer, New York, NY.

Jones, R. H., Lockaby, B. G., & Somers, G. L. (1996). Effects of microtopography and disturbance on fine-root dynamics in wetland forests of low-order stream floodplains. American Midland Naturalist, 57-71.

Jones, R. H., K. O. Henson, and G. L. Somers. (2000). Spatial, seasonal, and annual variation of fine root mass in a forested wetland. Journal of the Torrey Botanical Society 127:107-114.

Karban, R. (2008). Plant behaviour and communication. Ecology letters, 11(7), 727-739.

Kéfi, S., Holmgren, M., & Scheffer, M. (2016). When can positive interactions cause alternative stable states in ecosystems?. Functional Ecology, 30(1), 88-97.

Klooster, W. S., Herms, D. A., Knight, K. S., Herms, C. P., McCullough, D. G., Smith, A., ... & Cardina, J. (2014). Ash (Fraxinus spp.) mortality, regeneration, and seed bank dynamics in mixed hardwood forests following invasion by emerald ash borer (Agrilus planipennis). Biological Invasions,16(4), 859-873.

Kovacs, K. F., Haight, R. G., McCullough, D. G., Mercader, R. J., Siegert, N. W., & Liebhold, A. M. (2010). Cost of potential emerald ash borer damage in US communities, 2009–2019. Ecological Economics, 69(3), 569-578.

Kozlowski, T. T. (2002). Physiological-ecological impacts of flooding on riparian forest ecosystems. Wetlands, 22(3), 550-561.

Lai, D. Y. F. (2009). Methane dynamics in northern peatlands: a review. Pedosphere, 19(4), 409-421.

Lelito, J. P., Fraser, I., Mastro, V. C., Tumlinson, J. H., Böröczky, K., & Baker, T. C. (2007). Visually mediated 'paratrooper copulations' in the mating behavior of Agrilus planipennis (Coleoptera: Buprestidae), a highly destructive invasive pest of North American ash trees. Journal of Insect Behavior, 20(6), 537-552.

McKnight, J. S., Hook, D. D., Langdon, O. G., & Johnson, R. L. (1981). Paper 2 Flood Tolerance and related characteristics of trees of the bottomland forests of the southern United States.

Mitsch W. J, & Gosselink J. G. (2007) Wetlands. Hoboken (New Jersey): John Wiley & Sons, Inc. p. 158.

Moser, K. F., C. Ahn, and G. B. Noe. 2009. The Influence of Microtopography on Soil Nutrients in Created Mitigation Wetlands. Restoration Ecology 17:641-651.

Palik, B. J., Ostry, M. E., Venette, R. C., & Abdela, E. (2012). Tree regeneration in black ash (Fraxinus nigra) stands exhibiting crown dieback in Minnesota. Forest Ecology and Management, 269, 26-30.

Pawlik, Ł., Phillips, J. D., & Šamonil, P. (2016). Roots, rock, and regolith: Biomechanical and biochemical weathering by trees and its impact on hillslopes—A critical literature review. Earth-science reviews, 159, 142-159

Poland, T. M., & McCullough, D. G. (2006). Emerald ash borer: invasion of the urban forest and the threat to North America's ash resource. Journal of Forestry, 104(3), 118-124.

Ponnamperuma, F. N. (1984). Effects of flooding on soils. Flooding and plant growth, 9-45.

Porporato, A., D'odorico, P., Laio, F., & Rodriguez-Iturbe, I. (2003). Hydrologic controls on soil carbon and nitrogen cycles. I. Modeling scheme. Advances in Water Resources, 26(1), 45-58.

Ridolfi, L., D'Odorico, P., & Laio, F. (2006). Effect of vegetation–water table feedbacks on the stability and resilience of plant ecosystems. Water Resources Research, 42(1).

Ridolfi, L., D'Odorico, P., & Laio, F. (2007). Vegetation dynamics induced by phreatophyte–aquifer interactions. Journal of Theoretical Biology, 248(2), 301-310.

Rodriguez-Iturbe, I. (2000). Ecohydrology: A hydrologic perspective of climate-soil-vegetation dynamies. Water Resources Research, 36(1), 3-9.

Rodríguez-Iturbe, I., D'Odorico, P., Laio, F., Ridolfi, L., & Tamea, S. (2007). Challenges in humid land ecohydrology: Interactions of water table and unsaturated zone with climate, soil, and vegetation. Water Resources Research, 43(9).

Roy, V., Ruel, J. C., & Plamondon, A. P. (2000). Establishment, growth and survival of natural regeneration after clearcutting and drainage on forested wetlands. Forest Ecology and Management, 129(1), 253-267.

Scheffer, M., Carpenter, S., Foley, J. A., Folke, C., & Walker, B. (2001). Catastrophic shifts in ecosystems. Nature, 413(6856), 591-596.

Skopp, J., Jawson, M. D., & Doran, J. W. (1990). Steady-state aerobic microbial activity as a function of soil water content. Soil Science Society of America Journal, 54(6), 1619-1625.

Sleutel, S., Moeskops, B., Huybrechts, W., Vandenbossche, A., Salomez, J., De Bolle, S., ... & De Neve, S. (2008). Modeling soil moisture effects on net nitrogen mineralization in loamy wetland soils. Wetlands, 28(3), 724-734.

Sullivan, P. F., S.J. Arens, R.A. Chimner, and J.M. Welker. 2008. Temperature and microtopography interact to control carbon cycling in a high arctic fen. Ecosystems, 11(1), 61-76.

Titus, J. H. (1990). Microtopography and woody plant regeneration in a hardwood floodplain swamp in Florida. Bulletin of the Torrey Botanical Club, 429-437.

Troch, P. A., Lahmers, T., Meira, A., Mukherjee, R., Pedersen, J. W., Roy, T., & Valdés-Pineda, R. (2015). Catchment coevolution: A useful framework for improving predictions of hydrological change?. Water Resources Research, 51(7), 4903-4922.

Vitousek, P. M. (1994). Beyond global warming: ecology and global change. Ecology, 75(7), 1861-1876.

Vitousek, P. M., Loope, L. L., & Westbrooks, R. (2017). Biological invasions as global environmental change.

Vivian-Smith, G. 1997. Microtopographic Heterogeneity and Floristic Diversity in Experimental Wetland Communities. The Journal of Ecology 85:71-82.

Von Humboldt, A., & Bonpland, A. (1807). Essay on the geography of plants—with a physical tableau of the equinoctial regions. Essay on the Geography of Plants (2009), 61-155.

Wolf, K. L., C. Ahn, and G. B. Noe. 2011. Microtopography enhances nitrogen cycling and removal in created mitigation wetlands. Ecological Engineering 37:1398-1406.

CHAPTER 2: FORESTED *VERSUS* HERBACEOUS WETLANDS: CAN MANAGEMENT MITIGATE ECOHYDROLOGIC REGIME SHIFTS FROM EMERALD ASH BORER?

Authors

Jacob S. Diamond

Daniel L. McLaughlin

Robert A. Slesak

Anthony D'Amato

Brian Palik

2.1 Abstract

Wetlands self-organize through reciprocal controls between vegetation and hydrology, but external disturbance may disrupt these feedbacks with consequent changes to ecosystem state. Imminent and widespread emerald ash borer (EAB) infestation throughout North American forested wetlands has raised concern over possible ecosystem state shifts (i.e., wetter, more herbaceous systems) and loss of forest function, calling for informed landscape-scale management strategies. In response, we employed a large-scale manipulative study to assess the ecohydrologic response of black ash wetlands to three alternative EAB management strategies: 1) a do-nothing approach (i.e., simulated EAB infestation via tree girdling), 2) a preemptive, complete harvesting approach (i.e., clearcut), and 3) an overstory replacement approach via group selection. We analyzed six years of daily water table and evapotranspiration (ET) dynamics in six blocks comprising black ash wetlands (controls) and management strategy treatments to quantify potential for hydrologic change and subsequent recovery. In both the do-nothing approach and complete harvesting approach, we found persistent changes in hydrologic regime defined by shallower water tables and lower ET rates coupled with increased herbaceous vegetation growth, indicating ecosystem state shifts driven by vegetation-water table interactions. The do-nothing approach showed the least hydrologic recovery after five years, which we attribute to reduction in overstory transpiration as well as greater shade (via standing dead trees) that reduces open water evaporation and herbaceous layer transpiration compared to complete harvesting. We found no evidence

of ecohydrologic disturbance in the overstory replacement approach, highlighting its potential as a management strategy to preserve forested wetland habitat if periodically executed over time before EAB infestation. Although the scale of potential disturbance is daunting, our findings provide a baseline assessment for forest managers to develop preemptive mitigation strategies to address the threat of EAB to ecological functions in black ash wetlands.

2.2 Introduction

Wetlands self-organize through reciprocal controls between vegetation and hydrology. In contrast to uplands, hydrologic controls on wetland vegetation are generally the result of too much rather than too little water (Jackson and Colmer 2005). This abundance of water results in inadequate oxygen supply (Armstrong and Drew 2002) and accumulation of ethylene and anaerobic metabolism byproducts (Ponnamperuma 1984), limiting primary production and preferentially selecting for flora with special adaptations (Kozlowski 2002, Kreuzwieser and Rennenberg 2014). At the same time, wetland vegetation controls local hydrology directly through evapotranspiration (ET), which lowers water tables and reduces soil moisture (Marani et al. 2006). These ecohydrologic interactions often enable and promote ecosystem stability (Rodríguez-Iturbe et al. 2007). However, shifts to different ecosystem states can occur with disturbance to hydrologic setting (e.g., flooding, climate; Wang et al. 2015) or vegetation dynamics (e.g., widespread mortality, Heffernan 2008).

In black ash (*Fraxinus nigra* Marshall) wetlands of North America, looming threats of emerald ash borer (EAB; *Agrilus planipennis* Fairmaire 1888) infestation have drawn attention to possible large-scale tree mortality and a resultant whole-scale shift in ecosystem type and function. EAB causes nearly 100% mortality in all ash species within 3–6 years after infestation (Knight et al. 2013), and there is no known host physiological resistance or stand characteristic that inhibits infestation (Smith et al. 2015). Ash regeneration is also susceptible to EAB colonization once it reaches 2.5 cm in diameter (Klooster et al. 2013), limiting the potential for reestablishment in the presence of EAB. The extent of EAB infestation is widespread, occurring in 27 U.S. states and two Canadian Provinces as of 2017 (USDA 2017). Impending infestation throughout the upper Midwestern United States is particularly concerning, as black ash wetlands cover approximately 8,000 km^2 and provide myriad functions ranging from shelter and food for wildlife (Anderson and Nelson 2003) to timber and non-timber forest products (Wright and Rauscher 1990).

Widespread black ash mortality may equate to loss of a wetland foundational species (*sensu* Ellison et al. 2005), with important consequences for ecohydrologic interactions and successional trajectories (Youngquist et al. 2017). Throughout the upper

Midwestern United States, black ash wetlands are highly monospecific, with black ash comprising 75–100% of canopy cover. In these monospecific stands, complete canopy loss following EAB may cause the water table to rise (via reduced transpiration) and favor establishment and growth of other more water tolerant vegetation, particularly marsh species (Erdman et al. 1987). Recent studies support this general prediction, where canopy disturbance in black ash wetlands resulted in wetter conditions (Slesak et al. 2014) and associated large shifts in species composition towards an herbaceous community (Davis et al. 2017, Looney et al. 2017). Given the extensive coverage and regional importance of black ash wetlands, it is now important to explore possible consequences (and mitigation) of EAB disturbance on ecosystem interactions, state, and function.

Reduced ET is the putative mechanism for expected water table rise and ecosystem state shifts following EAB-induced mortality, but actual changes in ET and how such changes vary over time (seasons to years) and with vegetation structure remain largely unexplored. Although previous studies made a clear link between black ash mortality and altered hydrology (Slesak et al. 2014), the lack of direct ET measurements leaves open questions regarding how black ash regulates water tables compared to other vegetative communities. Post-disturbance community composition, growth, and associated ET rates are likely driven by both hydrologic regime and remnant vegetation structure and recovery, highlighting potential implications of management options that range from a do-nothing approach (i.e., leave standing dead trees) to different degrees of preemptive tree harvest (i.e., partial versus clearcutting). Confronting this knowledge gap, we posit a conceptual model of ET drivers that vary with vegetation structure and thus different management strategies (Figure 2.1a). This model includes availability of energy (e.g., shade from standing dead versus open canopy in a complete clear cut) and water (e.g., via differences in rooting depths), with associated feedbacks to water table regime and its control on post-disturbance vegetative communities. Evaluating this model will address more directly the interactions among energy, vegetation, and hydrology in black ash ecosystems, with implications for both recovery times and management options.

Here, we build upon earlier work (Slesak et al. 2014) by integrating multi-year measures of both daily water table and ET dynamics across black ash wetlands that represent different management options and thus vegetation structure: intact black ash stands (controls), simulated EAB-induced mortality (girdled; do-nothing approach), and two management mitigation options (clearcut and group selection harvest) (Figure 2.1b-d). Our overarching objective was to assess outcomes of both EAB infestation and management options on post-disturbance hydrologic regime. We hypothesized that: H1) water table regimes and their possible post-disturbance recovery will vary depending on management strategy and thus vegetation structure, and H2) that differences in water table regimes among management options can be explained by coincident differences in ET, where black ash trees exhibit unique ET regimes relative to post-disturbance replacement vegetation. Our research advances fundamental understanding of ecohydrologic interactions in black ash wetlands and has direct implications for management aimed at mitigating consequences of EAB infestation.

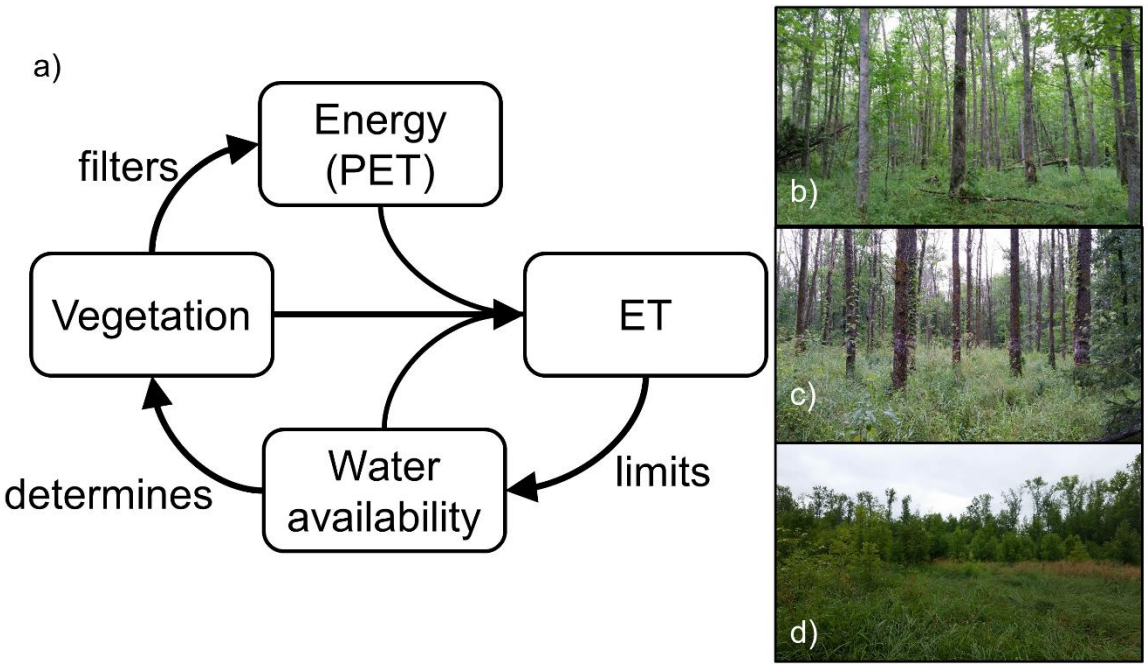

Figure 2.1 a) Conceptual model of feedbacks driving ecohydrology of black ash wetlands. Energy from solar radiation and wind (potential evapotranspiration, PET) is filtered through a cascading vegetation structure to drive evapotranspiration (ET) under the combined influence of vegetation and water availability. ET limits water availability through depletion and controls seasonal water table patterns, which in turn determine vegetation species composition and structure. Photos b-d are from treatment plots in August 2015 that are in similar in environmental conditions (e.g., climate, soils, and elevation) but differ in vegetation structure and its influence on energy partitioning: b) example of black ash wetland with energy filtered by the canopy strata; c) example of girdled black ash wetland to simulate EAB mortality with less energy filtered by the canopy strata; d) example of clearcut black ash wetland with increased growth of marsh vegetation due to large reduction in energy filtered from the canopy strata.

2.3 Methods

2.3.1 Landscape Setting

Our study sites were located within the Chippewa National Forest in northern Minnesota, USA, a 2,700 km^2 area with 1,600 km^2 of wetlands and over 1,300 lakes (Figure 2.2). The area encompasses a complex glacial landscape that is flat to gently rolling, with black ash wetlands found in the lowest landscape positions that commonly grade into aspen (*Populus*) or pine (*Pinus*)-dominated upland forests. Most of the black ash wetlands are underlain by lacustrine clay at a depth of 10–150 cm that acts as a confining layer and creates wetland hydrologic conditions (seasonal soil saturation and inundation). Specific soil types vary and include Typic Glossaqualfs with no O horizon,

Histic Humaquepts with a 30 cm deep O horizon, and Terric Haplosaprists with a 60 cm deep O horizon and no B horizon (Soil Survey Staff 2017). However, collected soil samples in our study sites did not significantly differ in overall soil chemistries (total carbon and nitrogen) or bulk densities (Table S2.1).

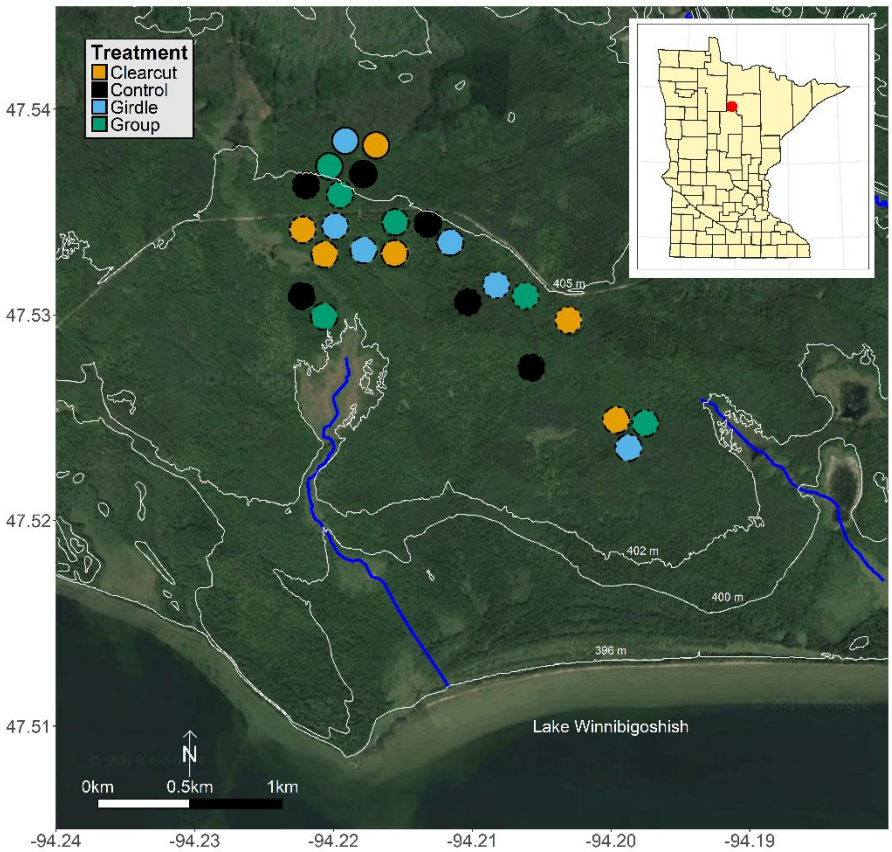

Figure 2.2 Experimental design of EAB study in Chippewa National Forest. Blocks 1–6 are shown. Line types surrounding experimental plots designate blocks. White lines are contour lines and dark blue lines are intermittent streams. Wells are located in the center of each plot, with two co-located rain gages in blocks 1 and 3 control plots.

Forest structure and composition in black ash stands in the region are characterized by black ash canopy dominance (75–100%) co-occurring with American elm (*Ulmus Americana* L.), balsam fir (*Abies balsamea* L. Mill.), basswood (*Tilia Americana* L.), red maple (*Acer rubrum* L.), yellow birch (*Betula alleghaniensis* Britt.), quaking aspen (*Populus tremuloides* Michx.), or white cedar (*Thuja occidentalis* L.). Stands are typically strongly uneven-aged and largely influenced by gap-scale disturbance processes with canopy tree ages ranging from 130–232 years (Looney et al.

2016). In our study sites, basal areas prior to treatment (see below) ranged from 23.0–39.2 m^2 ha^{-1}, and densities ranged from 563–917 stems ha^{-1} (minimum DBH 2.5 cm).

Mean annual precipitation at the study area is 70 cm, 60% of which is via rainfall. Mean growing season (May–September) temperature is 14.3 °C, and annual potential ET (PET) is 60–65 cm (Sebestyen et al. 2011). Hydrologic monitoring and water geochemistry investigations indicate that black ash wetlands are mostly disconnected from the regional groundwater system (via the shallow confining layer), and are largely precipitation driven with snowmelt in the spring and periodic inputs via rainfall throughout the growing season (Slesak et al. 2014). The regional confined groundwater system ranges in depth from 1.5 to 17 meters, with a general horizontal flow direction south towards Lake Winnibigoshish; vertical groundwater flow in the study area is minimal (Lindgren 1996).

2.3.2 Experimental design

We established a large-scale, manipulative study using a randomized complete block design with six blocks, each with four 1.6 ha circular treatment plots that were similar in elevation and soils (Figure 2.2). Blocks were delineated based on three criteria: 1) plot proximity, 2) general assessments of pretreatment hydrologic regime (e.g., wet vs. relatively drier), and 3) native plant communities. Four treatments were applied within each block, providing 6 replications of each treatment: 1) control, 2) girdling of all black ash trees down to 10 cm diameter at 1.3 m height ("girdle"), 3) group selection harvest (20% of stand in 0.04 ha gaps; "group selection"), and 4) clear cut harvest (complete removal of all trees; "clearcut"). The girdling treatment mimicked EAB induced mortality, including progressive ash mortality over several years and retention of standing dead trees on site. The two forest harvesting treatments represented possible management strategies to modify stand composition and facilitate natural regeneration or planting of alternative tree species to maintain forest ecosystem functioning following EAB infestation. All treatments were applied in winter of 2011–2012 during frozen ground conditions, and trees in girdle treatments were re-girdled in the winter of 2012–2013 to ensure 100% mortality. Drawknives were used for manual application of the girdle treatments, and cut-to-length mechanized harvest systems were used for the clearcut and group selection treatments. Previous research documented shifts from woody to

herbaceous species after girdle and clearcut treatments were implemented (Looney et al. 2016, Looney et al. 2017; Figure 2.1c,d). Clearcut treatments became dominated by Canada reedgrass (*Calamagrostis canadensis*), whereas girdle treatments promoted growth of rhizomatous ferns (*Matteuccia struthiopteris*) and sedges (*Carex radiata*).

2.3.3 Data collection

Over a six-year period (2011–2016), we monitored water table levels throughout the snow-free season (typically May through October) in all experimental plots using groundwater monitoring wells. Wells were constructed of 5-cm diameter, screened PVC pipe and located in the approximate center of each plot to a depth of 1.5 meters or until a confining layer was reached. We measured water levels with high-resolution total pressure transducers (Levelogger Gold Model 3001, Solinst Canada Ltd, Ontario, Canada; and HOBO U20L-04, Onset Computer Corp., Bourne, MA) at 15-minute intervals, and corrected for atmospheric pressure with a barometric pressure logger (Barologger, Solinst Canada Ltd, Ontario, Canada). We also recorded rainfall with four HOBO tipping-bucket rain gauges (model RG3-M, Onset Computer Corp., Bourne, MA) located on-site, and obtained local potential evapotranspiration (PET) values and total annual precipitation values (i.e., including snowfall) from the nearby RAWS Cutfoot station (http://www.raws.dri.edu/cgi-bin/rawMAIN.pl?sdMCUT). To assess effects of differences in canopy on energy budgets, air temperature was measured using Thermochron iButtons (model Ds1921G-F5, Maxim Integrated, San Jose CA) at 0.5 m height from 2013–2016 in controls, girdle, and clearcut treatments.

2.3.4 Data Analysis

We used collected data to quantify and compare pre- and post-treatment water table regimes and ET rates (also derived from water table data) across treatment groups. We first passed water table data through a digital, second-order Butterworth low-pass filter to improve the signal-to-noise ratio. For each well, we also removed all days when water tables were below sensor depth. We conducted all data processing and subsequent analyses using R (R Core Team 2016).

2.3.4.1 Water table regimes

To assess treatment-induced water table changes, we employed a paired-plot approach (*sensu* Pothier et al. 2003). Within each block, we calculated annual pretreatment (2011) and post-treatment (2012–2016) relationships between control water tables and water tables for each manipulative treatment (i.e., girdle, group, and clearcut) using simple linear regressions of average daily water tables. We then normalized all annual post-treatment relationships relative to pre-treatment relationships to account for pretreatment differences among blocks. Doing so allowed treatments to be pooled across replicates (i.e., across blocks) and for a more general interpretation of treatment effect (vis-à-vis 1:1 pretreatment relationships). To do so, we divided post-treatment slopes by pretreatment slopes (e.g., if the pre-treatment slope was 1.2 and the post-treatment slope was 0.6, then the normalized slope would be 0.5) and subtracted pre-treatment intercepts. To account for possible piecewise behavior in post-treatment normalized relationships (e.g., slope shifts at specific thresholds), we used the *segmented* package in R (Vito and Muggeo 2003, 2008) to test the null hypothesis of a constant linear predictor. Where this null hypothesis was rejected ($p < 0.05$), we conducted breakpoint analysis to estimate the fit for a model constrained to two slopes. Our model did not specify breakpoint values a priori, but instead optimized each breakpoint location by iteratively fitting standard iteratively-reweighted least squares models. For each normalized post-treatment relationship, we extracted relationship parameters (y-intercept, x-axis breakpoint, and slopes), pooled by treatment (via parameter means across replicates), and tested for significant differences both across treatments and compared to pretreatment predictions (null hypothesis: slope=1, intercept=0, and no breakpoint).

Normalized post-treatment relationships revealed effects of manipulative treatments in several ways. Deviations from pretreatment predictions (i.e., 1:1 relationship) indicated increased or decreased post-treatment water tables and under what conditions (e.g., shallow versus deep water tables). A normalized post-treatment slope less than unity indicated a reduced water table drawdown rate relative to pre-treatment predictions, whereas a slope greater than unity indicated a more rapid drawdown rate. The presence of breakpoint indicated a shift in drawdown rates at specific water table conditions. A normalized post-treatment intercept greater than zero indicated higher post-

treatment maximum water tables relative to pre-treatment predictions, and the opposite for an intercept less than zero. As such, annual normalized relationships allowed assessment of both treatment effects and degree of hydrologic recovery over time.

2.3.4.2 Evapotranspiration rates

We calculated daily ET using a modified White method (1932) first described by Loheide (2008), and used recently by Watras et al. (2017). The method is applied for non-rain days and assumes ET is negligible at night, allowing daily ET to be estimated from 24-hr change in water table and variable net groundwater inflow:

$$ET = S_y \times [r - S] \qquad (1)$$

where:
ET = daily evapotranspiration [L]
S_y = specific yield as a function of water table [-]
r = net groundwater inflow as a function of detrended water table [L]
S = 24-hr change in storage (change in daily water table) [L]

We estimated variable groundwater inflow (r) as a function of detrended water table data following methods described in Loheide (2008). We used a three-day sliding window to detrend the water table data because our data did not have one consistent trend over a season due to punctuated rain events and variable drawdown rates over the season. Eq. 1 also requires specific yield (S_y) values, defined as the depth of water released or gained from storage per unit change in water table. S_y varies with both below- (Duke 1972) and above-ground water levels (McLaughlin and Cohen 2014), requiring constructed relationships between S_y and water table levels. Similar to Watras et al. (2017) and following methods described in McLaughlin and Cohen (2014), we empirically estimated S_y values as ratios of rain (corrected for interception) to induced water table rise across different precipitation events (and water table levels) to construct S_y relationships for each plot. Across plots, our water table-dependent S_y functions followed an exponential curve from water tables levels at approximately -10 cm (10 cm below ground surface) to 5 cm above ground surface. Generally, below -10 cm, S_y was approximately constant at 0.05, and above 5 cm, S_y was approximately constant at 0.8.

We calculated daily ET for every day without rainfall at each of our plots. We conducted quality control by removing data with poor signal-to-noise ratios in diurnal water table variation (typically due to recent rainfall) that limited ET estimation. To evaluate differences in ET among treatments, we differenced daily ET in manipulative treatments (girdle, group, and clearcut) with daily control ET within each block ($ET_{treatment,i} - ET_{control,i}$), but only on days where both the treatment plot and the control plot within a block had ET estimates. Then we averaged daily differences by treatment (across blocks) and month for each year of the study. We also conducted unequal variances t-tests for each month to test the null hypothesis that controls versus manipulative treatments had equal mean monthly ET rates. Overall, we used 14,354 days for the ET analysis, 8,016 of which were days when we could compare control ET to treatment ET within a block.

To test our conceptual model, we employed a linear mixed-effects model to predict daily ET averaged by month using our hypothesized ET drivers as predictors (Figure 1a): 1) monthly average of daily PET for climatic demand; 2) average monthly water table position for water availability, 3) treatment for differences in both vegetation transpiration (e.g., via differences in water use efficiency and rooting depth) and structure (shading and canopy turbulence); and 4) vegetation phenology (i.e., leaf off or leaf on, assuming a leaf on period of June 1 to September 30). We used the control plots as our reference group. We also considered the interaction of average monthly water table position with treatment to account for the expected treatment differences in water table-dependent ET response. In addition to focusing on specific drivers, this combination of variables provided the lowest Bayesian Information Criterion scores and the highest likelihood scores relative to both simpler and more complex alternative models (e.g., no phenology term, multiple interaction terms, and no interaction terms). We modeled treatments nested within blocks as a random effect. We also used an autoregressive (AR1) correlation matrix structure to account for the high degree of autocorrelation among consecutive months; we confirmed this to be a reasonable correlation structure based on improvement of the autocovariance plot after implementation. We also found improvement in residual behavior, and note that residuals were normally distributed about zero. Finally, to allow for model estimate comparison between the two quantitative

variables (PET and average monthly water table), we also considered a model where PET and average monthly water table were centered and scaled to the same range.

2.4 Results

There were common hydrologic patterns across all treatments, best described as early season inundation followed by consistent summer drawdown with occasional punctuated rainfall events raising water tables Figure 2.3). We also observed consistent diel signals in water table data (Figure 2.3 inset) indicative of ET signals and their variability across treatments. There was little interannual variation among control treatment ET rates, with much greater variation in the timing and amount of total rainfall across years (Table 2.1); monthly rainfall and control ET were not correlated ($p = 0.33$) across years. Overall annual precipitation (obtained from the RAWS Cutfoot site) was greatest in 2016 (90.7 cm) and least in 2013 (59.2 cm). Rainfall was most frequent in 2013, 2014 and 2016, which experienced an average 0.4 events day-1, but 2016 had the largest events, with average event size 40% greater than other years. Despite this wide interannual variability in precipitation inputs, we observed coherent effects of manipulative treatments on both water table regimes and ET rates.

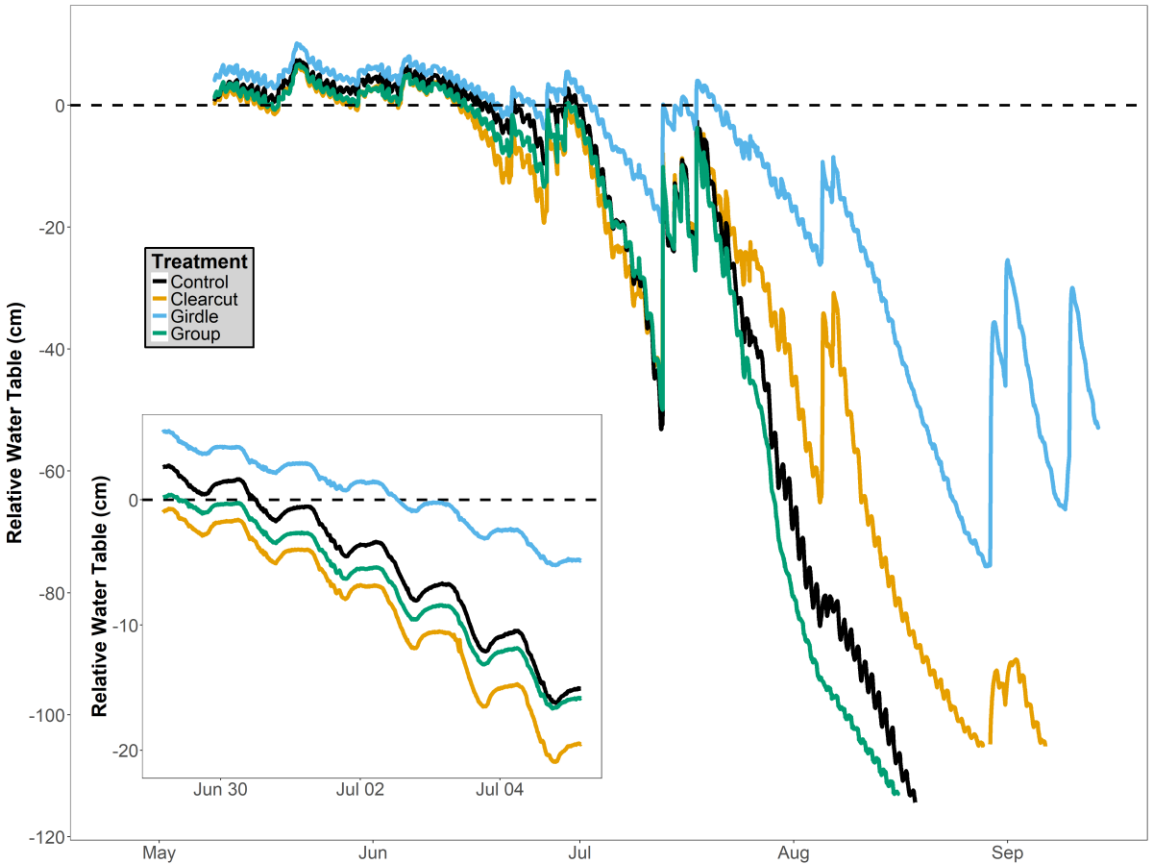

Figure 2.3 Example of water table patterns for each of the treatments (Block 1, 2013), with inset of diurnal patterns. Dashed line denotes ground surface.

2.4.1 Treatment effects on water table regimes

Across all plots, pre-treatment relationships between control and manipulative treatment daily water tables were highly linear, had slopes near 1 (slope = 1.1±0.6), and exhibited small variation about the best fit lines (R^2= 0.87±0.16), indicating a high degree of similarity in hydrologic behavior among plots within blocks (e.g., 2011 in Figure 2.4a). Plots exhibited common water table drawdown behavior across blocks and years with generally high early season water tables followed by drawdown leading to deeper late season water tables (Figure 2.4a, colors), corresponding with general trends shown in time series (Figure 2.3). Following treatment, there were significant differences between mean (across blocks) normalized post-treatment relationships and pre-treatment relationships (i.e., deviation from the 1:1 line) for both clearcut and girdle treatments, with water tables being consistently higher in these treatments relative to predicted values (Figure 2.4a, b). Deviation in girdle treatments was more evident following re-girdling in 2013, suggesting limited mortality in the first year. When water tables were deepest for

control plots (ca. -100 cm), clearcut and girdle treatment water tables were up to 50 cm higher on average than predicted (some replicates deviated by as much as 80 cm), but differences were markedly less at shallower water tables (Figure 2.4a, b). Clearcut and girdle treatments exhibited similar initial response to disturbance (compare clearcut in 2012 and girdle in 2013), but girdle treatments maintained shallower relative water tables and lower drawdown rates than clearcut treatments throughout the five-year study period (e.g., in 2014 when clearcut normalized slopes were not significantly different than unity; Figure 2.4b). Group treatments exhibited no significant departures from pre-treatment relationships in any year of the study period.

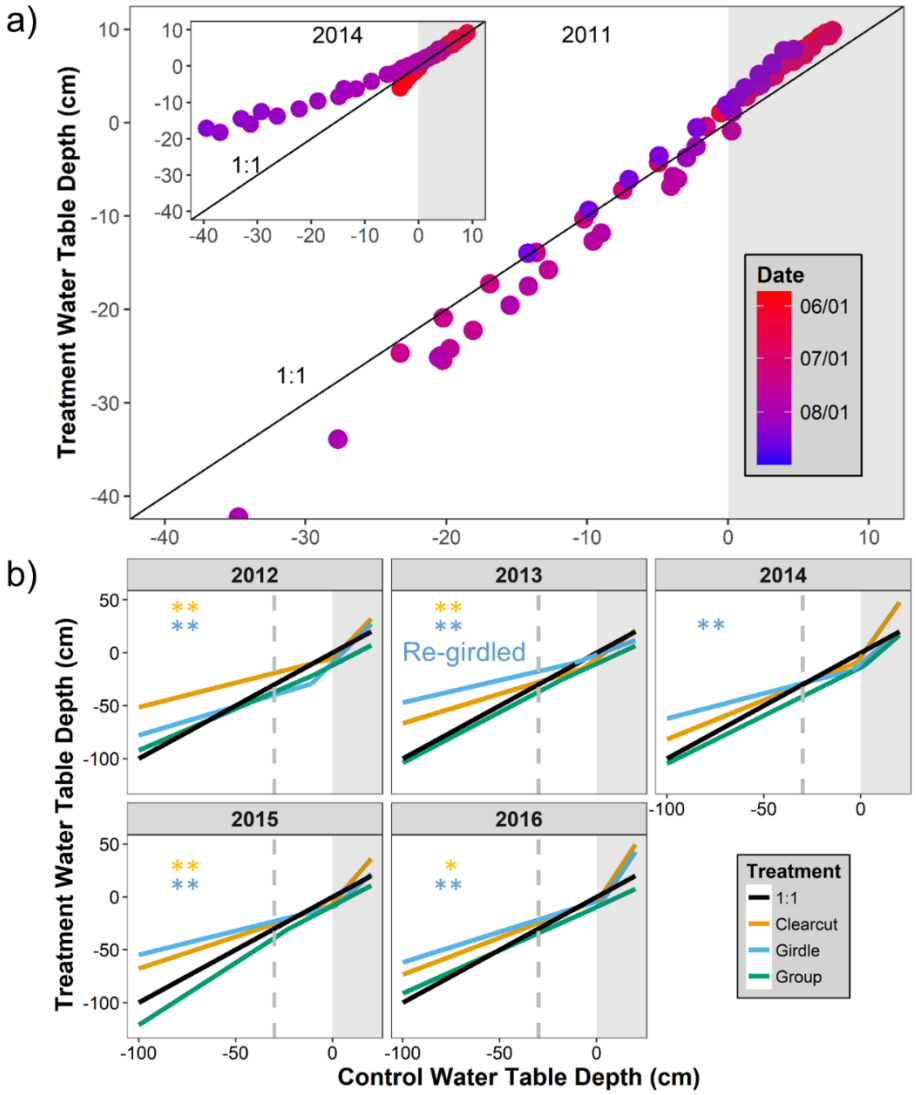

Figure 2.4 a) Example water table comparison in block 1 between girdle and control in pre-treatment year (2011) and post-treatment year (2014; inset). Points are colored by the date they were recorded. Note difference between near-identical 1:1 behavior in pre-treatment year (2011) compared to breakpoint behavior in post-treatment year (2014). b) Average water table response across 6 blocks. Black 1:1 line represents rescaled 2011 pre-treatment relationship. Asterisks represent slopes significantly different from the 1:1 line (, $p < 0.05$; **, $p < 0.01$). Slopes above breakpoints were often significantly greater than 1 within sites, but not when averaged among sites. Breakpoints predominately occurred at ground surface in the control (shading). Clearcut treatments appear to have a slightly faster recovery to pre-disturbance hydrology on average than girdle treatments, but both treatments maintain elevated water tables even after 5 years. The greatest differences in water table are observed below the grey line at 30 cm below ground surface. Group treatments do not significantly deviate from pre-treatment behavior.*

We observed ubiquitous piecewise post-treatment behavior across all blocks in both clearcut and girdle treatments (Figure 2.4b). In nearly all years, both clearcut and girdle treatments exhibited a mean normalized slope greater than unity above a mean breakpoint consistently centered on the ground surface (shaded region in Figure 2.4b). Below the breakpoint, however, normalized slopes were consistently less than unity. We also observed similarity between clearcut and girdle treatments in the relative location of departure from control water tables; the greatest differences between these treatments and controls were found below -30 cm (dashed line in Figure 2.4b).

When comparing normalized slopes below breakpoints among manipulative treatments, we found that girdle treatment slopes were significantly less than group treatment slopes for all years ($p < 0.05$), and were significantly less than clearcut normalized slopes in 2014 ($p = 0.04$). Clearcut normalized slopes were significantly less than group treatments for 2012, 2013, and 2015 ($p < 0.05$). We did not find any significant differences among treatments for normalized intercepts in any year.

2.4.2 Treatment effects on evapotranspiration rates

Differences in post-treatment water table relationships were coincident with differences in post-treatment ET between controls and clearcut and girdle treatments. We observed no significant differences in post-treatment ET for the group treatment, which aligns with water table observations; as such, the following results focus on clearcut and girdle treatments. In the pretreatment year (2011), there were generally no significant differences (i.e., standard error bars cross zero) in monthly averages of daily ET among treatments, but clear differences emerged for post-treatment years (2012–2016) for both girdle and clearcut treatments (Figure 2.5a). During the growing season for black ash (shaded area in Figure 2.5a), ET for clearcut and girdle treatments was consistently and often significantly ($p < 0.05$) less than control ET for post-treatment years. Average daily ET differences were greatest in June and July, with differences becoming less pronounced throughout the rest of the growing season. Frequently observed growing season differences on the order of -0.05– -0.1 cm d-1 amount to approximately 25% reductions in ET relative to control values (*cf.* column 2 in Table 2.1).

Table 2.1 Mean (± standard error) evapotranspiration and rainfall across control plots for study period (2011–2016).

Month	Average daily evapotranspiration (cm)	Average monthly evapotranspiration (cm)	Average monthly rainfall (cm)
5	0.21 ± 0.0056	6.4 ± 0.17	7.9 ± 0.37
6	0.31 ± 0.0078	9.2 ± 0.23	11 ± 1.3
7	0.42 ± 0.021	13 ± 0.63	7.5 ± 1.3
8	0.36 ± 0.041	11 ± 1.2	5.2 ± 0.18
9	0.17 ± 0.0053	5.0 ± 0.19	5.9 ± 2.0
10	0.12 ± 0.0053	3.6 ± 0.16	2.7 ± 1.4
11	0.040 ± 0.0043	1.2 ± 0.13	0.21 ± 0.15
Total	**–**	**49**	**40**

The trend of lower post-treatment ET in girdle and clearcut treatments relative to controls was often reversed in the dormant season, when black ash trees have no leaves. This dormant season increase in relative ET was most evident in 2013 and 2014, but also is present to a lesser extent in other post-treatment years. We note, however, that observations for fall dormant seasons are more limited due to low water tables, when dry well conditions in control plots often precluded ET comparison. Clearcut treatments typically exhibited the strongest adherence to this dormant season increase in ET relative to controls. These increases in clearcut ET relative to controls were approximately 0.025 cm d^{-1}, but could be as great as 0.1 cm d^{-1} (see 2013 in Figure 2.5a). Removing the large increases observed in 2013, these differences represent increases by approximately 10% in ET relative to controls (*cf.* column 2 in Table 2.1).

Interannual differences in precipitation and associated water tables partly explain interannual variability in post-treatment ET differences between controls and girdle and clearcut treatments (Figure 2.5b). The highest growing season monthly ET differences tended to occur during dry conditions with deep average water tables across all treatments (2012–2013 vs. 2016; Figure 2.5a, b). The effect of water table on differences in dormant season is less clear in part from limited observations. However, examining 2013 suggests that the greatest dormant-season ET increases occur during periods with higher dormant season water tables in girdle and clearcut treatments relative to controls. Greater growing season ET-induced water table decline in control plots led to large dormant season water table differences among treatments, subsequently magnifying differences in dormant season water availability and thus ET. Compare this to 2016,

when water tables remained high and were similar among treatments throughout the whole season yielding similar water availabilities; this year had the smallest overall differences in ET among treatments.

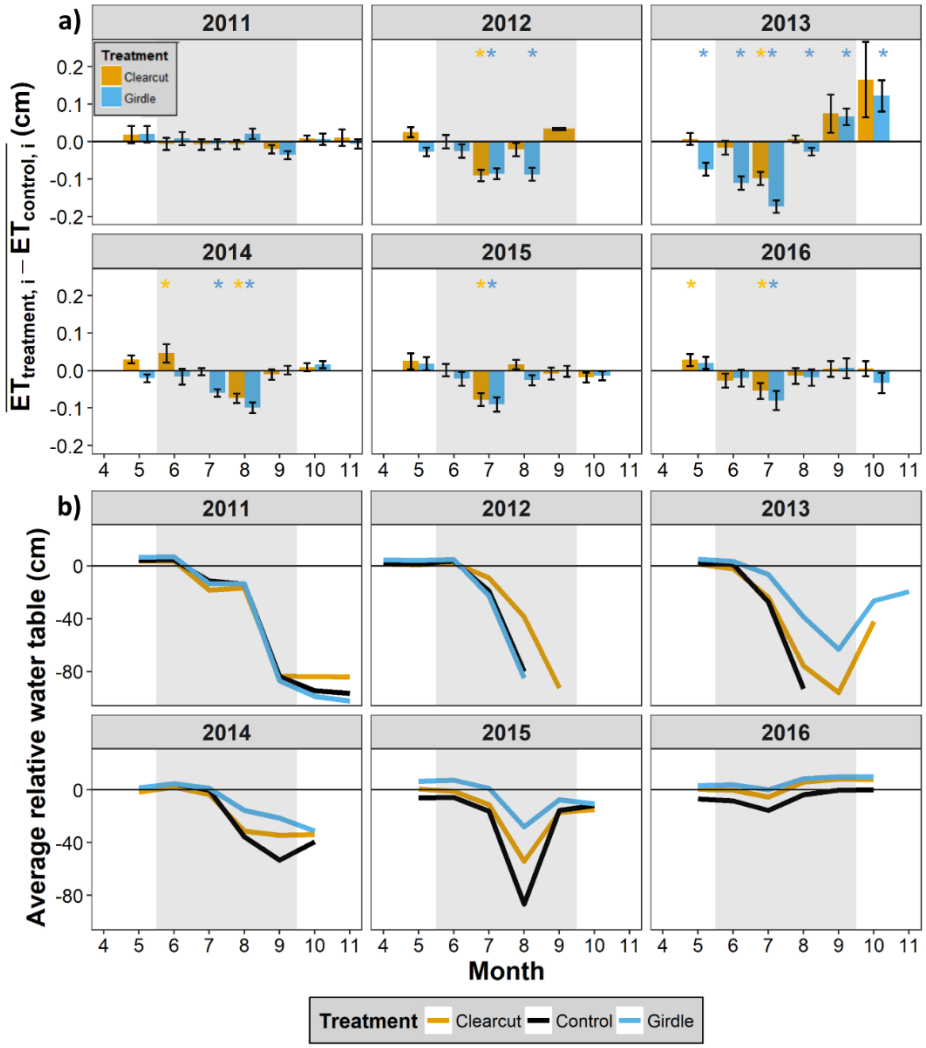

Figure 2.5 a) Sum of mean daily differences by month between controls and manipulative treatments, averaged across blocks. Bars are standard errors. Asterisks indicate significant differences ($p < 0.05$) for monthly average ET rates between controls and girdle and clearcut treatments. Pre-treatment year (2011) generally shows no significant differences among treatments. For post-treatment years (2012–2016), ET in controls is much greater than treatments during mid-summer, but these differences are muted or even reversed in late spring and late fall, especially for clearcuts. Shading indicates leaf on season. b) Average monthly water tables for block 1 (a representative block). Monthly values are missing when water tables were below recording depth. When water tables are similar among control and treatments, differences in daily ET are smallest. Note that not all blocks had water tables below recording depth during fall dormant season months.

Considering relative ET differences in both growing and dormant seasons, average cumulative differences for all post-treatment years were -0.16 cm yr^{-1} (-1.2 cm yr^{-1} without 2013) for clearcut and -5.1 cm yr^{-1} for girdle. These amount to overall reductions in post-treatment ET of 0.3% (2.4% without 2013) for clearcuts and 10% for girdle relative to controls. These numbers align with observed end-of-season differences in water tables after considering Sy and uncertainties involving unmeasured interception losses, adding confidence to the approach. That is, mean annual ET differences for clearcut (-1.2 cm) and girdle (-5.1 cm) yield expected mean differences in predicted and post-treatment water tables (24 cm and 102 cm, respectively).

Our linear mixed-effect model indicates significant effects of most candidate predictor variables (Table 2.2). The signs of the fixed effect parameter estimates align with expectations, lending credence to the structure of the model. PET and water table height exhibited positive influence on ET, and when rescaled in the model, it became clear that they had a similar magnitude of effect on ET (0.0133 versus 0.0134, Table 2.2). Comporting with ET observations, girdle and clearcut treatments (but not group) had negative influences on ET, although not significantly. However, treatment interaction with water table was positive for all treatments and was significant except for the group selection treatment. This implies that water table effects on ET differ from controls for clearcut and girdle, but not for group selection. Conditional (full model) and marginal (fixed effects only) coefficients of determination for the model were 0.32 and 0.23, respectively.

Table 2.2 Summary of linear mixed-effects model

Parameter	Estimate	SE	Df	t-value	p-value
Intercept	0.178 (0.234)	0.0183 (0.0127)	702	9.8 (18.4)	<0.0001 (<0.0001)
Average daily PET (cm)	0.273 (0.0133)	0.0557 (0.00272)	702	4.9	<0.0001
Leaf off/on	0.0433	0.00505	702	8.6	<0.0001
Clearcut	-0.0256	0.0162	14	-1.6	0.137
Girdle	-0.0271	0.0162	14	-1.7	0.116
Group	0.0231	0.0173	14	1.3	0.205
Control x WT	0.000435 (0.0134)	0.000139 (0.00427)	702	3.1	0.0018
Clearcut x WT	0.000695 (0.0259)	0.000275 (0.00786)	702	3.3	0.0010
Girdle x WT	0.000448 (0.0155)	0.000239 (0.00702)	702	2.2	0.0273

Group x WT	0.000144 (0.00396)	0.000240 (0.00685)	702	0.58	0.564

Values in parentheses refer to scaled and centered predictor variables.
Note: Control group is reference group

2.5 Discussion

In this work, we studied the ecohydrologic response of black ash wetlands to three alternative management strategies. Our work is motivated by concern over the impending EAB infestation in North American black ash wetlands, where evidence suggests potential for catastrophic shifts to wetter, non-forested wetland states. Our findings support this general prediction, provide insights into the ecohydrologic feedbacks of these systems, and highlight important differences among possible management strategies for mitigating consequences of EAB infestation.

2.5.1 Shifts in hydrologic regime

H1: Our results support our hypothesis (H1) that hydrologic regimes and their recovery vary depending on management strategy and its influence on vegetation structure. Group-selection treatment (20% harvest) exhibited no hydrologic response to treatment, aligning with expectations from upland systems where harvests of less than 20% produce no observable water yield effects (Bosch and Hewlett 1982). However, the clear and persistent "wetting up" behavior following clearcut and girdle treatments adds black ash wetlands to the numerous systems that exhibit this behavior with similar levels of disturbance, both in uplands (Bosch and Hewlett 1982, Arthur 1998, Bearup et al. 2014) and wetlands (Dubé et al. 1995, Sun et al. 2001, Bliss and Comerford 2002, Pothier et al. 2003). Similar post-clearcut water table rises observed in Michigan black ash wetland depressions (van Grinsven et al. 2017) imply that this response to disturbance is not unique to our study area, and may be common across any landscape or geomorphic position that is dominated by black ash.

Although immediate responses to disturbance may be expected, there is considerable variability among ecosystem hydrologic recovery times in the literature (Brown et al. 2005, Bosch and Hewlett 1982, Troendle and King 1985, Jones and Post 2004, Moore and Wondzell 2005, Aust 1997, Bliss and Comerford 2000, Sun et al. 2000). Importantly, we did not observe strong hydrologic recovery in our clearcut and girdled plots, even five years after treatment, although results suggest a more rapid

recovery trajectory for clearcut relative to girdle treatments (Figure 2.4). Such sustained water table rise has both local (i.e., controls on vegetation composition and growth) and landscape-scale consequences. For example, we estimate that end of growing season differences in water table (up to 50 cm in girdle treatments) due to black ash loss may increase annual water availability by up to 1 cm per hectare of loss. In Minnesota alone, which contains over 400,000 hectares of black ash forest (MN DNR 2003), this increase in water yield has the potential to substantially alter downstream hydrology by increasing headwater flows to the Mississippi River.

Post-disturbance shifts in hydrologic regime highlight unique black ash imprints on local ecohydrologic interactions. Hydrologic regime shifts were particularly evident from the coherent breakpoint patterning in annual post-treatment water table relationships. For both clearcut and girdle treatments, the consistent breakpoint patterning distinguishes early season, above-ground water levels that decline faster than pre-treatment from belowground water levels that decline slower (Figure 2.4b). Despite variable vegetation structure and composition between clearcut and girdle treatments (Looney et al. 2017), both treatments also exhibited similar breakpoint locations centered on ground surface and similar piecewise structure, suggesting common above- and below-ground hydrologic response to black ash mortality. Moreover, both clearcut and girdle treatments exhibited similar departures from pretreatment relationships (i.e., departures for both treatments begin around ~-30 cm, Figure 2.4b), highlighting the likely effect of black ash loss and its unique water uptake strategy (e.g., via relatively deeper roots) compared to herbaceous replacement vegetation (Looney et al. 2017). In combination, this interannual persistence of altered drawdown patterns (i.e., with a consistent break-point structure and 30 cm water table departure) indicates that black ash uniquely influences water table position, and imposes a hydrologic regime not observed under other vegetative configurations, underscoring its role as a foundation species in these ecosystems (Youngquist et. al. 2017).

H2: Our time series links observed hydrologic response (water table regimes) to the associated ET driver that varies with vegetation structure, and support our prediction (H2) that black ash communities imprint a unique ET signal relative to post-disturbance vegetation communities. Specifically, controls exhibited up to 30% greater ET during the

growing season but up to 50% less ET during the dormant season than clearcut and girdle treatments (Figure 2.5a). The presence of black ash clearly imparts different seasonal ET patterns and resulting water table patterns relative to herbaceous replacement vegetation, likely attributable to differences among phenology, filtering of PET, and rooting depth strategies. Despite these seasonal variations, controls maintained higher cumulative ET relative to treatments even after 5 years. These results support an analogous sap-flux study conducted in harvested black ash systems in Michigan, where findings suggested reductions in stand level transpiration in clearcut and girdle treatments during the growing season (van Grinsven et al. 2017). However, we note here that in addition to evaluating transpirative loss from black ash mortality, our study considers changes to ecosystem-scale ET that depend on increased understory contribution with decreasing canopy leaf area (Phillips and Oren, 2001). Black ash trees clearly have a significant influence on the magnitude and temporal structure of evapotranspirative fluxes.

2.5.2 Ecohydrologic Controls

Differences in ET and thus water table regimes among plots clearly reveal the importance of vegetation-specific ecohydrologic interactions that influence water availability (e.g., rooting depth) and energy partitioning (via canopy leaf area) (Figure 2.1a). Surprisingly, water-limitation due to shallow rooting may be an important control on ET in these wetland systems; our statistical model indicates that water table is equally as important as PET in predicting ET of black ash wetlands (controls) and possibly twice as important in clearcut treatments (Table 2.2, compare scaled and centered estimates). These results align with a black ash sap flux study that found significant soil moisture control on black ash transpiration, where highest sap fluxes occurred under saturated conditions and much lower sap flux when relative soil water saturation was still as high as 60% (Telander et al. 2015). Vegetation structure can further influence ET through effects to energy partitioning. For instance, canopy structure filters energy inputs for understory transpiration and direct evaporation of standing and/or soil water (Allen et al. 2017). Additionally, canopy structure likely influences snowfall interception and sublimation and wind redistribution that can result in less snow pack under ash relative to clearcut treatments (Molotch et al. 2007, LaMalfa et al. 2008, Veatch et al. 2009).

Changes in both rooting depths and canopy cover following disturbance likely play a large role in observed treatment effects.

Together, vegetation differences in both water access and energy partitioning help explain ET and water table differences among plots and over time. Clearcut treatments (and to a lesser extent, girdle treatments) commonly exhibited higher spring dormant season water tables than predicted pre-treatment relationships (Figure 2.4), possibly as a result of greater snowpack. However, clearcuts also often exhibited greater spring dormant season ET than controls and subsequently more rapid spring dormant season drawdown Figure 2.4b) likely due to more open water evaporation from a combination of reduced shading and greater boundary turbulence. We found clear support for the former control on ET, where clearcut (and to a lesser extent girdle) treatments experienced greater daily maximum temperatures compared to control treatments by up to 5° C (Figure S2.1). However, even though clearcut and girdle treatments received greater sub-canopy energy inputs throughout both dormant and growing seasons, they evapotranspired less than controls in the growing season and on an annual basis, likely due to limited growing season water access via shallow rooting Figure 2.4b). The greater reduction in growing season (and annual) ET and resulting shallower water tables for girdle treatments compared to clearcuts may be because girdle treatments experience the "worst of both worlds". That is, ash mortality results in both reduced overstory transpiration but also maintained shade to limit herbaceous transpiration and open water/soil evaporation (Slesak et al. 2014).

2.5.3 Consequent shifts in ecosystem state

The observed persistent shifts in hydrologic regime coupled with documented shifts in vegetation community from woody to herbaceous (e.g., Looney et al. 2017) indicate a clear change in ecosystem state for the highest levels of disturbance at these sites. Wetland plant communities can act as ecosystem engineers (*sensu* Jones et al. 1994) by regulating water table dynamics (via controls on ET) and creating conditions that enhance their own success (Ridolfi et al. 2006). However, the feedbacks that communities develop may be sensitive to abrupt shifts in ecosystem conditions, at which point new positive feedbacks arise, promoting an alternative stable state (Roy et al. 2000, van de Koppel et al. 2005, Kéfi et al. 2016 and references therein). Disturbances that alter

vegetation dynamics can cascade to hydrologic regime and, in turn, feedback to influence resultant vegetation composition (Figure 2.1a). In wetlands, where water table depth is a dominant control on oxygen and nutrient availability, even moderate rises in the water table following vegetation mortality (e.g., Dubé et al., 1995, Pothier et al. 2003) can alter recruiting vegetation communities (Rodríguez-Iturbe et al. 2007). As such, alternative stable states may be possible where less water tolerant species thrive on deep(er) water tables versus more water tolerant species thriving on shallow(er) water tables (Chambers and Linnerooth, 2001, Ridolfi et al. 2007). We suggest that we have observed such a change in feedbacks in this experiment where complete loss of black ash induced shifts in vegetation communities and their influence on hydrologic regimes, which will in turn likely continue to influence replacement vegetation composition and growth.

Whether this more herbaceous and wetter system will maintain itself through new feedbacks (i.e., become a new stable ecosystem configuration) or whether it will shift back to a forested wetland is uncertain. The stability of the post-disturbance system depends on the strength of the feedbacks that develop between replacement vegetation and hydrology. Explosive herbaceous layer growth following treatment application (Looney et al. 2017) in both the clearcut and girdle treatments may impose a negative feedback (via shade and competition) on establishment of tree seedlings (Terwilliger and Ewel 1986). However, we submit an additional negative feedback loop on black ash regeneration, where wetter conditions driven by reduced ET from replacement vegetation no longer favors forest plant communities. Evidence for this negative feedback is found throughout Minnesota, where increased wetness in black ash wetlands due to ponding and impoundment from roads correlates strongly with black ash crown dieback (Palik et al. 2011, Palik et al. 2012). Such overstory and seedling sensitivity to disturbed (wetter) hydrologic regime may be a common feature of forested wetlands, where replacement marsh communities are sustained until specific conditions (e.g., drought) support tree seedling regeneration (Aust 1997, Casey and Ewel 2006). Further, even if EAB-infested black ash wetlands experience ideal recovery conditions for ash seedling regeneration, it is uncertain whether new seedlings will survive due to perpetual mortality from EAB. These negative feedbacks suggest an alternative wetter, and more herbaceous stable state, where return to forested conditions will require intensive management (i.e., planting of

replacement tree species that can tolerate the hydrologic conditions, Looney et al. 2015). However, our study was limited to 5 years, and we cannot discount the plausibility of longer-term community succession and regrowth effects (particularly hardwood sprouting) to increase ET and result in more suitable hydrology for forests.

2.5.4 Management implications

Our work has direct implications for future management aimed at mitigating EAB impacts. EAB infestation, in the absence of mitigation strategies, is likely to result in large-scale loss of forested wetland area and shifts to wetter regimes. The group-selection method applied with small patches (ca. 0.05–0.1 ha covering 20% of stand area) maintained pre-disturbance hydrologic regime and could be used to slowly transition black ash stands to communities with other facultative wetland tree species. However, to be successful, this approach has to be implemented well before EAB infestation to allow for multiple harvests (i.e., to reduce black ash extent) with time between each for development of replanted patches. The effectiveness of this approach in operational settings is still unclear, but regional land management organizations are currently interested in utilizing these findings to address the looming EAB threat.

2.6 Conclusions

Our findings demonstrate clear influence of vegetation structure on ET and associated water table dynamics, highlighting potential consequences of EAB infestation and different management options. With a do-nothing approach, represented by our girdling treatment, EAB-induced tree mortality will likely generate the greatest hydrologic impact due to both reduced canopy transpiration and maintained shading by dead tree boles that limits subcanopy ET compensation. In this situation, elevated water tables and an herbaceous community may take over and persist for many years. The preemptive clearcut option will also likely result in a shift to wetter conditions, but water tables may recover faster than the do-nothing option. The least hydrologically impactful option that we studied was the group selection option (20% removal of black ash overstory), highlighting a potential mitigation strategy. Although the scale of potential disturbance is daunting, our findings and other related work are helping to inform such pre-emptive management actions to reduce EAB impacts on black ash wetlands.

Acknowledgments

This project was funded by the Minnesota Environmental and Natural Resources Trust Fund, the USDA Forest Service Northern Research Station, and the Minnesota Forest Resources Council. Additional funding was provided by the Virginia Tech Forest Resources and Environmental Conservation department, the Virginia Tech Institute for Critical Technology and Applied Science, and the Virginia Tech William J. Dann Fellowship. We gratefully acknowledge the field work and data collection assistance provided by Mitch Slater.

2.7 References

Allen, S. T., Reba, M. L., Edwards, B. L., & Keim, R. F. Evaporation and the sub-canopy energy environment in a flooded forest. *Hydrological Processes*, doi: 10.1002/hyp.11227.

Anderson, M. K., & Nelson, G. (2003). Black ash, Fraxinus nigra Marsh. NRCS plant guide. Natural Resource Conservation Service. http://plants.usda.gov/plantguide/pdf/csfrni.pdf.

Ann, Y., Reddy, K. R., & Delfino, J. J. (1999). Influence of redox potential on phosphorus solubility in chemically amended wetland organic soils. *Ecological Engineering*, 14(1), 169-180.

Arévalo, J. R., DeCoster, J. K., McAlister, S. D., & Palmer, M. W. (2000). Changes in two Minnesota forests during 14 years following catastrophic windthrow. *Journal of Vegetation Science*, 11(6), 833-840.

Armstrong, W., & Drew, M. C. (2002). Root growth and metabolism under oxygen deficiency. Plant roots: the hidden half, 3, 729-761.

Arthur, M. A., Coltharp, G. B., & Brown, D. L. (1998). Effects of best management practices on forest streamwater quality in eastern Kentucky. JAWRA Journal of the American Water Resources Association, 34(3), 481-495.

Aust, W. M., Schoenholtz, S. H., Zaebst, T. W., & Szabo, B. A. (1997). Recovery status of a tupelo-cypress wetland seven years after disturbance: silvicultural implications. Forest Ecology and Management, 90(2-3), 161-169.

Bearup, L. A., Maxwell, R. M., Clow, D. W., & McCray, J. E. (2014). Hydrological effects of forest transpiration loss in bark beetle-impacted watersheds. Nature Climate Change, 4(6), 481-486.

Belyea, L. R., & Clymo, R. S. (2001). Feedback control of the rate of peat formation. Proceedings of the Royal Society of London B: Biological Sciences, 268(1473), 1315-1321.

Bliss, C. M., & Comerford, N. B. (2002). Forest harvesting influence on water table dynamics in a Florida flatwoods landscape. Soil Science Society of America Journal, 66(4), 1344-1349.

Bond, B. J., Jones, J. A., Moore, G., Phillips, N., Post, D., & McDonnell, J. J. (2002). The zone of vegetation influence on baseflow revealed by diel patterns of streamflow and vegetation water use in a headwater basin. Hydrological Processes, 16(8), 1671-1677.

Bosch, J. M., & Hewlett, J. D. (1982). A review of catchment experiments to determine the effect of vegetation changes on water yield and evapotranspiration. Journal of hydrology, 55(1-4), 3-23.

Brinson, M. M., Lugo, A. E., & Brown, S. (1981). Primary productivity, decomposition and consumer activity in freshwater wetlands. Annual Review of Ecology and Systematics, 12, 123-161.

Brolsma, R. J., & Bierkens, M. F. P. (2007). Groundwater–soil water–vegetation dynamics in a temperate forest ecosystem along a slope. Water Resources Research, 43(1).

Brown, A. E., Zhang, L., McMahon, T. A., Western, A. W., & Vertessy, R. A. (2005). A review of paired catchment studies for determining changes in water yield resulting from alterations in vegetation. Journal of hydrology, 310(1), 28-61.

Bubier, J., Costello, A., Moore, T. R., Roulet, N. T., & Savage, K. (1993). Microtopography and methane flux in boreal peatlands, northern Ontario, Canada. Canadian Journal of Botany, 71(8), 1056-1063.

Bubier, J. L., Moore, T. R., Bellisario, L., Comer, N. T., & Crill, P. M. (1995). Ecological controls on methane emissions from a northern peatland complex in the zone of discontinuous permafrost, Manitoba, Canada. Global Biogeochemical Cycles, 9(4), 455-470.

Cappaert, D., McCullough, D.G., Poland T.M., & Siegert N.W. (2005). Emerald ash borer in North America: a research and regulatory challenge. American Entomologist, 51:152–63.

Carvalho, P., Thomaz S., Kobayashi, J. T., & Bini, L. (2013). Species richness increases the resilience of wetland plant communities in a tropical floodplain. Austral Ecology, 38(5), 592-598.

Casey, W. P., & Ewel, K. C. (2006). Patterns of succession in forested depressional wetlands in north Florida, USA. Wetlands, 26(1), 147-160.

Clément, J. C., Shrestha, J., Ehrenfeld, J. G., & Jaffé, P. R. (2005). Ammonium oxidation coupled to dissimilatory reduction of iron under anaerobic conditions in wetland soils. Soil Biology and Biochemistry, 37(12), 2323-2328.

Daly, E., Zinger, Y., Deletic, A., & Fletcher, T. D. (2009). A possible mechanism for soil moisture bimodality in humid-land environments. Geophysical Research Letters, 36(7).

Davis, J. C., Shannon, J. P., Bolton, N. W., Kolka, R. K., & Pypker, T. G. (2016). Vegetation responses to simulated emerald ash borer infestation in Fraxinus nigra dominated wetlands of Upper Michigan, USA. Canadian Journal of Forest Research, 47(3), 319-330.

Dettmann, U., & Bechtold, M. (2016). One-dimensional expression to calculate specific yield for shallow groundwater systems with microrelief. Hydrological Processes, 30(2), 334-340.

Devai, I., & Delaune, R. D. (1995). Formation of volatile sulfur compounds in salt marsh sediment as influenced by soil redox condition. Organic Geochemistry, 23(4), 283-287.

Diamond, A. K., & Emery, M. R. (2011). Black Ash (Fraxinus nigra Marsh.): Local Ecological Knowledge of Site Characteristics and Morphology Associated with Basket–Grade Specimens in New England (USA) 1. Economic Botany, 65(4), 422-426.

Dubé, S., Plamondon, A. P., & Rothwell, R. L. (1995). Watering up after clear-cutting on forested wetlands of the St. Lawrence lowland. Water Resources Research, 31(7), 1741-1750.

Duke, H. R. (1972). Capillary properties of soils-influence upon specific yield. Transactions of the ASAE, 15(4), 688-0691.

Erdmann, G. G., Crow, T. R., Ralph Jr, M., & Wilson, C. D. (1987). Managing black ash in the Lake States.

Ellison, A. M., Bank, M. S., Clinton, B. D., Colburn, E. A., Elliott, K., Ford, C. R., ... & Mohan, J. (2005). Loss of foundation species: consequences for the structure and dynamics of forested ecosystems. Frontiers in Ecology and the Environment, 3(9), 479-486.

Gandhi, K. J. K., Smith, A., Long, R. P., Taylor, R. A. J., & Herms, D. A. (2008). Three-year progression of emerald ash borer-induced decline and mortality in southeastern Michigan. In: Mastro, Victor; Lance, David; Reardon, Richard; Parra, Gregory, comps. Emerald ash borer research and development meeting; 2007 October 23-24; Pittsburgh, PA. FHTET 2008-07. Morgantown, WV: U.S. Department of Agriculture, Forest Service, Forest Health Technology Enterprise Team: 27.

Gill, K., Reinikainen, M., D'Amato, T., Fraver, S., Slesak, R., & Palik, B. (2015). Black ash ecology and management.

van Grinsven, M. J. (2015). Implications of emerald ash borer disturbance on black ash wetland watershed hydrology, soil carbon efflux, and dissolved organic matter composition (Doctoral Dissertation). Michigan Technical University, Houghton, MI.

Healy, R. W., & Cook, P. G. (2002). Using groundwater levels to estimate recharge. Hydrogeology Journal, 10(1), 91-109.

Heffernan, J. B. (2008). Wetlands as an alternative stable state in desert streams. Ecology, 89(5), 1261-1271.

Herms, D. A., & McCullough, D. G. (2014). Emerald ash borer invasion of North America: history, biology, ecology, impacts, and management. Annual Review of Entomology, 59, 13-30.

Huenneke, L. F., & Sharitz, R. R. (1986). Microsite abundance and distribution of woody seedlings in a South Carolina cypress-tupelo swamp. American Midland Naturalist, 328-335.

Jackson, M. B., & Colmer, T. D. (2005). Response and adaptation by plants to flooding stress. Annals of Botany, 96(4), 501-505.

Kéfi, S., Holmgren, M., & Scheffer, M. (2016). When can positive interactions cause alternative stable states in ecosystems?. Functional Ecology, 30(1), 88-97.

Klooster, W. S., Herms, D. A., Knight, K. S., Herms, C. P., McCullough, D. G., Smith, A., ... & Cardina, J. (2014). Ash (Fraxinus spp.) mortality, regeneration, and seed bank dynamics in mixed hardwood forests following invasion by emerald ash borer (Agrilus planipennis). Biological Invasions,16(4), 859-873.

Kozlowski, T. T. (2002). Physiological-ecological impacts of flooding on riparian forest ecosystems. Wetlands, 22(3), 550-561.

Kreuzwieser, J., & Rennenberg, H. (2014). Molecular and physiological responses of trees to waterlogging stress. Plant, cell & environment, 37(10), 2245-2259.

Lindgren, R. (1996). Hydrology and ground-water quality of glacial-drift aquifers, Leech Lake Indian Reservation, north-central Minnesota. U.S. Geological Survey Water-Resources Investigations report 95-4077.

Loheide, S. P., Butler, J. J., & Gorelick, S. M. (2005). Estimation of groundwater consumption by phreatophytes using diurnal water table fluctuations: a saturated-unsaturated flow assessment. Water Resources Research, 41(7).

Looney CE, D'Amato A.W., Palik B.J., & Slesak R.A. (2015). Overstory treatment and planting season affect survival of replacement tree species in emerald ash borer threatened *Fraxinus nigra* forests in Minnesota , USA. Canadian Journal of Forest Research 45:1728–1738.

Looney CE, D'Amato A.W., Fraver S., Palik B.J., & Reinikainen M.R. (2016). Examining the influences of tree-to-tree competition and climate on size-growth relationships in hydric, multi-aged Fraxinus nigra stands. Forest Ecology and Management 375:238-248.

Looney, C. E., D'Amato, A. W., Palik, B. J., Slesak, R. A., & Slater, M. A. (2017). The response of Fraxinus nigra forest ground-layer vegetation to emulated emerald ash borer mortality and management strategies in northern Minnesota, USA. Forest Ecology and Management, 389, 352-363.

LaMalfa, E. M., & Ryle, R. (2008). Differential snowpack accumulation and water dynamics in aspen and conifer communities: implications for water yield and ecosystem function. Ecosystems, 11(4), 569-581.

Marani, M., Silvestri, S., Belluco, E., Ursino, N., Comerlati, A., Tosatto, O., & Putti, M. (2006). Spatial organization and ecohydrological interactions in oxygen-limited vegetation ecosystems. Water Resources Research, 42(6).

McKee, W. H., & McKevlin, M. R. (1993). Geochemical processes and nutrient uptake by plants in hydric soils. Environmental Toxicology and Chemistry, 12(12), 2197-2207.

McKnight, J. S., Hook, D. D., Langdon, O. G., & Johnson, R. L. (1981). Paper 2 Flood Tolerance and related characteristics of trees of the bottomland forests of the southern United States.

McLaughlin, D. L., & Cohen, M. J. (2014). Ecosystem specific yield for estimating evapotranspiration and groundwater exchange from diel surface water variation. Hydrological Processes, 28(3), 1495-1506.

Minnesota Department of Natural Resources (MN DNR). (2003). Field guide to the native plant communities of Minnesota: The Laurentian Mixed Forest Province. Ecological Land Classification Program, Minnesota County Biological Survey, and Natural Heritage and Nongame Research Program. MNDNR St. Paul, MN.

Minnesota Department of Natural Resources (MN DNR). (2010). Guidelines for Managing Sites with Ash to Address the Threat of Emerald Ash Borer on Forestry Administered Lands. http://files.dnr.state.mn.us/forestry/ecssilviculture/policies/guidelinesManagingAshMinnesotaForestryLands-100723.pdf

Molotch, N. P., Blanken, P. D., Williams, M. W., Turnipseed, A. A., Monson, R. K., & Margulis, S. A. (2007). Estimating sublimation of intercepted and sub-canopy snow using eddy covariance systems. Hydrological Processes, 21(12), 1567-1575.

Moore, R., & Wondzell, S. M. (2005). Physical hydrology and the effects of forest harvesting in the Pacific Northwest: a review. JAWRA Journal of the American Water Resources Association, 41(4), 763-784.Nachabe, M. H. (2002). Analytical expressions for transient specific yield and shallow water table drainage. Water Resources Research, 38(10).

van Nes, E. H., & Scheffer, M. (2005). Implications of spatial heterogeneity for catastrophic regime shifts in ecosystems. Ecology, 86(7), 1797-1807.

Palik, B. J., Ostry, M. E., Venette, R. C., & Abdela, E. (2011). Fraxinus nigra (black ash) dieback in Minnesota: regional variation and potential contributing factors. Forest Ecology and Management, 261(1), 128-135.

Palik, B. J., Ostry, M. E., Venette, R. C., & Abdela, E. (2012). Tree regeneration in black ash (Fraxinus nigra) stands exhibiting crown dieback in Minnesota. Forest Ecology and Management, 269, 26-30.

Pataki, D. E., Bush, S. E., Gardner, P., Solomon, D. K., & Ehleringer, J. R. (2005). Ecohydrology in a Colorado River riparian forest: implications for the decline of Populus fremontii. Ecological Applications, 15(3), 1009-1018.

Petrice, T. R., & Haack, R. A. (2011). Effects of cutting time, stump height, and herbicide application on ash (Fraxinus spp.) stump sprouting and colonization by emerald ash borer (Agrilus planipennis). Northern Journal of Applied Forestry, 28(2), 79-83.

Phillips, N. and R. Oren, 2001. Intra- and Inter-Annual Variation in Transpiration of a Pine Forest. Ecological Applications 11:385-396

Poland, T. M., & McCullough, D. G. (2006). Emerald ash borer: invasion of the urban forest and the threat to North America's ash resource. Journal of Forestry, 104(3), 118-124.

Ponnamperuma, F. N. (1984). Effects of flooding on soils. Flooding and plant growth, 9-45.

Pothier, D., Prévost, M., & Auger, I. (2003). Using the shelterwood method to mitigate water table rise after forest harvesting. Forest Ecology and Management, 179(1), 573-583.

R Core Team. 2016. R: A language and environment for statistical computing. R Foundation for Statistical Computing, Vienna, Austria. URL: https://www.R-project.org/

Ridolfi, L., D'Odorico, P., & Laio, F. (2006). Effect of vegetation–water table feedbacks on the stability and resilience of plant ecosystems. Water Resources Research, 42(1).

Ridolfi, L., D'Odorico, P., & Laio, F. (2007). Vegetation dynamics induced by phreatophyte–aquifer interactions. Journal of Theoretical Biology, 248(2), 301-310.

Rodríguez-Iturbe, I., D'Odorico, P., Laio, F., Ridolfi, L., & Tamea, S. (2007). Challenges in humid land ecohydrology: Interactions of water table and unsaturated zone with climate, soil, and vegetation. Water Resources Research, 43(9).

Roy, V., Ruel, J. C., & Plamondon, A. P. (2000). Establishment, growth and survival of natural regeneration after clearcutting and drainage on forested wetlands. Forest Ecology and Management, 129(1), 253-267.

Scheffer, M., Carpenter, S., Foley, J. A., Folke, C., & Walker, B. (2001). Catastrophic shifts in ecosystems. Nature, 413(6856), 591-596.

Skopp, J., Jawson, M. D., & Doran, J. W. (1990). Steady-state aerobic microbial activity as a function of soil water content. Soil Science Society of America Journal, 54(6), 1619-1625.

Slesak, R. A., Lenhart, C. F., Brooks, K. N., D'Amato, A. W., & Palik, B. J. (2014). Water table response to harvesting and simulated emerald ash borer mortality in black ash wetlands in Minnesota, USA. Canadian Journal of Forest Research, 44(8), 961-968.

Soil Survey Staff, Natural Resources Conservation Service, United States Department of Agriculture. Web Soil Survey. Available online at the following link: https://websoilsurvey.sc.egov.usda.gov/. Accessed October 1, 2017.

Sumner, D. M. (2007). Effects of capillarity and microtopography on wetland specific yield. Wetlands, 27(3), 693-701.

Sun, G., Riekerk, H., & Kornhak, L. V. (2000). Ground-water-table rise after forest harvesting on cypress-pine flatwoods in Florida. Wetlands, 20(1), 101-112.

Sun, G., McNulty, S. G., Shepard, J. P., Amatya, D. M., Riekerk, H., Comerford, N. B., ... & Swift, L. (2001). Effects of timber management on the hydrology of wetland forests in the southern United States. Forest Ecology and Management, 143(1), 227-236.

Tamea, S., Muneepeerakul, R., Laio, F., Ridolfi, L., & Rodríguez-Iturbe, I. (2010). Stochastic description of water table fluctuations in wetlands. Geophysical Research Letters, 37(6).

Telander, A. C., Slesak, R. A., D'Amato, A. W., Palik, B. J., Brooks, K. N., & Lenhart, C. F. (2015). Sap flow of black ash in wetland forests of northern Minnesota, USA: hydrologic implications of tree mortality due to emerald ash borer. Agricultural and Forest Meteorology, 206, 4-11.

Titus, J. H. (1990). Microtopography and woody plant regeneration in a hardwood floodplain swamp in Florida. Bulletin of the Torrey Botanical Club, 429-437.

Troendle, C. A., & King, R. M. (1985). The effect of timber harvest on the Fool Creek watershed, 30 years later. Water Resources Research, 21(12), 1915-1922.

United States Department of Agriculture (USDA). (2017). Cooperative Emerald Ash Borer Project: Initial County EAB detections in North America. Accessed on October 1, 2017: http://www.emeraldashborer.info/documents/MultiState_EABpos.pdf

Van de Koppel, J., Wal, D. V. D., Bakker, J. P., & Herman, P. M. (2004). Self-organization and vegetation collapse in salt marsh ecosystems. The American Naturalist, 165(1), E1-E12.

Van Grinsven, M. J., Shannon, J. P., Davis, J. C., Bolton, N. W., Wagenbrenner, J. W., Kolka, R. K., & Grant Pypker, T. (2017). Source water contributions and hydrologic responses to simulated emerald ash borer infestations in depressional black ash wetlands. Ecohydrology.

Veatch, W., Brooks, P. D., Gustafson, J. R., & Molotch, N. P. (2009). Quantifying the effects of forest canopy cover on net snow accumulation at a continental, mid-latitude site. Ecohydrology, 2(2), 115-128.

White, W. N. (1932). A method of estimating ground-water supplies based on discharge by plants and evaporation from soil: results of investigations in Escalante Valley, Utah (Vol. 659). US Government Printing Office.

Wright, J. W., & Rauscher, H. M. (1990). Fraxinus nigra Marsh. black ash. Silvics of North America, 2, 344-347.

Youngquist, M. B., Eggert, S. L., D'Amato, A. W., Palik, B. J., & Slesak, R. A. (2017). Potential Effects of Foundation Species Loss on Wetland Communities: A Case Study of Black Ash Wetlands Threatened by Emerald Ash Borer. *Wetlands*, 1-13

2.8 Supplementary material

Table S2.1 Black ash system soil measurements for Chippewa Forest Sites

	Depth	
Soil Parameter	**0–15 cm**	**15–30 cm**
Bulk Density (g cm^{-3})	0.6 ± 0.4 *p = 0.057*	1.4 ± 0.3, *p = 0.54*
C (Mg ha^{-1})	88.4 ± 34.5 *p = 0.069*	22.8 ± 10.7 *p = 0.046*
N (Mg ha^{-1})	6.4 ± 2.6 *p = 0.94*	1.7 ± 0.9 *p = 0.057*
C:N	14.1 ± 1.6 *p = 0.0069*	14.9 ± 5.2 *p = 0.49*

Data from blocks 1, 2, 3, n = 32. Values are mean ± standard deviation.
ANOVA p-value in italics.

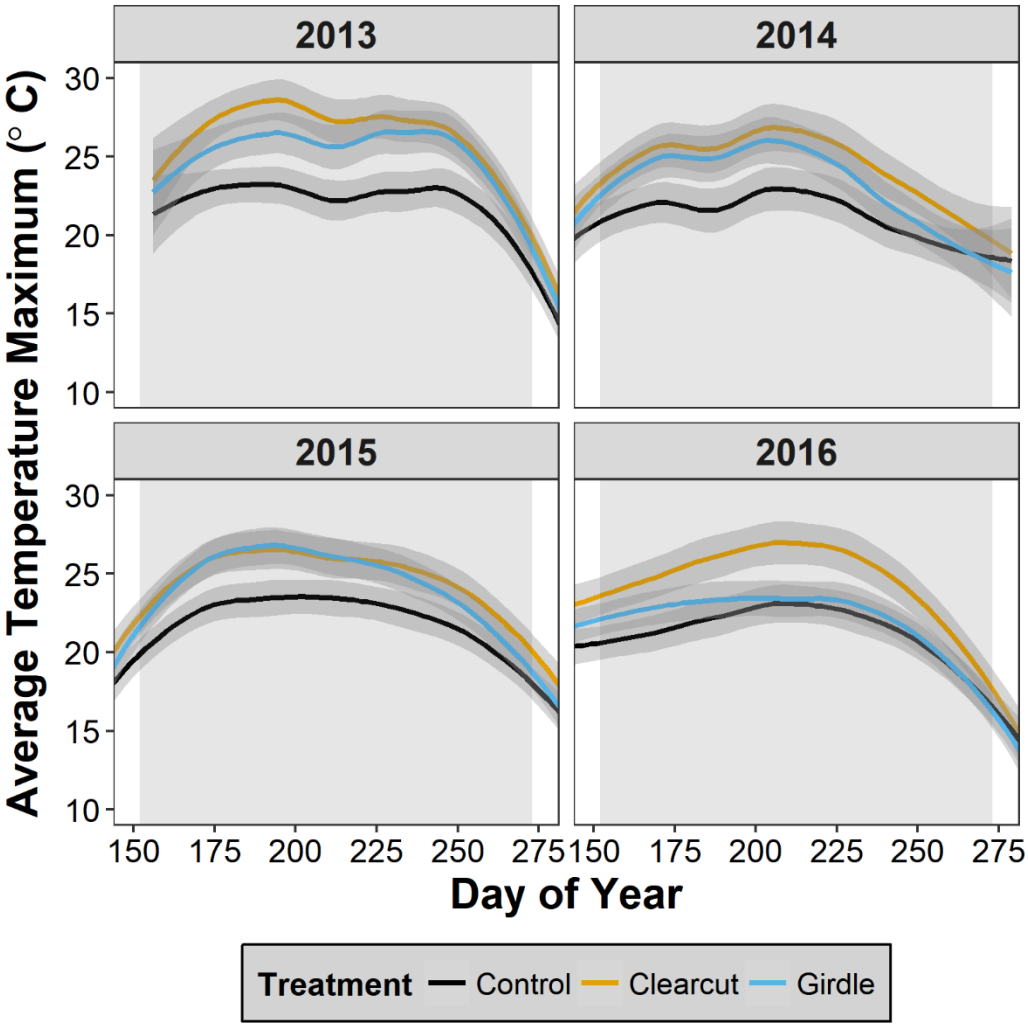

Figure S2.1 Daily maximum temperature comparison among treatments for 2013–2016. Clearcut and girdle treatments experience up to 6 degrees higher maximum daily temperatures than controls for most years except for 2016, where maximum temperatures in girdle treatment are similar to the control treatment. Shading indicates growing season.

CHAPTER 3: A MICROTOPOGRAPHIC SIGNATURE OF LIFE

3.1 Abstract

Microtopography in wetlands can be a visually striking landscape feature. Wetland microtopography also critically influences biogeochemical processes at both the scale of its observation (10^{-2}–10^{2} m^2) and at aggregate scales (10^{2}–10^{4} m^2). However, relatively little is known about how microtopography develops in wetlands or the factors that influence its structure and pattern. For example, wetland vegetation appears to have a strong affinity to elevated microsites, but the degree to which wetland vegetation simply preferentially occupies elevated microsites ("hummocks") *versus* the degree to which wetland vegetation reinforces and maintains these elevated microsites is not clear. Growing research across different ecosystems suggests that such reinforcing processes, or feedback loops, may be common between plants and their environment, and may result in characteristic, self-organized patch features, like hummocks. In this work, we made use of landscape ecology techniques and diagnostics to evaluate the plausibility of plant-environment feedback mechanisms in the maintenance of wetland microtopography. Using a novel terrestrial laser scanning (TLS) dataset, we were able to quantify the sizing and spatial distribution of hummocks in 10 black ash (*Fraxinus nigra* Marshall) wetlands in northern Minnesota, U.S.A. We observed clear elevation bimodality in our wettest sites, indicating microsite divergence into two states: elevated hummocks and base elevation hollows. We coupled the TLS dataset to a three-year water table record and synoptic soil-depth field campaign, and showed that hummock height is largely predicted by mean water table depth, with little-to-no influence of subsurface microtopography on surface microtopography. We further show that hummocks in wetter sites exhibit regular spatial patterning and overdispersion in contrast to hummocks in drier sites, which exhibit random spatial arrangements. We show that hummock size distributions (perimeters, areas, and volumes) are strongly lognormal, and that hummocks exhibit a characteristic patch area of approximately 1 m^2 across sites. Together, these results implicate hummocks in black ash wetlands as self-organized features. Finally, we show that hummocks may be responsible for increased reactive surface area in black ash wetlands by up to 32%, and may also influence surface water dynamics through modulation of specific yield by up to 30%. We suggest that vegetation develops and

maintains hummocks in response to anaerobic stresses from saturated soils, leading to a microtopographic signature of life.

3.2 Introduction

Biota permeate the Earth's surface, exerting direct control on surface processes and topographic features. Although topographic signatures of life at landscape scales remain elusive (Dietrich and Perron 2006), there is clear evidence of a biotic imprint on the land surface at the scale of biota (10^1 m; Lashermes et al. 2007, Roering et al. 2010), attributed to both animal (e.g., 1 m hill structures via burrowing; Gabet et al. 2014) and vegetative actions (e.g., 20–40 cm elevated ridges via organic inputs; Watts et al. 2010). Recently, vegetation's role in affecting critical zone processes and resulting structure has received considerable research attention (Amundson et al. 2007, Reinhardt et al. 2010, Corenblit et al. 2011). However, despite general understanding of the broad, directional effects that vegetation imposes on the critical zone environment (e.g., bedrock weathering and soil development), less is known regarding the reciprocal feedbacks that develop between vegetation and their environment (Pawlik et al. 2016, Brantley et al. 2017). Evidence suggests that some of these feedbacks may lead to reinforced and biotically maintained topographic structure (Eppinga et al. 2008), resulting in diagnostic (micro)topographic fingerprints of plants.

Microtopography, or the small-scale structured variation (10^{-1}–10^0 m) in ground surface height, can be a visually striking landscape signature. Wetland microtopography is particularly well studied, and is observed and detailed in freshwater marshes (Van de Koppel et al. 2006), fens (Sullivan et al. 2008), peat bogs (Nungesser 2003), forested swamps (Bledsoe and Shear 2000), tidal freshwater swamps (Duberstein et al. 2013), and coastal marshes (Stribling et al. 2007). Wetland microtopography is common enough that researchers in disparate systems collectively refer to local high points as "hummocks" and local low points as "hollows". Hollows are more frequently inundated and typically comprise large, flat or concave open spaces, whereas elevated hummocks tend to be dispersed throughout hollows (Nungesser 2003, Stribling et al. 2007). Elevated hummocks, even centimeters taller than adjacent hollows, can provide enough aeration to limit anaerobic stress to vegetation, promoting higher plant abundance and primary production (Strack et al. 2006, Rodríguez-Iturbe et al. 2007, Sullivan et al. 2008). Hence,

by simply changing the relative water table, microtopography inherently affects vegetative composition and growth in wetlands. However, the degree to which wetland vegetation simply preferentially occupies hummocks (sensu Jackson & Caldwell 1996) versus the degree to which wetland vegetation reinforces and maintains its own hummock microtopography and thus preferred environmental conditions is not clear. For example, seedlings may simply fare better on elevated microtopographic features such as downed woody debris or tree-fall mounds (Huenneke & Sharitz 1990). On the other hand, increased vegetation growth and associated organic matter inputs may support hummock expansion. Growing research across different ecosystems suggests that such reinforcing processes, or feedback loops, may be common between plants and their environment, and may result in characteristic, self-organized patch features (Rietkerk and van de Koppel 2008). By quantifying the structure and patterning of these features, we may therefore make process-based inferences about the latent feedback mechanisms (Turner, 2005).

Several diagnostic features implicate feedback mechanisms in the reinforcement and maintenance of landscape patches, like striping of vegetated patches in arid settings or maze-like patterns in mussel beds (Rietkerk and van de Koppel 2008). We suggest that such diagnostic features from landscape ecology are extensible to wetland microtopography, thereby allowing us to assess mechanisms of potential hummock self-organization. For example, multimodal distributions in environmental variables, such as vegetation composition, soil texture, and, in our case, elevation (and see Rietkerk et al. 2004, Eppinga et al. 2008, Watts et al. 2010), indicate patch self-organization (Scheffer and Carpenter 2003). Hypothesized mechanisms for patch self-organization rely on positive feedbacks that support so-called “local facilitation” (Pugnaire et al. 1996), where vegetation improves growth conditions locally by modifying plant-scale soil properties (e.g., soil nutrients, hydraulic conductivity) or structure (elevation), which then leads to greater vegetation growth, further soil modification, and thus reinforced patch expansion. However, this amplifying effect is ultimately constrained and stabilized by compensatory negative feedbacks (e.g., limiting nutrients, canopy competition for light; Rieterk and van de Koppel 2008; Schröder et al. 2005). Such negative feedbacks can limit patch growth both vertically (in the case of elevation; Heffernan et al. 2013) and laterally, constraining patch size. As such, patch size distributions may be used to query the scales at which

coupled positive and negative feedbacks operate. For example, landscapes with a characteristic patch size imply that limits to patch growth operate at local, or patch scales (Manor and Shnerb 2008, von Hardenberg et al. 2010). Such limits to growth result in a distinct absence of very large patches, and a truncation of the patch size distribution, which is modelled with lognormal or exponential functions (Kéfi et al. 2014, Watts et al. 2014). Characteristic patch sizes are also commonly accompanied by regular spatial patterning (Rietkerk et al. 2004), or spatial overdispersion of patches (i.e., uniformity of patch spacing is greater than expected by chance), which further implies local negative feedbacks to patch expansion (Watts et al. 2014). In contrast, patch size distributions may lack a characteristic spatial scale (e.g., Scanlon et al. 2007), which suggests lack of scale-dependent negative feedbacks to patch growth. Presence of very large patches characterize these scale-free patch size distributions, which are frequently modelled with power-law functions (Pascual and Guichard 2005). Here, we extend this inferential theoretical framework and specific diagnostics (multimodality, patch size distributions and patterning) to test predictions concerning the generation and maintenance of wetland microtopography.

Our broad hypothesis is that while there are many mechanisms that may initiate wetland microtopographic variation, structured and persistent (and possibly patterned) wetland microtopography results from self-organizing, reciprocal feedbacks between plant growth and hydrology (Figure 3.1). Microtopographic initiation mechanisms may include direct actions from biota (e.g., burrowing or mounding), indirect actions from biota (e.g., tree falls or preferential litter accumulation), and abiotic events that redistribute soils and sediment (e.g., extreme weather events). However, without reinforcement, or autogenic feedbacks that maintain such variations in soil elevation, this type of microtopography would be unstructured—indistinguishable from the random processes that create it, both vertically and laterally. On other hand, when operated on by autogenic feedbacks, these variations may take on a meaningful structure resulting from ecosystem processes. For example, slightly elevated microsites provide relief from adverse hydrologically induced anaerobic conditions, promoting plant establishment. Plant establishment further leads to increased organic matter or sediment accumulation through several potential mechanisms: 1) increased hummock gross primary productivity

(GPP) from reduced hydrologic stress (Conner 1995, Stribling et al. 2007, Hanan and Ross 2009), 2) sediment/organic floc accumulation around stems, roots, and shoots during periods of inundation (Barry et al. 1996, Peterson and Baldwin 2004), and 3) a directional hydraulic and dissolved nutrient gradient towards hummocks driven by increased evaporation on hummocks relative to hollows, which leads to increased GPP on hummocks (hummock "evapoconcentration"; Rietkerk et al. 2004, Eppinga et al. 2008). Thus, positive feedback loops develop where increased elevation induces greater plant productivity and sediment accumulation, which in turn lead to increased microsite elevation, and so on (top, solid loop in Figure 3.1). These positive feedbacks ultimately induce soil elevation bimodality, where microtopographic features belong either to a stable hummock and stable hollow elevation state (Rietkerk et al. 2004, Eppinga et al. 2008, Watts et al. 2010). Negative feedbacks eventually limit this growth; otherwise, hummocks would have no vertical or lateral limit. Vertical negative feedbacks may result from increased decomposition in hummocks as hummocks grow vertically and their soils become more aerobic (Courtwright and Findlay 2011; bottom, dashed loop in Figure 3.1). Lateral negative feedbacks may result from canopy competition for light among trees located on hummocks, or from competition for nutrients among hummocks (Rietkerk et al. 2004), leading to characteristic patch sizes and spatial overdisperion of patches.

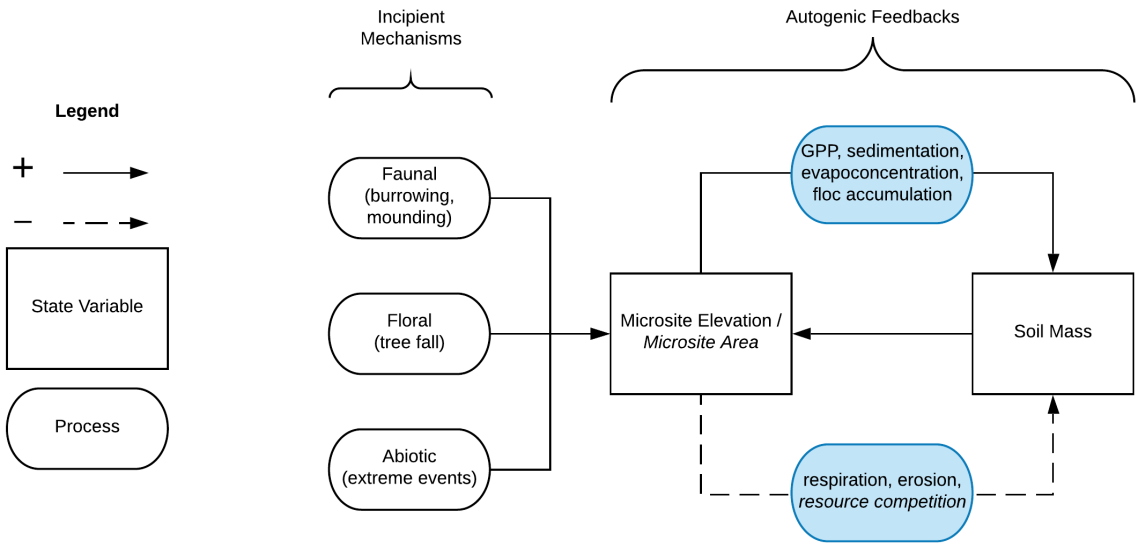

Figure 3.1 Conceptual model for autogenic hummock maintenance in wetlands. Incipient mechanisms create small-scale variation in soil elevation that is amplified by autogenic feedbacks, which grow and maintain elevated hummock structures. Solid lines indicate positive feedback loops and dashed lines indicate negative feedback loops. Font in italics refer to feedback processes hypothesized to only affect lateral hummock extent (thus hummock area), whereas non-italic font indicates mechanisms that affect both vertical and lateral hummock extent. Processes in blue indicate that these mechanisms are influenced by hydrology.

In wetlands, the posited positive and negative feedback loops that grow and maintain hummocks are likely under the strong influence of both site- and hummock-scale hydrology (blue shading in Figure 3.1). Consequently, we hypothesize that soil wetness is predictive of the strength of the autogenic processes that structure wetland microtopography. For example, drier sites may obviate the feedback loop between elevation and productivity/decomposition (*cf.* Watts et al. 2010), because soils are nearly always unsaturated and aerobic. Additionally, dissolved solutes may less easily flow along directional hydraulic routes in unsaturated soils compared to unsaturated soils, reducing the evapoconcentration effect. In contrast, we predict that in wetter sites both the elevation-productivity and evapoconcentration feedbacks will be more important, and will therefore lead to more clear and structured hummock-hollow features. In this framework, we view wetland hummocks as self-organizing, created autogenically by bidirectional feedbacks among vegetation, soil, and hydrology. Although our broad hypothesis has previously been tested in non-forested peatland environments (Belyea and Baird 2006, Eppinga et al. 2009), we seek here to expand and more directly quantify our

understanding of the pattern and development of wetland microtopography in forested-wetland systems with a focus on hydrologic controls.

A potential null hypothesis of self-organizing, autogenic wetland microtopography is that hummocks and hollows are simply just reflections of similar undulations in some underlying soil horizon. This null hypothesis, however, is easily tested through co-located measurements of surface soil horizon depth and underlying soil horizon topography. We would fail to reject this null hypothesis if we observe no correlation (slope = 0) between these variables, where surface soil depth is constant and thus surface microtopography is a reflection of subsurface microtopography. However, if we observe deviations from this no-correlation case, then we may reject this null hypothesis. For example, we may observe a completely negative correlation (slope = -1) between surface soil depth and subsurface elevation, indicating a completely flat surface over a varying subsurface due to soil accumulation. Further still, deviations above this -1:1 line imply surface elevations above a flat surface, indicating variable surface elevations unexplained by subsurface elevation. This method therefore provides a litmus test of this first-order null hypothesis.

In this study, we assessed our self-organizing hummocks hypothesis by evaluating wetland soil elevations, hummock properties and patterning, and hydrologic regimes in black ash forested wetlands in northern Minnesota, U.S.A. To do so, we characterized microtopography with a 1-cm spatial resolution dataset from a terrestrial laser scanning campaign. We also evaluated subsurface mineral layer topography and daily water tables to determine the extent that that these influenced observed surface microtopography. Specifically, we tested the following predictions:

1. Elevation will exhibit a bimodal distribution within black ash wetlands. A bimodal distribution of microtopography requires sharp boundaries between hummocks and hollows (Eppinga et al. 2009), which are indicative of positive feedbacks between biota and hummock growth (top feedback in Figure 3.1), and therefore suggest biotically controlled hummock development.
2. Surface soil depth will exhibit a -1:1 relationship with underlying mineral layer topography, but hummocks will plot above this line. In other words, hummocks

and hollows are not simply reflections of the ups and downs of subsurface layers, but instead reflect surface-level self-organization of soil elevation.

3. Hummock heights will be positively correlated to site wetness. This prediction follows from the idea that hummocks are self-organizing, but only organize in response to elevated water tables. This prediction implies that drier sites may exhibit no microtopography because average water tables are low enough to where the feedbacks that support hummock expansion do not develop. Moreover, within-site variability in hydrology may also result in within-site variability in hummock heights.
4. Hummocks will be regularly spatial patterned. Regular spatial patterning requires coupling of scale-dependent positive and negative feedbacks (Rietkerk and van de Koppel 2008). Overdispersion and regular hummock spatial patterning may therefore arise when the increased local productivity on hummocks (i.e., local positive feedback as predicted in the previous hypothesis) inhibits the formation of hummocks at some distance away (e.g., canopy light and/or nutrient competition among trees on hummocks). However, we predict that regular patterning will only be clear in wetter sites with more pronounced microtopography (see 3 above).
5. Cumulative distribution (cdf) of individual hummock areas will correspond to a family of truncated distributions (e.g., exponential or lognormal). This type of patch-size distribution implies a characteristic patch size, and tends to emerge for patches that grow with local facilitation but also a local constraint that limits their maximum size (e.g., resource competition). We hypothesized that light and nutrients would be limiting to plant growth in these systems, both of which may act at the scale of hummocks, thus leading to truncated hummock patch size distributions.

3.3 Methods

3.3.1 Site descriptions

To test our hypotheses, we investigated ten black ash (*Fraxinus nigra*) wetlands of varying size and hydrogeomorphic landscape position in northern Minnesota, U.S.A. (Figure 3.2; Table 3.1). Thousands of meters of sedimentary rocks overlay an Archean

granite bedrock geology in this region. Study sites are located on a glacial moraine landscape (400–430 m ASL) that is flat to gently rolling, with the black ash wetlands found in lower landscape positions that commonly grade into aspen or pine-dominated upland forests. The climate is continental, with mean annual precipitation of 700 mm and a mean growing season (May–October) temperature of 14.3°C (mean annual temperature = -1.1°C – 4.8°C; WRCC 2019). Annual precipitation is approximately two-thirds rain and one-third snowfall. Potential ET (PET) is approximately 600–650 mm per year (Sebestyen et al. 2011). Detailed site histories were unavailable for the ten study wetlands, but silvicultural practices in black ash wetlands have been historically limited in extent (D'Amato et al. 2018). Based on the available information (e.g., Erdmann et al. 1987, Kurmis and Kim 1989), we surmise that our sites are late successional or climax communities and have not been harvested for at least a century.

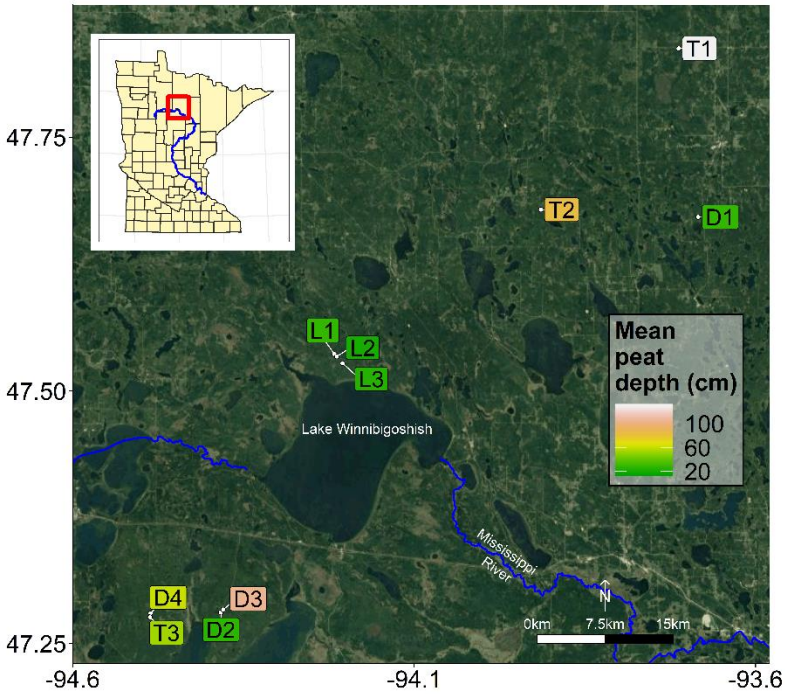

Figure 3.2 Map of black ash wetland sites. Sites are colored by their mean organic horizon depth.

As part of a larger effort to understand and characterize black ash wetlands (D'Amato et al. 2018), we categorized and grouped each wetland by its hydrogeomorphic characteristics as follows: 1) depression sites ("D", n = 4) characterized by a convex, pool-type geometry with geographical isolation from other surface water bodies and

surrounded by uplands, 2) lowland sites ("L", n = 3) characterized by extensive wetland complexes on flat, gently sloping topography, and 3) transition sites ("T", n = 3) characterized as flat, linear boundaries between uplands and black spruce (*Picea nigra*) bogs (Figure 3.2). The three lowland sites were control plots from a long-term experimental randomized block design on black ash wetlands (blocks 1, 3, and 6; Slesak et al. 2014, Diamond et al. 2018). We considered hydrogeomorphic variability among sites an important criterion, as it allowed us to capture expected differences in hydrologic regime and thus differences in the strength of our predicted control on microtopographic generation (Figure 3.3). Ground slopes across sites ranged from 0–1%. Hydrology of black ash wetlands is typically dominated by precipitation and evapotranspiration (ET), with shallow water tables following a common annual trajectory of late-spring/early-summer inundation followed by summer drawdown from ET (Slesak et al. 2014, Diamond et al. 2018). However, the degree of drawdown depends on local hydrogeomorphic setting; we observed considerably wetter conditions at depression sites and transition sites than lowland sites.

Table 3.1 Site information for ten black ash study wetlands

Site	Latitude	Longitude	Elevation (m ASL)	Size (ha)	Average organic horizon depth (cm)
D1	47.67168	-93.68438	447	5.697	28.9 ± 9.1
D2	47.28097	-94.38353	425	6.499	27.7 ± 11.3
D3	47.28380	-94.37992	429	6.062	105.3 ± 32.2
D4	47.28021	-94.48627	442	0.491	60.6 ± 22.1
L1	47.53685	-94.21786	403	2.191	28.8 ± 9.5
L2	47.53444	-94.21320	391	6.845	19.6 ± 7.2
L3	47.52744	-94.20573	394	1.455	24.5 ± 10.1
T1	47.83737	-93.71288	424	15.659	129.4 ± 3.6
T2	47.67887	-93.91441	447	8.618	84 ± 26.2
T3	47.27623	-94.48689	432	1.938	53.6 ± 28.5

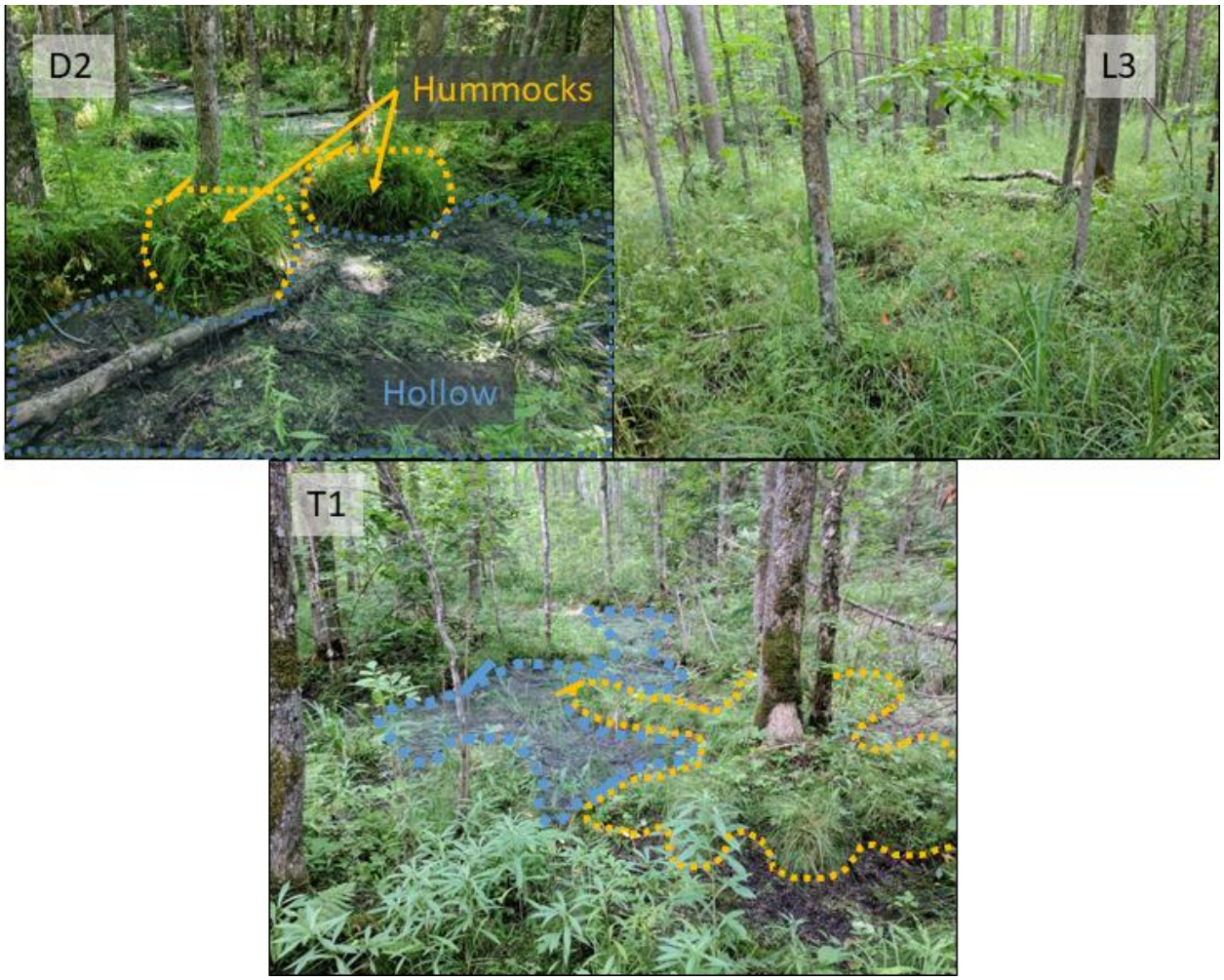

Figure 3.3 Photos of observed black ash wetland microtopography from a site in each hydrogeomorphic category. Hummocks are outlined in yellow/orange dashed lines, and hollows are outlined and lightly shaded in blue. Lowland site hummocks and hollows are difficult to discern in summer time due to heavy understory cover and are additionally less pronounced, so they are not drawn here.

3.3.1.1 Vegetation

Overstory vegetation at the ten sites is dominated by black ash. At the lowland sites, other overstory species were negligible, but at the depression and transition sites there were minor cohorts of northern white-cedar (*Thuja occidentalis* L.), green ash (*Fraxinus pennsylvanica* Marshall), red maple (*Acer rubrum* L.), yellow birch (*Betula alleghaniensis* Britt.), balsam poplar (*Populus balsamifera* L.), and black spruce (*Picea mariana* Mill. Britton). Still, except at one transition site (T1), where northern white cedar represented a significant overstory component, black ash represented over 75% of overstory cover across all sites. Black ash also made up the dominant midstory

component in each site, but was regularly found with balsam fir (*Abies balsamea* L. Mill.) and speckled alder (*Alnus incana* L. Moench) in minor components, and greater abundances of American elm (*Ulmus Americana* L.) at lowland sites. Black ash stands are commonly highly uneven-aged (Erdmann et al. 1987), with canopy tree ages ranging from 130–232 years, and stand development under a gap-scale disturbance regime (D'Amato et al. 2018). Black ash are also typically slow-growing, achieving heights of only 10–15 m and diameters at breast height of only 25–30 cm after 100 years (Erdmann et al. 1987).

3.3.1.2 Soils

Soils in black ash wetlands in this region tend to be Histosols characterized by deep mucky peats underlain by silty clay mineral horizons, although there were clear differences among site groups (NRCS 2019). Depression sites were commonly associated with Terric haplosaprists of the poorly drained Cathro or Rifle series with O horizons approximately 30–150 cm deep (Table 3.1). Lowland sites were associated with lowland Histic inceptisols of the Wildwood series, which consist of deep, poorly drained mineral soils with a thin O horizon (< 10 cm) underlain by clayey till or glacial lacustrine sediments. Transition sites typically had the deepest O horizons (> 100 cm), and were associated with typic haplosaprists of the Seelyeville series and Typic haplohemists (NRCS 2019). Both depression and transition sites had much deeper O horizons than lowland sites, but depression site organic soils were typically muckier and more decomposed than more peat-like transition site organic soils.

3.3.2 TLS

3.3.2.1 Data collection

To characterize the microtopography of our sites, we conducted a synoptic terrestrial laser scanning (TLS) campaign from October 20–24, 2017. We chose this period to ensure high-quality TLS acquisitions, as it coincided with the time of least vegetative cover and the least likelihood for inundated conditions. During scanning, leaves from all deciduous canopy trees were off, grasses had largely senesced, and standing water was present at portions of only three of the sites. Where standing water

was present, it was typically less than 10 cm deep and constrained to small pools (*ca*. 0.5–2 m^2) dispersed across the site.

We used a Faro Focus 120 3D phase-shift TLS (905 nm λ) to scan three randomly established, non-overlapping 10 m diameter sampling plots at each site (see Stovall et al. [in revision] for exact methodological details). For each site, we merged our plot-level TLS data to a single 900 m^2 site-level point-cloud using 30 strategically placed and scanned 7.62 cm radius polystyrene registration spheres set atop 1.2 m stakes. We further referenced each site to a datum located at each site's base well elevation.

To validate the eventual TLS surface model products, we installed sixty 2.54 cm radius spheres on fiberglass stakes exactly 1.2 m above ground surface at each site. Hence, for each site we knew the exact elevation (i.e., 1.2 m below a scanned sphere) of 60 points in space. We placed 39 (13 at each plot) of these validation spheres at points according to a random walk sampling design, and placed 21 (7 at each plot) of these validation spheres on distinctive hummock-hollow transitions. We placed the 1.2 m tall validation spheres approximately plumb to reduce errors due to horizontal misalignment.

We processed the point clouds generated from the TLS sampling campaign to generate two products: 1) site-level 1 cm resolution ground surface models, and 2) site-level delineations of hummocks and hollows. The details and validation of this method are described completely in Stovall et al. (in review), but a brief outline is provided here.

3.3.2.2 Surface model processing and validation

For each site, we first filtered the site-level point-clouds in the CloudCompare software (Othmani et al. 2011) and created an initial surface model with the absolute minima in a moving 0.5 cm grid. We removed tree trunks from this initial surface model using a slope analysis and implemented a final outlier removal filter to ensure all points above ground level were excluded. Our final site-level surface models meshed the remaining slope-filtered point cloud using a local minima approach at 1 cm resolution. We validated this final 1 cm surface model using 60 validation spheres per site.

Before we analyzed surface models from each site, we first detrended sites that exhibited site-scale elevation gradients (e.g., 0.02 cm m^{-1}). These gradients may obscure analysis of site-level relative elevation distributions (Planchon et al. 2002), and our hypothesis relates to relative elevations of hummocks and hollows and not their absolute

elevations. We chose the best-detrended surface model based on adjusted R^2 values and observation of resultant residuals and elevation distributions from three options: no detrend, linear detrend, and quadratic detrend (P. Five sites were detrended: L2 was detrended with a linear model, and D1, D2, D4, and T1 were detrended with quadratic models. We then subsampled each surface model to 10,000 points to speed up processing time as original surface models were approximately 100,000,000 points. We observed no significant difference in results from the original surface model based on our subsampling routine.

3.3.2.3 Hummock delineation and validation

We classified the final surface model into two elevation categories: hummocks and hollows. We first filled gaps in the original surface model (e.g., where the TLS scans did not get returns) with a buffered model using the R package, *lidR* (Roussel and Auty, 2018). Because of their broader extent and simpler features, we first classified hollows using a combination of normalized elevation and slope thresholds: hollows have less than average elevation and less than average slope. This combined elevation and slope approach avoided confounding hollows with the tops of hummocks (tops of hummocks are typically flat or shallow sloped). We used the remaining point cloud after hollow classification and removal as our domain of potential hummocks.

We used this potential hummock domain to segment hummocks into individual point clouds and thereby create a hummock-level surface model for each site. We first used the local maxima (Roussel and Auty, 2018) of a moving window to identify potential microtopographic structures for segmentation. The local maxima served as "seed points" from which we then applied a modified watershed delineation approach (Pau et al. 2010). The watershed delineation is an inverse watershed function, inverting the elevation values in the point cloud and finding the edge of the "watershed", which in our case was hummock edges. The defined boundary was used to clip and segment an identified hummock area into an individual hummock point cloud surface model.

For each delineated hummock within each site, we calculated perimeter length, total area, volume, and height distributions relative both to local hollow datum and to a site level datum. To calculate area, volume, and perimeter, we first converted hummock point clouds into rasters with a resolution of 1 cm^2. This method creates a horizontal

projection of the original 3D point cloud with constant pixel resolution. To calculate area, we summed total number of points in each hummock raster multiplied by the model resolution (1 cm^2). We calculated volume was using the same method as area, but further multiplied by each points' height above the hollow surface. Perimeter was conservatively estimated by converting our raster-based hummock features into polygons and extracting the edge length from each hummock. We estimated side hummock area (analogous to the surface area of a cylinder without a top or bottom) by multiplying the perimeter of each hummock by its 20th percentile height, which we determined to be a conservative representation of the average height around the perimeter of the hummock.

To validate the hummock delineation, we compared manually delineated and automatically delineated hummock size distributions at one depression site (D2) and one transition site (T1), both with clearly defined hummock features. We omitted using a lowland site for validation because none of these sites had obvious hummock features that we could manually delineate with confidence. We manually delineated hummocks for the D2 and T1 sites with a qualitative visual analysis of raw TLS scans using the clipping tool in CloudCompare (2018). We relied on area, perimeter, and volume estimates for the comparison and tested for significant differences in the manual and automatic hummock segmentations using a two-tailed t-test for unequal variances and a Kolmogorov-Smirnov test.

After the automatic delineation procedure and subsequent validation, we performed a data cleaning procedure by manually inspecting outputs in the CloudCompare software. We eliminated clear hummock mischaracterization that was especially prevalent at the edges of sites, where point densities were low. We also excluded downed woody debris from further hummock analysis because, although these features may serve as nucleation points for future hummocks, they are not traditionally considered hummocks and their distribution does not relate to our broad hypotheses. Finally, we excluded delineated hummocks that were less than 0.1 m^2 in area because we did not observe hummocks less than this size during our field visits. This delineation and manual cleaning process yielded point clouds of hummocks and hollows for every site that could be further analyzed.

3.3.3 Field data collection

3.3.3.1 Mineral layer depth measurements

To quantify the control that underlying mineral layer microtopography has on surface microtopography, we conducted synoptic measurements of mineral layer depth and thus organic soil thickness at each site. Within each of the 10 m diameter plots used for TLS at each site, we took 13 measurements (co-located with the randomly established validation spheres) of depth to mineral layer using a steel 1.2 m rod. At each point the steel rod was gently pushed into the soil with consistent pressure until resistance was met – we performed this resistance test twice at each point and recorded the average depth until resistance (resolution = 1 cm) as the depth to mineral layer. At nearly every point, there was a clear difference in resistance when a mineral layer was reached. In cases where it was unclear whether the steel rod reached a mineral layer (e.g., hitting a tree root), three measurements were taken in the surrounding 50 cm region and averaged. At each measurement point, we placed an orange survey flag for future comparison and replication. Later, we tied each of these depth-to-mineral-layer measurements with a soil elevation based on TLS data and the site-level datum (i.e., elevation at the base of each site's well, see Data collection 3.3.2.1).

3.3.3.2 Hydrology

To address our hypothesis that hydrology is a controlling variable of microtopographic expression in black ash wetlands, we instrumented all 10 sites to monitor water level dynamics and continuous precipitation. Three sites (L1, L2, and L3; Slesak et al. 2014) were instrumented in 2011 and seven in June 2016 following the same protocols. At each site, we placed a fully-slotted observation well (schedule 40 PVC, 2-inch diameter, 0.010-inch-wide slots) at approximately the lowest elevation, although at the flatter L sites, wells were placed at the approximate geographic center of each site. We instrumented each well with a high-resolution total pressure transducer (HOBO U20L-04, resolution = 0.14 cm, average error = 0.4 cm) to record water level time series at 15-minute intervals. We dug each well with a hand auger to a depth associated with the local clay mineral layer and did not penetrate the mineral layer, which ranged from 30 cm below the soil surface to depths greater than 200 cm. We then backfilled each well with a clean, fine sand (20-40 grade). At each site, we also placed a dry well with the same

pressure transducer model to measure temperature-buffered barometric pressure and frequency for barometric pressure compensation (McLaughlin and Cohen 2011). We also placed five tipping-bucket rain gages equipped with high-resolution data loggers (HOBO UA-003-64 Pendant, resolution = 0.254 mm) in open spaces within 1 km of the seven well locations.

3.3.4 Data analysis

3.3.4.1 Hydrology

We calculated simple hydrologic metrics based on the three years of water table data for each site. For each site, we calculated the mean and variance of water table elevation relative to ground surface at the well. A positive water table value indicates that the water table is above the soil surface (inundated conditions), and a negative water table indicates that the water table is below the soil surface. We also calculated the average hydroperiod of each site by counting the number of days that the mean daily water table was above the soil surface at the well each year, and averaging across years.

3.3.4.2 Elevation distributions

Our first line of inquiry was to evaluate the general spatial distribution of elevation at each site. We first calculated site-level omni-directional and directional (0°, 45°, 90°, 135°) semivariograms using the *gstat* package in R (Pebesma 2004 and Gräler 2016). We calculated directional variograms to test for effects of anisotropy (directional dependence) of elevation. Semivariogram analysis is regularly used in spatial ecology to determine spatial correlation between measurements (Ettema and Wardle 2002). The sill, which is the horizontal asymptote of the semivariogram, is approximately the total variance in parameter measurements. The nugget is the semivariogram y-intercept, and it represents the parameter variance due to sampling error or the inability of sampling resolution to capture parameter variance at small scales. The larger the difference between the sill and the nugget (the “partial sill”), the more spatially predictable the parameter. If the semivariogram is entirely represented by the nugget (i.e., slope = 0), the parameter is randomly spatially distributed. The semivariogram range is the distance where the semivariogram reaches its sill, and it represents the spatial extent (patch size) of heterogeneity, beyond which data are randomly distributed. When spatial dependence

is present, semivariance will be low at short distances, increase for intermediate distances, and reach its sill when data are separated by large distances. We used detrended elevation models for this analysis to assess more directly the importance of microtopography on elevation variation as opposed to having it obscured by site-level elevation gradients. From these semivariograms we calculated the best-fit semivariogram model among exponential, Matérn, or Matérn with Stein parameterization model forms (Minasny and McBratney 2005). We also extracted semivariogram nuggets, ranges, sills, and partial sills.

Our second line of inquiry was to evaluate the degree of elevation bimodality in these systems, which is indicative of a positive feedback between hummock growth and hummock height (Eppinga et al. 2008). Based on the classification into hummock or hollow from our delineation algorithm, we plotted site-level detrended elevation distributions for hummocks and hollows and determined a best-fit Gaussian mixture model with Bayesian Information Criteria (BIC) using the *mclust* package (Scrucca et al. 2016) in R (R Core Team 2018), which uses an expectation-maximization algorithm. Mixture models were allowed to have either equal or unequal variance, and were constrained to a comparison of bimodal versus a unimodal mixture distribution.

3.3.4.3 Subsurface topographic control on microtopography

We assessed the importance of mineral layer microtopography on soil surface microtopography by comparing the depth-to-mineral-layer measurements with the soil surface elevation TLS measurements. We first calculated the elevation of the mineral layer relative to each site-level datum by subtracting the depth-to-mineral-layer measurement from its co-located soil elevation measurement estimated from the TLS campaign. We then plotted the depth-to-mineral-layer measurement (hereafter referred to as “organic soil thickness”) as a function of this mineral layer elevation, noting which points were on hummocks or hollows as determined from the TLS delineation algorithm. We fit linear models to these points and compared the regression slopes to the expected slopes from: 1) a scenario where surface microtopography is simply a reflection of subsurface microtopography (slope = 0, or constant organic soil thickness), and 2) a scenario of flat soil surface where organic soil thickness negatively corresponds to varying mineral layer elevation (slope = -1, or varying soil thickness). Again, the first

observation would suggest that surface microtopography mimics subsurface microtopography, whereas the second would suggest organic matter/surface soil accumulation and smoothing over a varying subsurface topography. Observations above the -1:1 line would indicate surface processes that increase elevation above expectations for a flat surface.

3.3.4.4 Hydrologic controls on microtopography

To test our hypothesis that hydrology is a broad, site-level control on hummock height, we first regressed site mean hummock height against site mean daily water table. We also conducted a within-site regression of individual hummock heights against their local mean daily water table. To do so we first calculated a local relative mean water table for each delineated hummock location by subtracting the elevation minimum of the hummock (i.e., the elevation at the base of the hummock) from the site-level mean water table. This calculation assumes that the water table is flat across the site, which is likely valid for the high permeability organic soils at each site and relatively small areas that we assessed. This within-site regression allowed us to understand more local-scale controls on hummock height.

3.3.4.5 Hummock spatial distributions

To test whether there was regular spatial patterning of hummocks at each site, we compared the observed distribution of hummocks against a theoretical distribution of hummocks subject to complete spatial randomness (CSR) with the R package *spatstat* (Baddeley et al. 2015). We first extracted the centroids and areas of the hummocks from the hummock delineation and created a marked point pattern of the data. Using this point pattern, we conducted a nearest-neighbor analysis (Diggle 2002), which evaluates the degree of dispersion in a spatial point process (i.e., how far apart on average hummocks are from each other). If hummocks are on average further apart (using the mean nearest neighbor distance, μ_{NN}) compared to what would be expected under CSR (μ_{exp}), the hummocks are said to be overdispersed and subject to regular spacing; if hummocks are closer together than what CSR predicts, they are said to be underdispersed and subject to clustering. We compared the ratio of μ_{NN} and μ_{exp}, where values greater than 1 indicate overdispersion and values below 1 indicate clustering, and calculated a z-score (z_{ANN}) and subsequent p-value to evaluate the significance of overdispersion or clustering

(Diggle 2002, Watts et al. 2014). We computed the z-score from the difference between μ_{NN} and μ_{exp} scaled by the standard error. We also evaluated the probability distribution of observed nearest neighbor distances to visualize further the dispersion of wetlands in the landscape.

3.3.4.6 Hummock size distributions

To test the prediction that hummock sizes are constrained by patch-scale negative feedbacks, we plotted site-level rank frequency curves (inverse cumulative distribution functions) for hummock perimeter, area, and volume. These curves trace the cumulative probability of a hummock dimension (perimeter, area, or volume) being greater than or equal to a certain value ($P[X \geq x]$). We then compared best-fit power ($P[X \geq x] = \alpha X^{\beta}$), log-normal ($P[X \geq x] = \beta \ln(X) + \beta_0$), and exponential ($P[X \geq x] = \alpha e^{\beta X}$) distributions for these curves using AIC values. Power-scaling of these curves occurs where negative feedbacks to hummock size are controlled at the landscape-scale (i.e., hummocks have equal probability to be found at all size classes). Truncated scaling of these curves, as in the case of exponential or lognormal distributions, occurs when negative feedbacks to hummock size are controlled at the patch-scale (Scanlon et al. 2007, Watts et al. 2014).

3.4 Results

3.4.1 TLS

A complete description of the performance and validation of the TLS methods and hummock delineation are provided in Stovall et al. (in revision), but a concise presentation of the results is provided here.

3.4.1.1 Surface model performance

Validation of surface models using the validation spheres indicated that surface models were precise (RMSE = 3.67 ± 1 cm) and accurate (bias = 1.26 ± 0.1 cm) across all sites (Stovall et al. in revision). The gently sloping lowland sites (L) had substantially higher RMSE and bias than the transition (T) and depression (D) sites. The relatively high error of lowland site validation points resulted from either low point density or a complete absence of LiDAR returns. We observed overestimation of the surface model when TLS scans were unable to reach the ground surface, leading to the greatest overestimations in sites with dense grass cover (lowland sites). Overestimation was also

common in locations with no LiDAR returns, such as small hollows, where the scanner's oblique view angle was unable to reach. Nonetheless, examination of the surface models indicated clear ability of the TLS to capture surface microtopography (Figure 3.4).

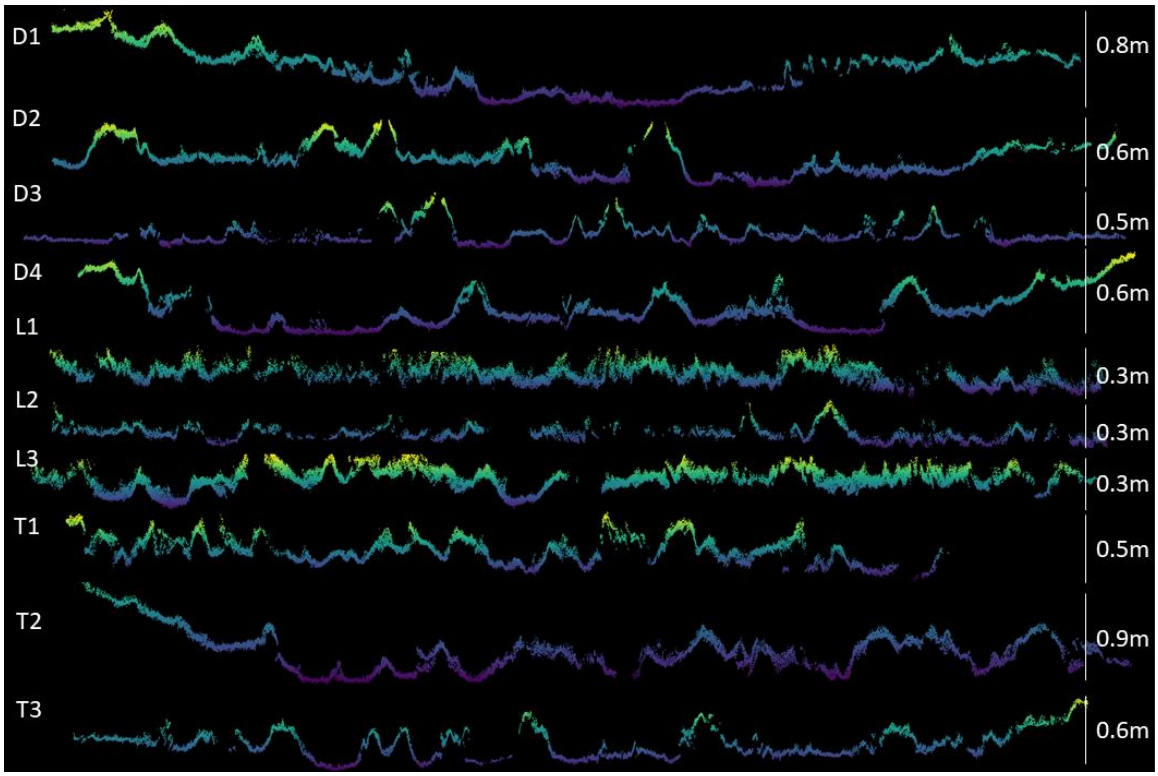

Figure 3.4 Example surface model profiles from each site with scales on the left (5:1 scaling in z:x). Hummocks are clearly visible in most sites.

3.4.1.2 Hummock delineation performance

Hummocks delineated from our algorithm were generally consistent in distribution and dimension with manually delineated hummocks. However, the automatic delineation located hundreds of small (<0.1 m^2) "hummock" features that were not captured with manual delineation, which we attribute to our detrending procedure. We did not consider automatically delineated hummocks less than 0.1 m^2 in further analyses, as we did not observe hummocks smaller than this in the field (see 3.3.2.3). Both area and volume size distributions from the manual and automatic delineations were statistically indistinguishable for both t-test (p-value = 0.84 and 0.51, respectively) and Kolmogorov-Smirnov test (p-value = 0.40 and 0.88, respectively). Automatically delineated hummock area, perimeter:area, and volume estimates had 23%, 19.6%, and 24.1% RMSE, respectively, and the estimates were either unbiased or slightly negatively biased (-9.8 %,

0.2 %, and -11.9 %, respectively). We consider these errors to be well within the range of plausibility, especially considering the uncertainty involved in manual delineation of hummocks, both in the field and on the computer. Final delineations showed clear visual differences among site types in the spatial distributions of hummocks (Figure 3.5).

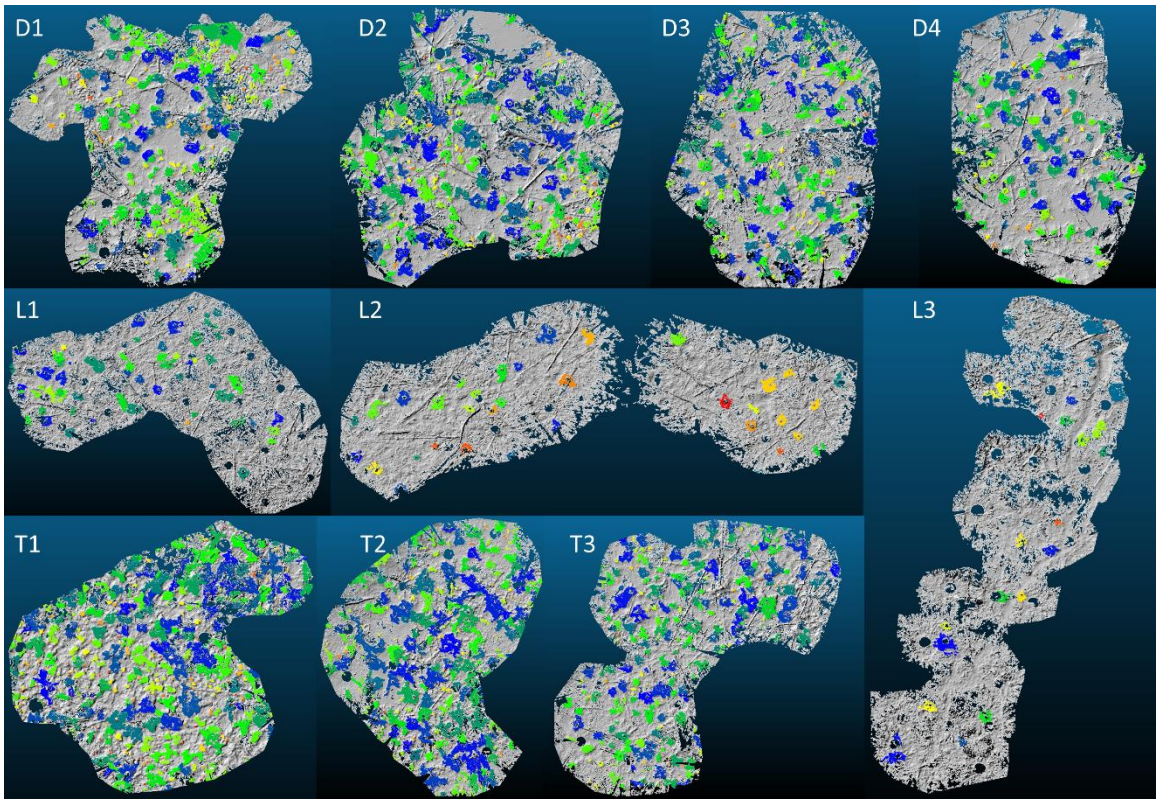

Figure 3.5 Automatically delineated hummocks for every site with hill-shaded surface models in the background. Hummocks are colored in each site by a unique identifier. Although some hummocks have similar colors to their neighbors indicating that they are the same hummock, if they are separated by grey space, they are unique.

3.4.2 Hydrology

Hydrology varied across sites, but largely corresponded to hydrogeomorphic categories (Table 3.2). Depressions sites were the wettest sites (mean daily water table = -0.010 m), followed by transition sites (-0.039 m), and lowland sites (-0.324 m). Lowland sites also exhibited significantly more variability in water table than transition or depression sites, whose water tables were consistently within 0.4 m of the soil surface. Although lowland sites exhibited greater water table drawdown during the growing season, they were able to rapidly re-wet after rain events.

Table 3.2 Daily water table summary statistics for black ash study wetlands

Site	Mean (m)	Median (m)	Standard deviation (m)	Mean hydroperiod (d)
D1	0.012	0.088	0.179	105
D2	-0.098	0.042	0.156	96
D3	0.053	0.143	0.196	117
D4	-0.008	0.003	0.151	77
L1	-0.255	-0.046	0.462	67
L2	-0.346	-0.046	0.543	77
L3	-0.370	-0.076	0.502	61
T1	-0.001	0.034	0.125	105
T2	-0.048	0.044	0.202	101
T3	-0.069	0.016	0.217	84

3.4.3 Elevation distributions

During field sampling, we observed distinct differences in microtopography among site categories. Depression sites were dominated by hollow features, which were punctuated with hummocks associated with black ash trees. Transition sites were microtopographically similar to depression sites, but tended to have more of their area covered with hummocks. Transition site hummocks were also more regularly occupied by canopy species other than black ash, most commonly northern white-cedar, and hummocks were often covered entirely by moss species, especially *Sphagnum spp.* Lowland sites had considerably less variability in microtopography than depression or transition sites, and during the summer were covered in grasses and sedges that obscured hummock and hollow features. However, during late autumn, it became clear that there were some distinctive hummock features associated with black ash trees, but these hummocks were far less numerous and less pronounced than those at depression or transition sites. Most areas of these lowland sites were of intermediate elevation, belonging neither to what would be traditionally considered hummock nor hollow categories.

In support of our observations, semivariograms demonstrated much more pronounced elevation variability at depression and transition sites than at lowland sites (Figure 3.6). In general, lowland sites reached overall site elevation variance (sills, horizontal dashed lines) within 5 meters, but best-fit ranges (dotted vertical lines in Figure 3.6) were less than 1 m. In contrast, best-fit semivariogram ranges for depression and transition sites were several times greater. Therefore, depression and transitions sites

have much larger ranges of spatial autocorrelation for elevation than lowland sites. Semivariograms were all best fit with Matérn models with Stein parameterizations, and nugget effects were extremely small in all cases (average <0.001), which we attribute to the very high precision of the TLS method. As such, partial sills were quite large (i.e., the difference between the sill and nugget), indicating that very little elevation variation is at scales less than our surface model resolution (1 cm); the remaining variation is found over site-level ranges of autocorrelation. We did not observe major differences in directional semivariograms compared to the omnidirectional semivariogram, implying isotropic variability in elevation, and do not present them here

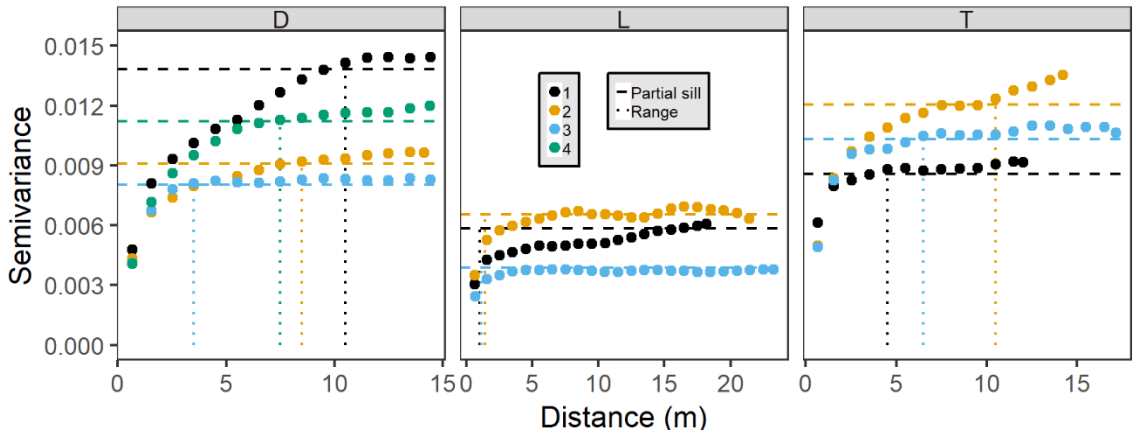

Figure 3.6 Omni-directional semivariograms for site elevations by hydrogeomorphic category (D = depression, L = lowland, T = transition). Sites are colored according to their number within their hydrogeomorphic category. Dotted vertical lines indicate best-fit ranges and horizontal dashed lines indicate best-fit partial sills (sill – nugget).

We observed bimodal elevation distributions at every site, with hummocks clearly belonging to a distinct elevation class separate from hollows (Figure 3.7). Bimodal mixture models of two normal distributions were always better fit to the data than unimodal models based on BIC values. Differences in mean elevations between these two classes ranged from 12 cm at the lowland sites to 20 cm at depression sites, and hummock elevations were more variable than hollow elevations across sites. Across sites, 27±10% of all elevations did not fall into either a hummock or a hollow category, with lowland sites having considerably more elevations failing to fall into these binary categories (36–44%) than depression (22–27%) or transition sites (16–22%). However, we emphasize that even when considering the entire site elevation distribution (i.e., including elevations that did not fall into a hummock or hollow category), bimodal fits

were still better than unimodal fits, but to a lesser extent for lowland sites (Figure S3.2). Delineated hummocks varied in number and size across and within sites. We observed the greatest number of hummocks in the depression and transition sites, with approximately an order of magnitude less hummocks found in lowland sites (Figure 3.7).

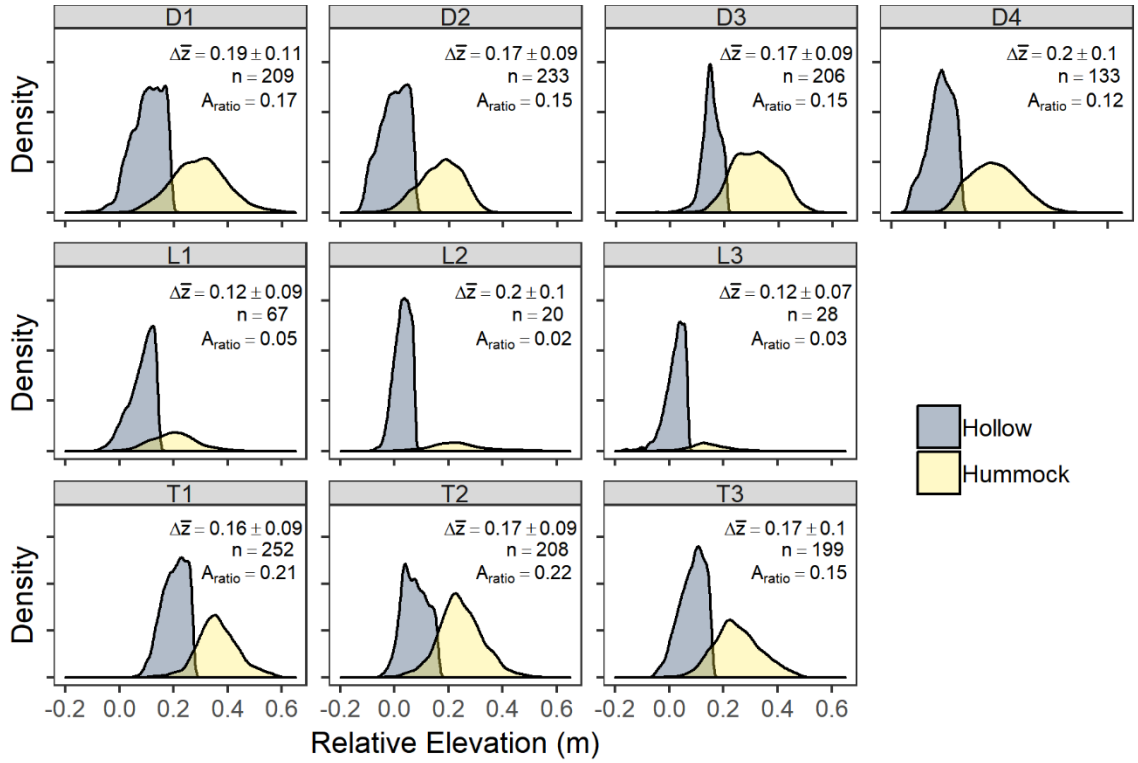

Figure 3.7 Relative elevation probability densities for each site, colored by hummock and hollow. Text indicates the difference in mean elevation (Δz; m) between hummock and hollow at each site (± standard deviation), the total number of hummocks identified at each site (n), and the ratio of hummock area to total site area (A_{ratio}). Depression sites (D) occupy the top row, followed by lowland sites (L), and transition sites (T)

3.4.4 Subsurface topographic control on microtopography

Across sites, depth to resistance ("organic soil thickness") varied and was greatest at the lowest mineral layer elevations, indicating that surface microtopography is not simply a reflection of subsurface mineral layer topography with constant overlying organic thickness (as illustrated with 0-slope line in Figure 3.8). In contrast, at most sites, except for possibly D1 and L2, there was a strong negative linear relationship between soil thickness and mineral layer elevation, with five sites exhibiting slopes near -1, which we define as the smooth surface model of soil elevation (dashed -1:1 line in Figure 3.8). If only hollows (open circles; Figure 3.8) were used in the regression, then D1 also

exhibited a significant (p<0.001) negative slope in this relationship (-0.4, R^2 = 0.52). A majority of depth to mineral layer measurements at D3 were below detection limit with our 1.5 m steel rod, and all but one measurement at T1 were below detection limit. At sites D2 and L2, there was indication that some hollows were actually better represented by the subsurface reflection model (i.e., slope = 0). However, at all sites, though to a lesser extent at lowland sites, hummocks (closed circles; Figure 3.8) tend to plot above hollows and above the -1:1 line, even when at the same soil thickness as hollows, indicating that their elevation is greater than would be expected for a smooth surface model.

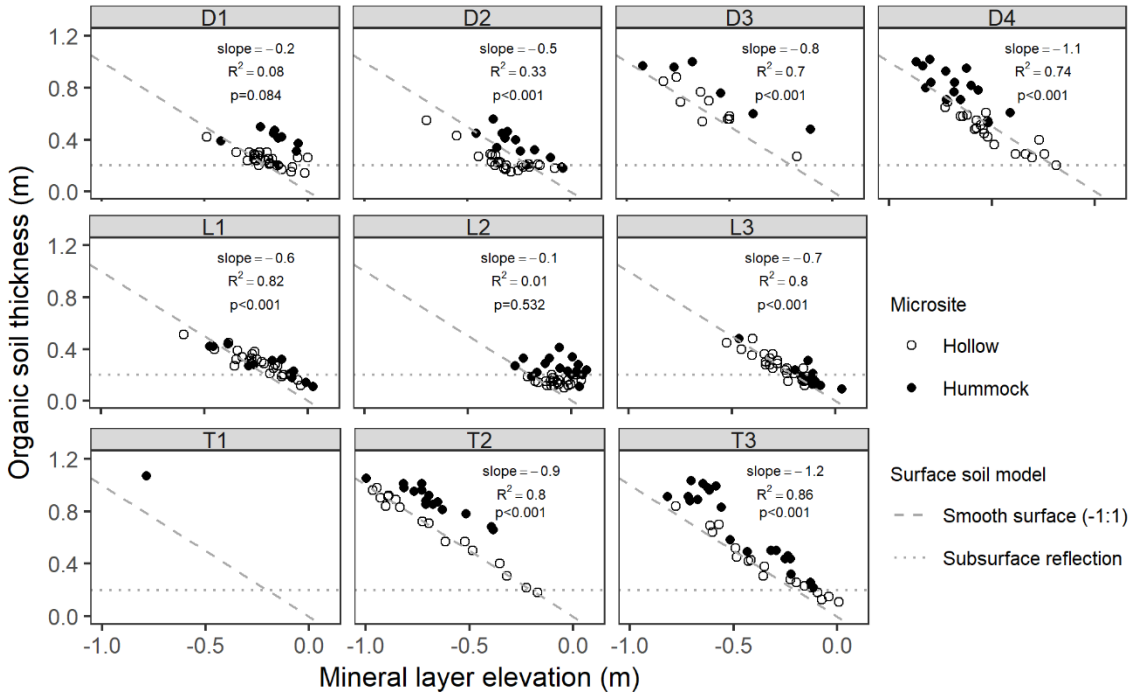

Figure 3.8 Organic soil thickness (measured as depth to resistance) as a function of mineral layer elevation. Points are filled by their microsite. Dashed -1:1 line indicates a smooth surface soil model and dotted horizontal line indicates a subsurface reflection model. Text values are slopes, R^2, and p-value of best-fit linear model for aggregated hummock and hollow points.

3.4.5 Hydrologic control on microtopography

We observed a significant (p<0.001) positive linear relationship between site level mean hummock height and site level mean daily water table (Figure 3.9). Because lowland sites were clearly influential points on this linear relationship, we also conducted this regression excluding the lowland sites and still found a significant (p = 0.007)

positive linear trend between these variables with reasonable predictive power (R^2=0.8) — wetter sites have on average have taller hummocks than drier sites. We found very little variability in average hummock heights across sites when relative to site-level mean water table elevation (mean normalized hummock height = 0.31±0.06 m), indicating that hummocks were generally about 30 cm higher than the site mean water table.

Within sites, we also observed clear positive relationships between individual hummock heights and their local mean daily water table (Figure 3.9). At all but two of the sites (D4 and L1), individual hummock heights within a site were significantly ($p<0.01$) taller at wetter locations than drier locations. Slopes for these individual hummock regressions varied among sites, ranging from 0.4–1.1 (mean±sd = 0.7±0.2), and local hummock mean water table was able to explain 12–56% (mean±sd = 0.36±0.14) of variability in hummock height within a site.

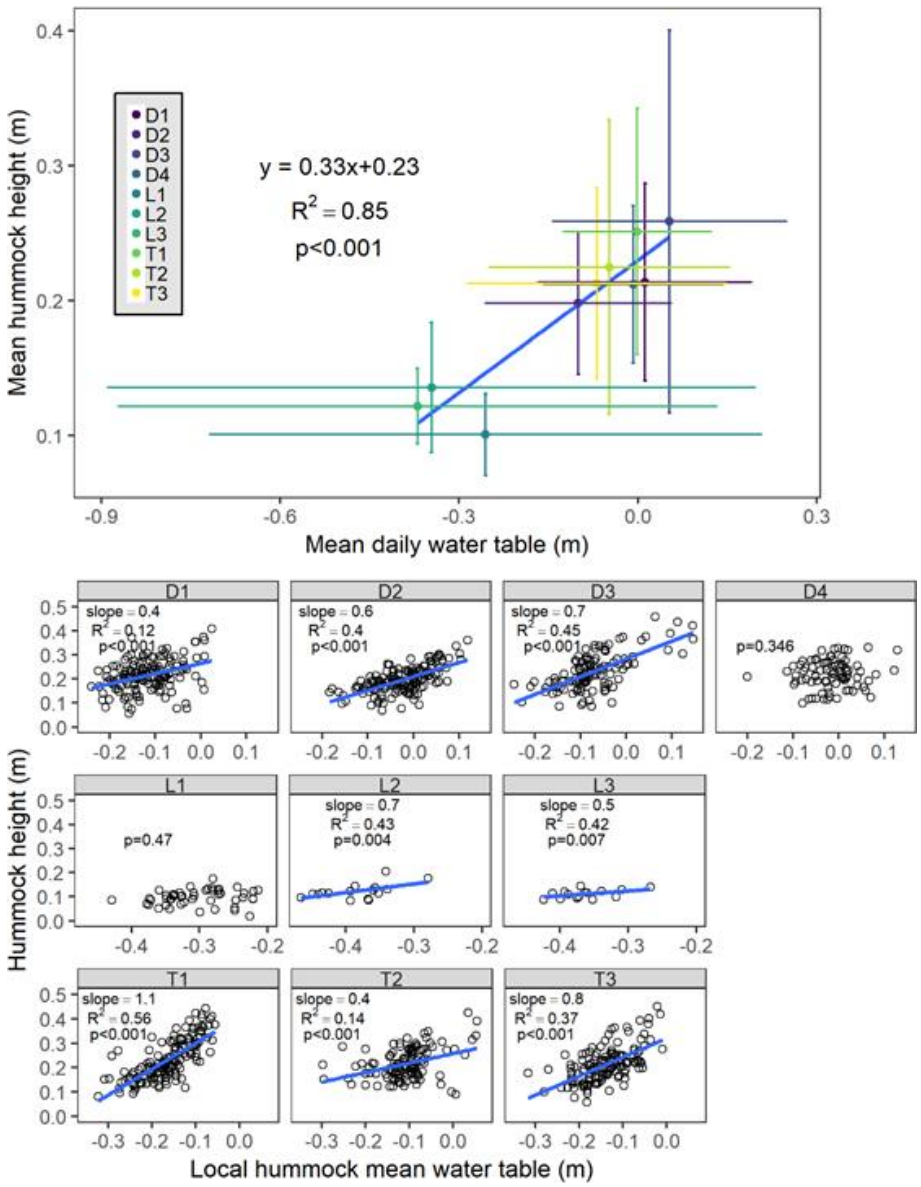

Figure 3.9 Hummock height as a function of mean water table. (Top) mean site-level hummock height (± sd) versus mean site-level daily water table (± sd), and (Bottom) individual hummock height versus local daily mean water table. Slope, R2, and p-value for best fit linear model (blue line) presented.

3.4.6 Hummock spatial distributions

All sites characterized as depressions or transitions exhibited significant ($p < 0.001$) overdispersion of hummocks compared to what would be predicted under complete spatial randomness (Figure 3.10). For these sites, the nearest neighbor ratios (μ_{NN}:μ_{exp}) indicated that hummocks are 25–30% further apart than would be expected with complete spatial randomness, with spacing ca. 1.5 meters, as evidenced by the narrow distributions in nearest neighbor histograms (Figure 3.10). In contrast, all lowland

sites, while having hummock nearest neighbor distances 2–3 times as far apart as depression of transition sites, were not significantly different than what would predicted under complete spatial randomness (p = 0.129, 0.125, 0.04 for sites L1, L2, and L3, respectively).

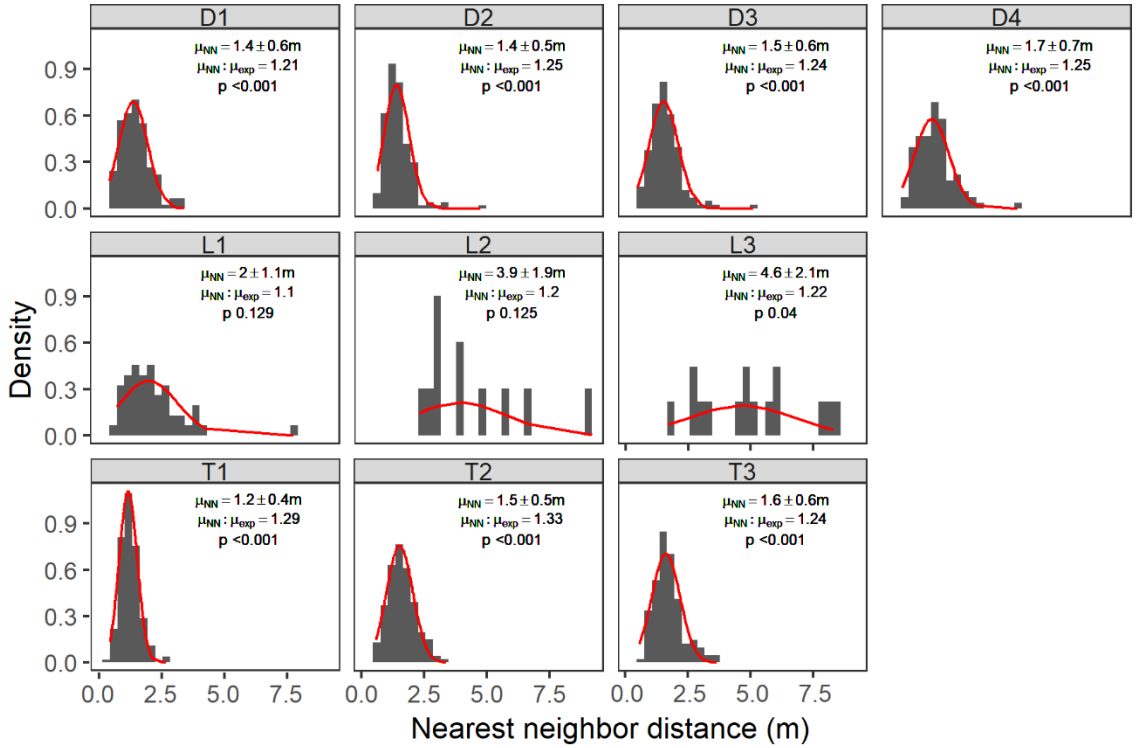

Figure 3.10 Hummock nearest-neighbor distance distributions across sites. Bars are scaled density histograms overlain with best-fit normal distributions (red lines). Text indicates the mean nearest-neighbor distance (μ_{NN} ± standard error); the ratio of the measured mean nearest-neighbor distance and the expected nearest neighbor distance for complete spatial randomness (μ_{exp}); and the p-value for a z-score comparison between μ_{NN} and μ_{exp}. p-values less than 0.001 indicate that hummocks are significantly overdispersed.

3.4.7 Hummock size distributions

Hummock dimensions (perimeter, area, and volume) were strongly lognormally distributed across sites (Figure 3.11), though exponential models were typically only slightly worse fits. For each hummock dimension, site fits were similar within site hydrogeomorphic categories, but drier lowland site distributions were clearly different from wetter depression and transition site distributions, which were more similar (Figure 3.11). Lowland sites had significantly lower ($p < 0.05$) coefficients for hummock property model fits than depression or transition sites, with slopes approximately 20%

more negative on average, indicating more rapid truncation of size distributions. Across sites, average hummock perimeter was 4.2±0.8 m, average hummock area was 1.7±0.5 m^2, and average hummock volume was 0.17±0.06 m^3. Hummock areas were typically less than 1 m^2 in size at all sites (Figure 3.11). Similar to hummock spatial density, hummock area per site (ratio of hummock area to site area) was lower at drier lowland sites (2–5%) compared to wetter depression and transition sites (12–22%) (Figure 3.7).

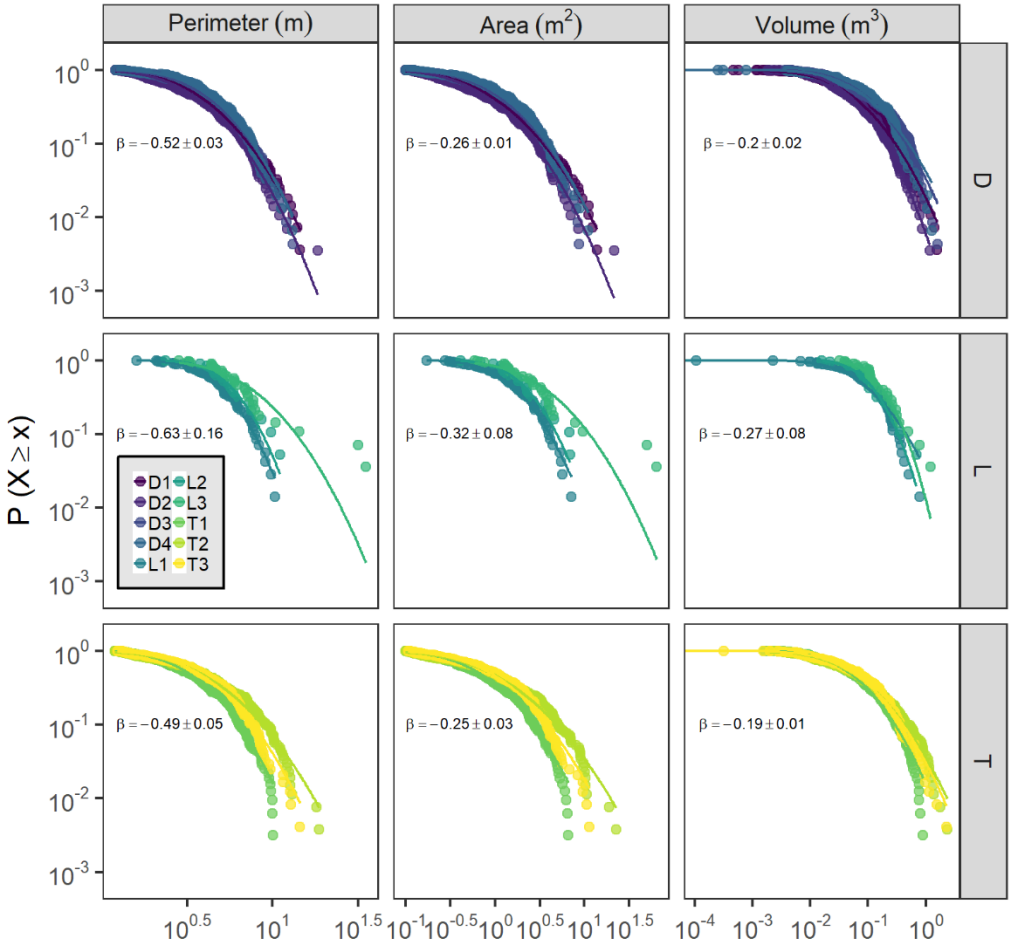

Figure 3.11 Inverse cumulative distributions of hummock dimensions (perimeter, area, and volume) across sites (points), split by hummock dimension and site type. The y-axis is the probability that a hummock dimension value is greater than or equal to the corresponding value on the x-axis. Best-fit lognormal distributions are shown for each site as lines. All fits were highly significant ($p<<0.001$). Text indicates mean (±sd) within-group coefficient for a model of the form $P(X\geq x)=\beta*ln(dimension\_value) + \beta_0$.

3.5 Discussion

We tested our hypothesis that microtopography in black ash wetlands self-organizes in response to hydrologic drivers (Figure 3.1) using an array of diagnostic tests including

analyses of multimodal elevation distributions, spatial patterning, and patch size distributions. We further analysed the influence of hydrology on these diagnostic measures and tested a potential null hypothesis that surface microtopography was simply a reflection of subsurface microtopography. All diagnostic tests aligned with hypothesized predictions, which when taken together with a clear influence of hydrology on microtopographic structure and pattern, provide strong support for our hypothesis.

3.5.1 Controls on microtopographic structure

Bimodal soil elevation distributions at all sites suggest that the microsite separation into hummocks and hollows is a common attribute of black ash wetlands. Soil elevation bimodality was most evident at depression and transition sites, where hummocks were more numerous and consequently occupied a higher fraction of overall site area (15–20%). Sharp boundaries between hummocks and hollows were not always observed in soil elevation probability densities (Figure 3.7), which may be indicative of weaker-than-predicted positive feedbacks between primary productivity and elevation (Rietkerk et al. 2004; Figure 3.1). On the other hand, modeling predictions indicate that if evapoconcentration feedbacks are strong, boundaries between hummocks and hollows will be less sharp (Eppinga et al. 2009), possibly implicating hummock evapoconcentration as an additional feedback to hummock maintenance (Figure 3.1).

Our results provide clear evidence of decoupling between surface microtopography and mineral layer microtopography at all of our sites. A smooth surface model, with a relatively constant surface elevation despite variable underlying mineral soil elevation, best represented hollows. Importantly, we also observed that regardless of underlying mineral layer, hummocks had greater soil thickness than hollows did (Figure 3.8). To clarify, irrespective of mineral layer microtopography, hummocks are maintained at local elevations that are higher than would be predicted for a smooth soil surface. We interpret this as evidence for self-organization of wetland microtopography. Smoothing of soil surfaces relative to variability in underlying mineral layers or bedrock is observed in other wetland systems where soil creation is dominated by organic matter accumulation (Watts et al. 2014), implying that deviations from this smooth surface are related to other surface-level processes.

Hummock heights relative to site-level water table were approximately 30 cm, aligning with field observations of relatively constant hummock height within sites. Generally consistent hummock height across sites in conjunction with clear bimodality in soil elevations supports the contention that hummocks and hollows are discrete, self-organized ecosystem states (*sensu* Watts et al. 2010). However, variability in site-level hummock heights–especially at depression and transition sites–may partially be attributable to hummocks in non-equilibrium states. From our feedback model (Figure 3.1), it seems reasonable that within a site, some hummocks may be in growing states (e.g., elevation-GPP positive feedback) and some may be in shrinking states (e.g., elevation-respiration negative feedback), the combination of which may result in a distribution of hummock heights centered around an equilibrium hummock height.

We observed strong control of local hydrology on hummock height, providing evidence for our hypothesis that hummocks are a biogeomorphic response to hydrologic stresses in wetlands. Vegetation patches like hummocks are most commonly found in conditions with strong environmental stressors. In particular, water stress—both too little (Deblauwe et al. 2008, Scanlon et al. 2007) and too much (Eppinga et al. 2009)—appears to be an important regulator of microhabitat size and its spatial distribution across the landscape. Wetlands are characterized by regular water stresses from periodic inundation with nearly all biogeochemical processes under the fundamental influence of hydrology (Rodriguez-Iturbe et al. 2007). It is therefore perhaps unsurprising that hydrology also controls the scale-dependent feedbacks that create and maintain hummock sizes and their spatial patterning. We found support for this contention at both the site level and at the hummock level, with the tallest hummocks being found in the wettest sites and in the wettest zones within sites. In fact, distance from mean water table explained on average 35% of the variability in hummock height (Figure 3.9); prevalence of non-equilibrium hummock states may explain much of the additional variability. The considerable variation in the ability of hydrology to explain hummock height within sites (adjusted R^2 =0.12–0.56), and also in the strength of that relationship (linear regression slopes=0.4–1.1) may be attributed to two factors: 1) the across-site flat water table assumption, and 2) lack of long trends for hydrology. The flat water table assumption is likely to be a minor effect in transition sites with deep organic wetland soils (e.g., Nungesser 2003, Wallis

and Raulings 2011, Cobb et al. 2017), but could be significant at depression and lowland sites with shallower O horizons. Lack of sufficient data to characterize mean water table may also be an issue at several of our sites, because hummocks likely develop over the course of decades or more, whereas our hydrology data only span three years.

To our knowledge, this study represents the first empirical evidence of the positive relationship between hummock height and hydrology in forested wetlands. These results are consistent with previous research on tussocks of northern wet meadows (Peach and Zedler 2006, Lawrence and Zedler 2011) and shrub hummocks in brackish wetlands (Wallis and Raulings 2011). The concordance in hydrologic control in these disparate systems suggests a common mechanism of soil building and accumulation on hummocks that may result from increased vegetation growth from reduced water stress and/or from transport and accumulation of nutrients (Eppinga et al. 2009, Sullivan et al. 2011, Heffernan et al., 2013).

3.5.2 Controls on microtopographic patterning

We found clear support for our hypothesis that hummocks are non-randomly distributed in the wettest sites of our study area, further supporting the posited interactions among hydrology, vegetation, and soils. Hummocks exhibited spatial overdispersion in all sites, but this overdispersion was only significant at depression and transition sites (Figure 3.10). Significant spatial overdispersion is indicative of regular hummock spacing in contrast to clustered distributions or completely random placement. Regular patterning of landscape elements is observed across climates, regions, and ecosystems (Rietkerk and van de Koppel 2008), but to our knowledge, this study is the first to demonstrate regular patterning in forested wetland microtopography and the hydrologic control on this regular pattern emergence. Hydrology appears to be a common driver in regular pattern formation in wetlands (Heffernan et al. 2013), drylands (Scanlon et al. 2007), and tidal flats (Weerman et al. 2011) through a diverse array of mechanisms (e.g., Watts et al. 2014). However, most observed regular patterning in wetlands ultimately develops only through coupling between biota and hydrology (Rietkerk and van de Koppel 2008), underscoring the importance of biota in structuring their own environment.

We observed lognormal hummock size distributions, suggesting that some hummocks may attain very large areas (i.e., over 10 m^2), but the majority of hummocks (~80%) are less than 1 m^2 (Figure 3.11). This finding aligns with field observations, where most hummocks were associated with a single black ash tree, but some hummocks appeared to have merged over time to create large patches. Truncated patch size distributions are common in other systems as well, like the stretched exponential distribution for geographically isolated wetlands (Watts et al. 2014) or the lognormal distribution for desert soil crusts (Bowker et al. 2013). These types of distributions have much fewer large patches than would be expected for systems without patch-scale negative feedbacks, and have a central tendency towards a common patch size. Hence, truncation in hummock size distributions comports with hypothesized patch-scale negative feedbacks (i.e., tree competition for light and nutrients) that inhibit expansion. Hummocks at drier lowland sites did not conform to size distributions or spatial patterns from wetter depression and transition sites, supporting our hypothesis that the feedbacks that control hummock maintenance and distribution are governed by hydrology and amplified in wetter conditions. Larger hummock patches were especially obvious at transition sites that had significant *Sphagnum spp.* moss cover, which tended to blend and expand hummock areas. This work adds to recent efforts across climates and systems to use patch size distributions to infer drivers and processes of ecosystem self-organization and response to environmental conditions and abiotic drivers (Kefi et al. 2007, Maestre and Escudero 2009, Weerman et al. 2011, Schoelynck et al. 2012, Tamarelli et al. 2017).

Characteristic hummock sizes in association with overdispersion in black ash wetlands suggest that hummocks are laterally limited in size by negative feedbacks on the scale of meters (Manor and Shnerb 2008). We posit that there are two patch-scale negative feedbacks: 1) overstory competition for nutrients and 2) understory and overstory competition for light. Hummocks associated with black ash trees, which account for more than 85% of measured hummocks, are likely limited in area by the radial growth of the tree's root system. Evapoconcentration feedbacks bring nutrients to the tree roots, limiting the degree to which roots must search for them (Karban 2008), and therefore limiting root lateral expansion. Moreover, finite nutrient pools may lead to development of similarly sized nutrient source basins for each hummock, further limiting

expansion (Rietkerk et al. 2004, Eppinga et al. 2008). Black ash trees must also compete for light with other ash trees, but leaf area is typically low in these systems (<2.5 leaf area index [LAI]; Telander et al. 2015; Figure 3.12). Low LAI and observed canopy shyness (*sensu* Long and Smith 1992) in black ash wetlands may imply less competition among individuals than would be expected in mixed stands (Franco 1986). On the other hand, low canopy competition for light in the overstory may increase light availability for understory hummock species, and therefore allow subsequent hummock expansion from the understory.

Figure 3.12 Open canopies in black ash wetlands

3.5.3 Broader implications

The consequences of wetland microtopography are clear at small scales, but there is also some evidence that the presence of microtopography has site- and regional-scale importance. For example, microtopographic expression results in a drastic increase in surface area within wetlands. We estimate an average of 19% and up to 32% relative increase in surface area due to the presence of hummocks (i.e., that additional area provided by the sides of hummocks; Table 3.2). These estimates comport with studies in tussock meadows that found tussocks of an average of 20 cm tall increased surface area

by up to 40% (Peach and Zedler 2006). Increases in the diversity of biogeochemical processes occurring at the individual hummock or hollow scale (Deng et al. 2014) likely aggregate to influence ecosystem functioning at large scales. For example, microtopographic niche expansion allows for local material and solute exchange between hummocks and hollows, creating coupled aerobic-anaerobic conditions with emergent outcomes for denitrification (Frei et al. 2012) and carbon emission (Bubier et al. 1995).

Table 3.3 Relative area increase by hummocks across sites

Site	**Survey area (m^2)**	**Hummock side surface area (m^2)**	**Relative area increase by hummocks**
D1	1234	175	0.17
D2	919	151	0.14
D3	1221	223	0.20
D4	1045	107	0.09
L1	1041	55	0.04
L2	1093	40	0.04
L3	1164	41	0.03
T1	731	237	0.32
T2	994	227	0.23
T3	1198	179	0.15
Average		144±74	0.14±0.09
(Average, no L)		(186±44)	(0.19±0.07)

While our results implicate hydrology as a major determinant of microtopographic structure and pattern, microtopography can reciprocally influence system-scale hydraulic properties. Results from our hummock property analysis indicate that hummock volume displacement may be a significant factor in water table dynamics of wetlands. Specific yield, which controls water table response to hydrologic fluxes, is commonly assumed to be unity when wetlands are inundated. However, inclusion of microtopography may render this assumption invalid, with hummock volumes up to 30% of site volumes (Table 3.3). These observations are supported in other studies of microtopographic effects of specific yield (Sumner 2007, McLaughlin and Cohen 2014, Dettmann and Bechtold 2016). Therefore, while hydrology exerts clear control on the geometry of hummocks, hummocks may exert reciprocal control on hydrology by amplifying small hydrologic fluxes into large water table variations

Table 3.4 Hummock volume displacement ratios for all sites

Site	Site height† (m)	Site volume‡ (m^3)	Hummock volume (m^3)	Hummock volume displacement ratio
D1	0.17	179	33	0.18
D2	0.15	155	26	0.17
D3	0.21	233	41	0.18
D4	0.17	200	24	0.12
L1	0.15	181	10	0.05
L2	0.26	242	5	0.02
L3	0.21	255	6	0.02
T1	0.18	134	37	0.28
T2	0.16	157	46	0.30
T3	0.17	199	37	0.18
Average			**27±14**	**0.15±0.09**
(Average, no L)			**(35±7)**	**(0.20±0.06)**

†Site height is estimated as the mean 80th percentile of hummock heights across the site
‡Site volume is estimated as by multiplying site height by site area

Last, hummocks also provide unique microsite conditions that support increased vegetation growth and diversity (Bledsoe and Shear 2000, Peach and Zedler 2006, Økland et al. 2008). Evidence abounds for both increased understory richness and improved seedling regeneration on hummocks relative to hollows (Koponen et al. 2004, Dubertstein and Connor 2009, Courtwright and Findlay 2011). To this point, recent wetland restoration efforts have begun to use microtopography as a restoration strategy to promote planted seedling success and long-term project viability (Larkin et al. 2006; Bannister et al. 2013; Lieffers et al. 2017). Indeed, and in light of recent concerns over regime shift to marsh like states from black ash loss to EAB (Diamond et al. 2018), we posit that hummock presence and persistence may allow for future tree seedlings to survive wetting up periods following ash loss (Slesak et al. 2014), and for consequent resilience of swamp ecosystem states.

3.6 Conclusions

Although observations of the presence and significance of wetland microtopography abound in the literature, this is the first study, to our knowledge, to detail the structure, pattern, and drivers of wetland microtopography in forested systems. This study adds to the growing body of evidence that the structure and regular patterning of wetland microtopography is an autogenic response to hydrology. Although the imprint of biota on landscapes may be masked by the signature of larger scale physical processes (Dietrich and Perron, 2006), we show clear evidence here for a microtopographic signature of life.

Acknowledgments

This project was funded by the Minnesota Environmental and Natural Resources Trust Fund, the USDA Forest Service Northern Research Station, and the Minnesota Forest Resources Council. Additional funding was provided by the Virginia Tech Forest Resources and Environmental Conservation department, the Virginia Tech Institute for Critical Technology and Applied Science, and the Virginia Tech William J. Dann Fellowship. We gratefully acknowledge the field work and data collection assistance provided by Mitch Slater, Alan Toczydlowksi, and Hannah Friesen.

3.7 References

Amundson, R., Richter, D. D., Humphreys, G. S., Jobbágy, E. G., & Gaillardet, J. (2007). Coupling between biota and earth materials in the critical zone. Elements, 3(5), 327-332.

Baddeley A., Rubak, E., and Turner, R. (2015). Spatial Point Patterns: Methodology and Applications with R. London: Chapman and Hall/CRC Press, 2015. URL http://www.crcpress.com/Spatial-Point-Patterns-Methodology-and-Applications-with-R/Baddeley-Rubak-Turner/9781482210200/

Bannister, J. R., R. E. Coopman, P. J. Donoso, and J. Bauhus. 2013. The Importance of Microtopography and Nurse Canopy for Successful Restoration Planting of the Slow-Growing Conifer Pilgerodendron uviferum. Forests 4:85-103

Belyea, L. R., & Baird, A. J. (2006). Beyond "the limits to peat bog growth": Cross-scale feedback in peatland development. Ecological Monographs, 76(3), 299-322.

Bledsoe, B. P. and T. H. Shear. (2000). Vegetation along hydrologic and edaphic gradients in a North Carolina coastal plain creek bottom and implications for restoration. Wetlands 20:126-147.

Bowker, M. A., Maestre, F. T., & Mau, R. L. (2013). Diversity and patch-size distributions of biological soil crusts regulate dryland ecosystem multifunctionality. Ecosystems, 16(6), 923-933.

Brantley, S. L., Eissenstat, D. M., Marshall, J. A., Godsey, S. E., Balogh-Brunstad, Z., Karwan, D. L., ... & Chadwick, O. (2017). Reviews and syntheses: on the roles trees play in building and plumbing the critical zone. Biogeosciences (Online), 14(22).

Bubier, J. L., Moore, T. R., Bellisario, L., Comer, N. T., & Crill, P. M. (1995a). Ecological controls on methane emissions from a northern peatland complex in the zone of discontinuous permafrost, Manitoba, Canada. Global Biogeochemical Cycles, 9(4), 455-470.

Cobb, A. R., Hoyt, A. M., Gandois, L., Eri, J., Dommain, R., Salim, K. A., ... & Harvey, C. F. (2017). How temporal patterns in rainfall determine the geomorphology and carbon fluxes of tropical peatlands. Proceedings of the National Academy of Sciences, 114(26), E5187-E5196.

Conner, W. H. 1995. Woody plant regeneration in three South Carolina Taxodium/Nyssa stands following Hurricane Hugo. Ecological Engineering 4:227-287

Corenblit, D., Baas, A. C., Bornette, G., Darrozes, J., Delmotte, S., Francis, R. A., ... & Steiger, J. (2011). Feedbacks between geomorphology and biota controlling Earth surface processes and landforms: a review of foundation concepts and current understandings. Earth-Science Reviews, 106(3-4), 307-331.

Courtwright, J., & Findlay, S. E. (2011). Effects of microtopography on hydrology, physicochemistry, and vegetation in a tidal swamp of the Hudson River. Wetlands, 31(2), 239-249.

D'Amato, A., Palik, B., Slesak, R., Edge, G., Matula, C., & Bronson, D. (2018). Evaluating Adaptive Management Options for Black Ash Forests in the Face of Emerald Ash Borer Invasion. Forests, 9(6), 348.

Deblauwe, V., Barbier, N., Couteron, P., Lejeune, O., & Bogaert, J. (2008). The global biogeography of semi-arid periodic vegetation patterns. Global Ecology and Biogeography, 17(6), 715-723.

Deng, Y., X. Cui, M. Hernández, and M. G. Dumont. 2014. Microbial Diversity in Hummock and Hollow Soils of Three Wetlands on the Qinghai-Tibetan Plateau Revealed by 16S rRNA Pyrosequencing. PLOS ONE 9:e103115.

Dettmann, U., & Bechtold, M. (2016). One-dimensional expression to calculate specific yield for shallow groundwater systems with microrelief. Hydrological Processes, 30(2), 334-340.

Dietrich, W. E., & Perron, J. T. (2006). The search for a topographic signature of life. Nature, 439(7075), 411.

Diggle PJ. 2002. Statistical Analysis of Spatial Point Patterns, 2nd edn. Hodder Education: London; 288.

Duberstein, J. A., K. W. Krauss, W. H. Conner, W. C. Bridges (Jr.), and V. B. Shelburne. 2013. Do Hummocks Provide a Physiological Advantage to Even the Most Flood Tolerant of Tidal Freshwater Trees? Wetlands 33: 399-408.

Eppinga, M. B., De Ruiter, P. C., Wassen, M. J., & Rietkerk, M. (2009). Nutrients and hydrology indicate the driving mechanisms of peatland surface patterning. The American Naturalist, 173(6), 803-818.

Erdmann, G. G., Crow, T. R., Ralph Jr, M., & Wilson, C. D. (1987). Managing black ash in the Lake States. General Technical Report NC-115. St. Paul, MN: US Dept. of Agriculture, Forest Service, North Central Forest Experiment Station, 115.

Ettema, C. H., & Wardle, D. A. (2002). Spatial soil ecology. Trends in ecology & evolution, 17(4), 177-183.

Foti, R., del Jesus, M., Rinaldo, A., & Rodriguez-Iturbe, I. (2012). Hydroperiod regime controls the organization of plant species in wetlands. Proceedings of the National Academy of Sciences, 109(48), 19596-19600.

Franco, M. (1986). The influence of neighbours on the growth of modular organisms with an example from trees. Philosophical Transactions of the Royal Society of London. B, Biological Sciences, 313(1159), 209-225.

Frei, S., Knorr, K. H., Peiffer, S., & Fleckenstein, J. H. (2012). Surface micro-topography causes hot spots of biogeochemical activity in wetland systems: A virtual modeling experiment. Journal of Geophysical Research: Biogeosciences, 117(G4).

Gabet, E. J., Perron, J. T., & Johnson, D. L. (2014). Biotic origin for Mima mounds supported by numerical modeling. Geomorphology, 206, 58-66.

Gräler, B., Pebesma, E., and Heuvelink G. (2016). Spatio-Temporal Interpolation using gstat. The R Journal 8(1), 204-218.

Heffernan, J. B., Watts, D. L., & Cohen, M. J. (2013). Discharge competence and pattern formation in peatlands: a meta-ecosystem model of the Everglades ridge-slough landscape. PloS one, 8(5), e64174.

Huenneke, L. F., & Sharitz, R. R. (1990). Substrate heterogeneity and regeneration of a swamp tree, Nyssa aquatica. American Journal of Botany, 77(3), 413-419.

Jackson, R. B., & Caldwell, M. M. (1996). Integrating resource heterogeneity and plant plasticity: modelling nitrate and phosphate uptake in a patchy soil environment. Journal of Ecology, 891-903.

Karban, R. (2008). Plant behaviour and communication. Ecology letters, 11(7), 727-739.

Kéfi, S., Rietkerk, M., Alados, C. L., Pueyo, Y., Papanastasis, V. P., ElAich, A., & De Ruiter, P. C. (2007). Spatial vegetation patterns and imminent desertification in Mediterranean arid ecosystems. Nature, 449(7159), 213.

Kéfi, S., Rietkerk, M., Roy, M., Franc, A., De Ruiter, P. C., & Pascual, M. (2011). Robust scaling in ecosystems and the meltdown of patch size distributions before extinction. Ecology letters, 14(1), 29-35.

Koponen, P., Nygren, P., Sabatier, D., Rousteau, A., & Saur, E. (2004). Tree species diversity and forest structure in relation to microtopography in a tropical freshwater swamp forest in French Guiana. Plant Ecology, 173(1), 17-32.

Kurmis, V., & Kim, J. H. (1989). Black ash stand composition and structure in Carlton County, Minnesota.

Larkin, D. J., G. Vivian-Smith, and J. B. Zedler. 2006. Topographic heterogeneity theory and ecological restoration. In: Falk, D. A., M. A. Palmer, and J. B. Zedler, (eds). Foundations of restoration ecology. Island Press, Washington, D.C., USA.

Larsen, L. G., & Harvey, J. W. (2011). Modeling of hydroecological feedbacks predicts distinct classes of landscape pattern, process, and restoration potential in shallow aquatic ecosystems. Geomorphology, 126(3-4), 279-296.

Lashermes, B., Foufoula-Georgiou, E., & Dietrich, W. E. (2007). Channel network extraction from high resolution topography using wavelets. Geophysical Research Letters, 34(23).

Lawrence, B. A., & Zedler, J. B. (2011). Formation of tussocks by sedges: effects of hydroperiod and nutrients. Ecological Applications, 21(5), 1745-1759.

Lieffers, V. J., R. T. Caners, and H. Ge. 2017. Re-establishment of hummock topography promotes tree regeneration on highly disturbed moderate-rich fens. Journal of Environmental Management 197:258-264.

Long, J. N., & Smith, F. W. (1992). Volume increment in Pinus contorta var. latifolia: the influence of stand development and crown dynamics. Forest Ecology and Management, 53(1-4), 53-64.

Maestre, F. T., & Escudero, A. (2009). Is the patch size distribution of vegetation a suitable indicator of desertification processes?. Ecology, 90(7), 1729-1735.

Manor, A., & Shnerb, N. M. (2008). Facilitation, competition, and vegetation patchiness: from scale free distribution to patterns. Journal of theoretical biology, 253(4), 838-842.

McLaughlin, D. L., & Cohen, M. J. (2014). Ecosystem specific yield for estimating evapotranspiration and groundwater exchange from diel surface water variation. Hydrological Processes, 28(3), 1495-1506.

Minasny, B., & McBratney, A. B. (2005). The Matérn function as a general model for soil variograms. Geoderma, 128(3-4), 192-207.

Nungesser, M. K. (2003). Modelling microtopography in boreal peatlands: hummocks and hollows. Ecological Modelling, 165(2-3), 175-207.

Økland, R. H., Rydgren, K., & Ø kland, T. (2008). Species richness in boreal swamp forests of SE Norway: The role of surface microtopography. Journal of Vegetation Science, 19(1), 67-74.

Othmani, A., Piboule, A., Krebs, M., Stolz, C., Voon, L.L.Y. (2011). Towards automated and operational forest inventories with T-Lidar, in: 11th International Conference on LiDAR Applications for Assessing Forest Ecosystems (SilviLaser 2011).

Pascual, M., Roy, M., Guichard, F., & Flierl, G. (2002). Cluster size distributions: signatures of self–organization in spatial ecologies. Philosophical Transactions of the Royal Society of London. Series B: Biological Sciences, 357(1421), 657-666.

Pascual, M., & Guichard, F. (2005). Criticality and disturbance in spatial ecological systems. Trends in ecology & evolution, 20(2), 88-95.

Pau, G., Fuchs, F., Sklyar, O., Boutros, M., Huber, W., 2010. EBImage--an R package for image processing with applications to cellular phenotypes. Bioinformatics 26, 979–981. https://doi.org/10.1093/bioinformatics/btq046

Pawlik, Ł., Phillips, J. D., & Šamonil, P. (2016). Roots, rock, and regolith: Biomechanical and biochemical weathering by trees and its impact on hillslopes—A critical literature review. Earth-science reviews, 159, 142-159.

Peach, M., & Zedler, J. B. (2006). How tussocks structure sedge meadow vegetation. Wetlands, 26(2), 322-335.

Pebesma, E.J. (2004). Multivariable geostatistics in S: the gstat package. Computers & Geosciences, 30: 683-691.

Peterson, J. E., and A. H. Baldwin. 2004. Variation in wetland seed banks across a tidal freshwater landscape. American Journal of Botany 91:1251-1259.

Planchon, O., Esteves, M., Silvera, N., & Lapetite, J. M. (2002). Microrelief induced by tillage: measurement and modelling of surface storage capacity. Catena, 46(2-3), 141-157.

Pugnaire, F. I., Haase, P., & Puigdefabregas, J. (1996). Facilitation between higher plant species in a semiarid environment. Ecology, 77(5), 1420-1426.

R Core Team (2018). R: A language and environment for statistical computing. R Foundation for Statistical Computing, Vienna, Austria. URL https://www.R-project.org/.

Reinhardt, L., Jerolmack, D., Cardinale, B. J., Vanacker, V., & Wright, J. (2010). Dynamic interactions of life and its landscape: feedbacks at the interface of geomorphology and ecology. Earth Surface Processes and Landforms, 35(1), 78-101.

Rietkerk, M., Dekker, S. C., Wassen, M. J., Verkroost, A. W. M., & Bierkens, M. F. P. (2004). A putative mechanism for bog patterning. The American Naturalist, 163(5), 699-708.

Rietkerk, M., & Van de Koppel, J. (2008). Regular pattern formation in real ecosystems. Trends in ecology & evolution, 23(3), 169-175.

Roering, J. J., Marshall, J., Booth, A. M., Mort, M., & Jin, Q. (2010). Evidence for biotic controls on topography and soil production. Earth and Planetary Science Letters, 298(1-2), 183-190.

Roussel, J.-R., Auty, D., 2018. lidR: Airborne LiDAR Data Manipulation and Visualization for Forestry Applications.

Scanlon, T. M., Caylor, K. K., Levin, S. A., & Rodriguez-Iturbe, I. (2007). Positive feedbacks promote power-law clustering of Kalahari vegetation. Nature, 449(7159), 209.

Scheffer, M., & Carpenter, S. R. (2003). Catastrophic regime shifts in ecosystems: linking theory to observation. Trends in ecology & evolution, 18(12), 648-656.

Schoelynck, J., De Groote, T., Bal, K., Vandenbruwaene, W., Meire, P., & Temmerman, S. (2012). Self-organised patchiness and scale-dependent bio-geomorphic feedbacks in aquatic river vegetation. Ecography, 35(8), 760-768.

Schröder, A., Persson, L., & De Roos, A. M. (2005). Direct experimental evidence for alternative stable states: a review. Oikos, 110(1), 3-19.

Scrucca L., Fop M., Murphy T. B. and Raftery A. E. (2016). mclust 5: clustering, classification and density estimation using Gaussian finite mixture models The R Journal 8/1, pp. 205-233.

Sebestyen, S.D., Dorrance, C., Olson, D.M., Verry, E.S., Kolka, R.K., Elling, A.E., & Kyllander, R. (2011). Chapter 2. Long-term monitoring sites and trends at the Marcell Experimental Forest. In Peatland biogeochemistry and watershed hydrology at the Marcell Experimental Forest. Edited by R.K. Kolka, S.D. Sebestyen, E.S. Verry, and K.N. Brooks. Boca Raton, FL: CRC Press: 15–71.

Soil Survey Staff, Natural Resources Conservation Service, United States Department of Agriculture. Web Soil Survey. Available online at the following link: https://websoilsurvey.sc.egov.usda.gov/. Accessed February 11, 2019.

Strack, M., Waddington, J. M., Rochefort, L., & Tuittila, E. S. 2006. Response of vegetation and net ecosystem carbon dioxide exchange at different peatland microforms following water table drawdown. Journal of Geophysical Research: Biogeosciences, 111(G2).

Stribling, J. M., J. C. Cornwell, and O. A. Glahn. 2007. Microtopography in tidal marshes: Ecosystem engineering by vegetation? Estuaries and Coasts 30:1007-1015.

Sullivan, P. F., S.J. Arens, R.A. Chimner, and J.M. Welker. 2008. Temperature and microtopography interact to control carbon cycling in a high arctic fen. Ecosystems, 11(1), 61-76.

Sumner, D. M. (2007). Effects of capillarity and microtopography on wetland specific yield. Wetlands, 27(3), 693-701.

Taramelli, A., Valentini, E., Cornacchia, L., & Bozzeda, F. (2017). A hybrid power law approach for spatial and temporal pattern analysis of salt marsh evolution. Journal of Coastal Research, 77(sp1), 62-72.

Telander, A. C., Slesak, R. A., D'Amato, A. W., Palik, B. J., Brooks, K. N., & Lenhart, C. F. (2015). Sap flow of black ash in wetland forests of northern Minnesota, USA: Hydrologic implications of tree mortality due to emerald ash borer. Agricultural and forest meteorology, 206, 4-11.

Turner, M. G. (2005). Landscape ecology: what is the state of the science?. Annu. Rev. Ecol. Evol. Syst., 36, 319-344.

van de Koppel, J., & Rietkerk, M. (2004). Spatial interactions and resilience in arid ecosystems. The American Naturalist, 163(1), 113-121.

van De Koppel, J. and C. M. Crain. 2006. Scale-Dependent Inhibition Drives Regular Tussock Spacing in a Freshwater Marsh. The American Naturalist 168:E136-E147.

von Hardenberg, J., Kletter, A. Y., Yizhaq, H., Nathan, J., & Meron, E. (2010). Periodic versus scale-free patterns in dryland vegetation. Proceedings of the Royal Society B: Biological Sciences, 277(1688), 1771-1776.

Wallis, E., & Raulings, E. (2011). Relationship between water regime and hummock-building by Melaleuca ericifolia and Phragmites australis in a brackish wetland. Aquatic Botany, 95(3), 182-188.

Watts, D. L., Cohen, M. J., Heffernan, J. B., & Osborne, T. Z. (2010). Hydrologic modification and the loss of self-organized patterning in the ridge–slough mosaic of the Everglades. Ecosystems, 13(6), 813-827.

Watts, A. C., Watts, D. L., Cohen, M. J., Heffernan, J. B., McLaughlin, D. L., Martin, J. B., ... & Kobziar, L. N. (2014). Evidence of biogeomorphic patterning in a low-relief karst landscape. Earth Surface Processes and Landforms, 39(15), 2027-2037.

Weerman, E. J., Van Belzen, J., Rietkerk, M., Temmerman, S., Kéfi, S., Herman, P. M. J., & de Koppel, J. V. (2012). Changes in diatom patch-size distribution and degradation in a spatially self-organized intertidal mudflat ecosystem. Ecology, 93(3), 608-618.

Western Regional Climate Center [WRCC]. (2019). Cooperative Climatological Data Summaries. Retrieved from https://wrcc.dri.edu/cgi-bin/cliMAIN.pl?mn4652 /

Wolf, K. L., C. Ahn, and G. B. Noe. (2011). Microtopography enhances nitrogen cycling and removal in created mitigation wetlands. Ecological Engineering 37:1398-1406.

3.8 Supplementary material

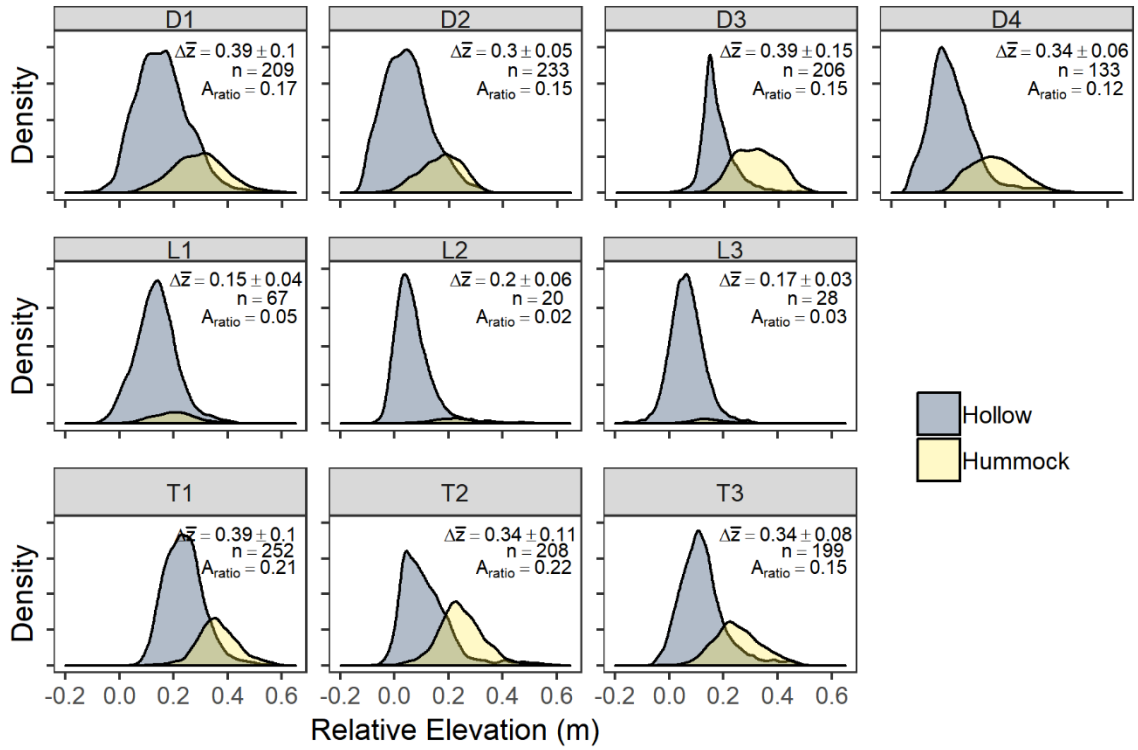

Figure S3.2 Relative elevation probability densities for each site, but using a binary classification system where anything not defined as a hummock is a hollow. Text indicates the difference in mean elevation (Δz; m) between hummock and hollow at each site (± standard deviation), the total number of hummocks identified at each site (n), and the ratio of hummock area to total site area (A_{ratio}).

CHAPTER 4: MICROTOPOGRAPHY IS A FUNDAMENTAL ORGANIZING STRUCTURE IN BLACK ASH WETLANDS

4.1 Abstract

All wetland ecosystems are controlled by water table and soil saturation dynamics, so any local scale deviation in soil elevation represents variability in this primary control. Wetland microtopography is the structured variability in soil elevation, and across systems it is typically categorized into a binary classification of local high points ("hummocks") and local low points ("hollows"). While microtopography's influence on biogeochemical processes and vegetation has received attention in wetlands around the globe, its role in in forested wetlands is still poorly understood. To improve this understanding, we studied the influence of microtopography on understory vegetation communities, canopy biomass, and soil chemistry in 10 black ash (*Fraxinus nigra* Marshall) wetlands in northern Minnesota, U.S.A. To do so, we combined a 1 cm resolution surface model generated from terrestrial laser scanning (TLS) with a long-term water table record and vegetation and soils data from a synoptic field sampling campaign. We observed a strong influence of microtopography across sites, where hummocks were loci of greater species richness, greater canopy biomass, and higher soil concentrations of chloride, phosphorus, and base cations. In contrast, hollows were associated with higher soil concentrations of nitrogen and sulfate. We also found that microtopography's influence on vegetation and soils was greater at wetter sites than at drier sites, suggesting that distance to mean water table is a primary determinant of wetland biogeochemistry. Higher soil concentrations of chloride and phosphorus on hummocks are potentially suggestive of evapoconcentration of mobile solutes from hollows towards hummocks. Although we did not measure it, greater evapotranspiration from trees preferentially located on hummocks may drive this mechanism. This work provides strong support for the notion that microtopography is a fundamental organizing structure in black ash wetlands.

4.2 Introduction

Microtopography is a topic of great interest to wetland ecologists because it so clearly influences a host of fundamental wetland processes. To first order, all wetland

ecosystems are controlled by shallow water table and soil saturation dynamics (Rodriguez-Iturbe et al. 2007), so any local scale deviation in soil elevation represents variability in this primary control (Wallis and Raulings 2011). For example, perhaps incredibly, experimental treatments have demonstrated that even soil surface variability of 2 cm can dramatically increase wetland vegetation germination, overall biomass, and species richness relative to flat soil surfaces (Vivian-Smith 1997). This microtopographic effect on vegetation community structure is also borne out in real wetlands (though with elevation variation on the order of 10–50 cm), ranging from freshwater sedge meadows (Werner and Zedler 2002, Peach and Zedler 2006) to salt marshes (Windham et al. 1999, Fogel et al. 2004). Further, in many wetlands, primary productivity tends to increase with distance from the water table (Belyea and Clymo 2001), and high points are often loci of greater primary productivity compared to low points (Strack et al. 2006, Sullivan et al. 2008). Relatedly, elevation variation from wetland microtopography augments the spatial extent of soil redox gradients (Frei et al. 2012) that might otherwise only be present at wetland-upland boundaries, areas which disproportionately influence aggregate wetland reactivity (Cohen et al. 2016). However, by far, most studies on wetland microtopography have focused on northern bog systems dominated by *Sphagnum spp.* mosses or non-forested wetlands, leaving open questions regarding the commonality of microtopographic influence on wetland processes in forested systems.

The relationship between wetland process and microtopography is thought to be reciprocal, where vegetation and biogeochemical interactions can in turn support expansion of microtopographic features (Eppinga et al. 2009). That is, wetland microtopography can result from feedbacks among hydrology, vegetation, and soil processes that induce soil elevation divergence into two modes: 1) a high elevation mode (“hummocks”) and 2) a low elevation mode (“hollows”) (Rietkerk et al. 2004, Eppinga et al. 2008, Heffernan et al. 2013; Chapter 3). This divergence likely initiates on seed, or nucleation, points that may result from a treefall mound, sediment collection around woody debris (Huenneke and Sharitz 1986), or from animal activity (Palmer and Mazzotti 2004). Subsequent preferential colonization by plants on slightly elevated sites leads to local buildup of organic matter via primary productivity and sediment accretion around roots, and further increased elevation (Gunnarsson and Rydin 1998, Pouliot et al.

2011). This productivity-elevation positive feedback is constrained and stabilized by increased decomposition rates of accumulated organic matter as hummocks become more aerobic (Belyea and Clymo 2001, Watts et al. 2010), from increased instability in substrate and consequent erosion (Larsen and Harvey 2010), or resource limitations (e.g., nutrients; Wetzel et al. 2005). The resulting microtopographic signature often displays a clear structure, with observations of marked spatial patterns in open bog (Eppinga et al. 2009) and marsh systems (Casey et al. 2016).

An additional feedback mechanism that can reinforce and maintain wetland microtopography is preferential hummock evapoconcentration of nutrients. Greater productivity and thus greater evapotranspiration rates on hummocks compared to hollows drive a net flow of water and dissolved nutrients toward hummocks (Rietkerk et al. 2004, Wetzel et al. 2005, Eppinga et al. 2008, Eppinga et al. 2009). Nutrients are consequently rapidly cycled through vascular plant uptake and plant litter mineralization on the more aerobic hummocks (Malmer et al. 2003), leading to local nutrient concentration effects. This localized nutrient concentration purportedly leads to increased primary productivity, which leads to more nutrient evapoconcentration, and so on: an autogenic process (Ross et al. 2006). In other words, hummocks harvest nutrients from hollows, concentrating them there. One clear prediction from this hypothesis is greater nutrient—and conservative water tracer—concentrations in hummock soil relative to hollow soil. To the best of our knowledge, this mechanism remains untested in forested wetlands with hummock-hollow terrain.

In this work, we had two main objectives: 1) to determine microtopographic influences on vegetation and soil chemistry in a forested wetland system and 2) to assess the plausibility of an evapoconcentration feedback to hummock maintenance in forested wetlands. We used black ash (*Fraxinus nigra*) wetlands as our model forested wetland ecosystem to address these objectives. Black ash trees are unique among ash species because they often occur in nearly pure stands (i.e., over 90% canopy cover) in wetland conditions with very little regeneration of other tree species (Palik et al. 2012). Observations in black ash wetlands suggest that black ash trees are unable to fully occupy the available growing space, implicating preferential establishment on suitable microsites (Looney et al. 2016). Field observations and recent work also support this result of

hummock colonization by black ash, but highlight the importance of hydrology on this behavior, with wetter sites exhibiting more pronounced microtopography than drier sites (see Chapter 3). Hence, we expect that drier black ash wetlands may not support the conditions that allow amplification of feedback loops like the evapoconcentration and productivity mechanisms. The diverse hydrologic conditions among and within black ash wetlands suggest that these may be candidate systems to investigate feedbacks (*sensu* Wilson and Agnew 1992) between black ash and microtopography.

Based on previous research showing that hummocks are loci of reduced anaerobic stress (e.g., Bruland and Richardson 2005, Wolf et al. 2011), we hypothesized that black ash wetland hummocks would be important zones for species diversity, primary productivity, and unique biogeochemical processes. Additionally, research in a similar species of the same genus (*Fraxinus excelsior*) indicates that black ash may be highly effective at oxidizing their rhizosphere (Iremonger and Kelly 1988), with important effects for nutrient recycling within hummocks. Black ash hummocks are also expected to be zones of relatively high evapotranspiration (Duberstein et al. 2013). Consequently, we further hypothesized that black ash hummocks will exhibit a nutrient evapoconcentration effect and that under wet conditions, this effect results in a productivity feedback that generates and maintains hummocks.

Specifically we predicted the following:

1) We predicted the primary control on understory species richness would be elevation relative to water table. This prediction follows from observations in other wetland systems, where dry microsites are often zones of greater species diversity. We expected the following: a) greater understory richness at drier sites compared to wetter sites, b) greater understory richness on hummocks than hollows, and c) positive linear correlation between richness and elevation relative to water table.
2) We also predicted that the primary control on midstory and canopy-level biomass (inferred from basal area [BA]) would be elevation relative to water table. This prediction follows from observations in non-forested wetlands, where lower anaerobic stress to roots on hummocks results in greater local primary productivity (e.g., Strack et al. 2006, Sullivan et al. 2008). We expected the following: a) greater basal area at drier sites compared to wetter sites, b) greater basal area on hummocks

than hollows, and c) positive linear correlation between basal area and elevation relative to water table.

3) Finally, we predicted that elevation variation would result in spatial differences in soil chemistry. This prediction follows from expectations from the evapoconcentration mechanism (Eppinga et al. 2008) where sites of greater evapotranspiration [ET] (i.e., hummocks) concentrate nutrients from surrounding areas of lower ET (i.e., hollows). We therefore expected the following: a) site-to-site differences in overall soil chemistry related to hydrology, with drier sites having less within-site soil chemistry variation than wetter sites, b) greater nutrient and conservative tracer (chloride) soil concentrations on hummocks than hollows, and c) positive linear correlation between both soil nutrients and conservative tracers and elevation relative to water table.

4.3 Methods

4.3.1 Site descriptions

To test our hypotheses, we investigated ten black ash (*Fraxinus nigra* Marshall) wetlands of varying size (0.5–15.6 ha) and hydrogeomorphic landscape position in northern Minnesota, U.S.A. (Figure 4.1). As part of a larger effort to understand and characterize black ash wetlands (D'Amato et al. 2018), we categorized and grouped each wetland by its hydrogeomorphic characteristics as follows: 1) depression sites ("D", n = 4) characterized by a convex, pool-type geometry with geographical isolation from other surface water bodies, 2) lowland sites ("L", n = 3) characterized by flat, gently sloping topography, and 3) transition sites ("T", n = 3) characterized as flat, linear boundaries between uplands and black spruce (*Picea mariana* Mill. Britton.) bogs. Ground slopes across sites ranged from 0 to 1 percent. Detailed site histories were unavailable for the ten study wetlands, but silvicultural practices in black ash wetlands have been historically limited in extent (D'Amato et al. 2018). Based on the available information (e.g., Erdmann et al. 1987, Kurmis and Kim 1989), we surmise that our sites are late successional or climax communities and have not been harvested for at least a century.

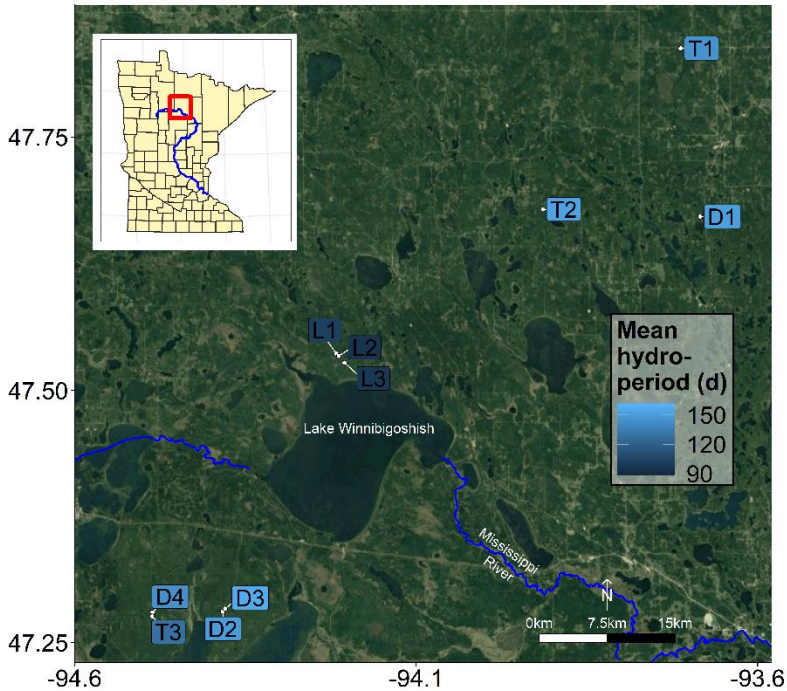

Figure 4.1 Map of the ten black ash study wetlands in northern Minnesota, U.S.A., with sites colored by average annual hydroperiod (i.e., number of surface-inundation days per year from the May to November time period) for 2015–2018.

Soils at our sites tend to be Histosols characterized by deep mucky peats underlain by silty clay mineral horizons, although there were clear differences among site groups (NRCS 2019). Depression sites were commonly associated with Terric haplosaprists of the poorly drained Cathro or Rifle series with O horizons approximately 30–150 cm deep (Table 3.1). Lowland sites were associated with lowland Histic inceptisols of the Wildwood series, which consist of deep, poorly drained mineral soils with a thin O horizon (< 10 cm) underlain by clayey till or glacial lacustrine sediments. Transition sites typically had the deepest O horizons (> 100 cm), and were associated with typic haplosaprists of the Seelyeville series and Typic haplohemists (NRCS 2019). Both depression and transition sites had much deeper O horizons than lowland sites, but depression site organic soils were typically muckier and more decomposed than more peat-like transition site organic soils.

We previously characterized hydrology at these sites using ground water wells and rain gages (see Chapter 3) and found that lowland sites were considerably drier on average than depression or transition sites (note hydroperiods in Fig. 4.1), and exhibited much more water table variability (Table 4.1). Depression sites were typically wetter than

transition sites and were more frequently inundated. Depression and transition sites also exhibited significantly more microtopographic structure than lowland sites, with over twice as much elevation variability on average (see Chapter 3).

Table 4.1 Daily water table summary statistics for black ash study wetlands

Site	Mean (m)	Median (m)	Standard deviation (m)	Mean hydroperiod (d)
D1	0.012	0.088	0.179	105
D2	-0.098	0.042	0.156	96
D3	0.053	0.143	0.196	117
D4	-0.008	0.003	0.151	77
L1	-0.255	-0.046	0.462	67
L2	-0.346	-0.046	0.543	77
L3	-0.370	-0.076	0.502	61
T1	-0.001	0.034	0.125	105
T2	-0.048	0.044	0.202	101
T3	-0.069	0.016	0.217	84

4.3.2 Field measurements

We conducted two field measurement campaigns to characterize soil and vegetation properties of our study systems. We then coupled these data to previously characterized hydrology and elevation data (Chapter 3) to address our hypotheses and predictions. With these data, we were able to calculate for each measurement point a relative elevation above mean water table by subtracting the mean water table elevation from the sampling point elevation.

4.3.2.1 Understory vegetation community

To measure understory vegetation communities, we used a quasi-random walk sampling scheme within three, 300 m^2 circular plots at each site. These plots were previously established during terrestrial laser scanning (TLS) measurements in October 2017, when we acquired high resolution (1 cm) digital elevation models of our sites. We term the study design quasi-random because we constrained the random sampling locations by quadrant, allowing us to sample each quadrant of a circular plot approximately equally (Figure 4.2). We used a random walk study design as opposed to a hummock-hollow stratified sampling design because one of our hypotheses was that elevation above water table—not just microsite category—is an important predictor of understory richness (and overstory biomass and soil chemistry). Hence, a random walk

design allowed us to sample the entire site elevation distribution instead of a potentially bimodal, clustered elevation distribution. To create the plot-level random walk design, we generated a sequence of 12 random integers between 1 and 10 that represented the number of steps to take between sampling points. Sampling point 1 was always the plot center, from which we proceeded to sample at a central point in the northern half of the plot (point 2 in Figure 4.2). We then sampled at points orthogonal to this central point (e.g., points 3 and 4 in Figure 4.2), and repeated this clockwise in cardinal directions (i.e., sample point at a central point along cardinal direction with two sample points orthogonal to the central point). To summarize, we randomly sampled 13 points per plot, with three plots per site, for 39 samples per site, and 390 points across all sites.

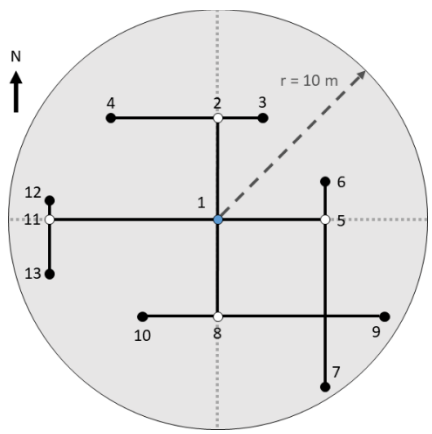

Figure 4.2 Example of plot-level (3 per site) quasi-random walk sampling design with 13 sampling points per plot. Points are the samples (numbers are the sequential sampling order) and black, solid line segments refer to walking path, where path length was determined by a sequence of 12 random generated integers. White points indicate central points along cardinal directions and blue point indicates plot center and first sampling point. Dotted lines demarcate circle quadrants, which this design allowed us to sample approximately equally.

To assess the prediction (H1) that understory plant richness and diversity will be greater on higher elevation features, we measured understory vegetation communities at each sampling point in the random walk design during July 2017, coinciding with peak vegetation presence. Using a 0.25 m^2 square PVC quadrat, we classified vascular and moss individuals to the species level, visually estimated their percent foliar cover, and recorded stem count (if possible) for vascular species. We chose a 0.25 m^2 size quadrat as it corresponded to the smallest hummock areas that we observed in the field, and thus was on the scale of elevation variation at each site. Species that we were unable to

identify in the field we assigned a genus or standard unknown code and collected in a bag for later identification. At each point, we also classified the sampling point as a hummock or a hollow and briefly described the local conditions.

4.3.2.2 Stand structure

To assess the prediction that canopy basal area will be greater on higher elevation features (H2), we used data from two parts of a larger study investigating black ash wetlands. The first data source was species-level stand metrics, including basal area and trees per hectare for both the midstory and canopy level, for each site. For each midstory and canopy species, we calculated site-level basal area, summarized overall basal area across species, and determined the fraction of total basal area occupied by black ash. We also calculated average stems per hectare for each site to a minimum diameter and breast height (DBH) of 2.5 cm.

The second data source was plot-scale point clouds of forest structure from the aforementioned TLS campaign in October 2017 at six of the ten sites (see Chapter 3 or Stovall et al. [in revision]). We estimated overstory DBH (i.e., > 2.5 cm) from the TLS point clouds with the SimpleTree algorithm implemented in CompuTree (Hackenberg et al. 2015). We were only able to apply the algorithm on a fraction of our scanned areas (approximately 300 m^2 at six sites) due to resolution issues and understory noise that precluded DBH analysis. The SimpleTree algorithm models trees as cylinders by automatically segmenting trees using an iterative nearest neighbor approach that moves vertically from an initial seed point along the stem while expanding in area with increasing crown size. The best least squares cylinder at approximately 1.3 m above ground provided estimates of DBH. Following DBH analysis, we matched each processed tree with an elevation value associated with surface models from our TLS analysis (Stovall et al. [in revision]).

4.3.2.3 Soil chemistry

To assess the prediction that soil chemistry heterogeneity will covary with elevation variability, we cored soil at a subsample of the 390 sampling points in the previously described quasi-random walk sampling design. We determined the subsampling points prior to site arrival with the intention to sample all points at a

minimum of one plot (13 points) per site. We sampled one plot at sites D2, D3, D4, and T3, but two plots at the remaining sites for 208 sampling points out of our original 390.

We used a 15 cm beveled and serrated soil knife to extract our soil samples. To obtain a soil sample, we first cleared litter, moss, and/or root mats if they occurred and then placed the wiped-clean knife into the soil to a depth of 10 cm (occasionally sawing through roots with the serrated edge). Then, in a sawing motion with the serrated edge, we rotated the knife counterclockwise to create a circle diameter of 2.5 cm. Once we cut the 2.5 cm diameter, 10 cm tall core, we extracted it with the knife using a lever motion. We then placed the extracted core into a labeled Ziploc bag, making sure not to touch it with bare hands. We did not use a constant-volume soil core because the majority of measurements on hummocks quickly proved this method unfeasible due to tree roots. Our goal was to assess relative concentrations of extractable soil elements and this soil-knife method proved to be rapid, efficient, and effective for obtaining consistent sized samples of the upper 10 cm of soil.

4.3.3 Soil processing and laboratory analyses

We placed all soil samples in paper bags and air-dried them to a constant weight over 2 weeks. We then removed visible roots (typically greater than 2 mm in diameter). We hand-ground, mixed, and sieved soils to pass a 2 mm mesh to create a representative sample of the 10 cm soil profile, and weighed the soils for a final dry weight to the nearest 0.01 g

Total C and N concentration was determined with dry combustion on 0.25 g subsamples with a CN Elemental Analyzer (Elementar Analysensysteme GmbH vario Max; Langenselbold, Germany). For anions and cations, we used a modified water extraction method (Jones and Willett 2006) where we created a slurry at 1:50 soil to deionized water (20°C) that were mixed using a reciprocating shaker for one hour at 200 rpm. We then centrifuged mixtures for 10 minutes at 6000 rpm, after which we decanted supernatant liquids, immediately filtered through a 0.45 µm filter, and froze the filtrate in sterile 50 mL HDPE scintillation bottles (Fisher Scientific, Pittsburgh, PA) until analysis. Nitrate (NO_3^-) and phosphate (PO_4^{3-}) were analyzed colorimetrically with a segmented flow analyzer (SEAL AA3; SEAL Analytical, Mequon, WI) using equipment methods G-200-97 and G-175-96, respectively. Chloride (Cl^-), sulfate (SO_4^{2-}), calcium (Ca^{2+}), and

magnesium (Mg^{2+}) were analyzed with ion chromatography (Standard Methods 4110, Dionex ICS 3000; Thermo Fisher Scientific, Waltham, MA). For each analysis, we included 22 subsample replicates (10% of total samples) to quantify error in the extraction process and the instrument analysis.

4.3.4 Data Analysis

Across our different analyses, we took the following approach: 1) test for site-scale differences in environmental variables focusing on hydrology as a predicting variable, 2) test for microsite-scale (hummock vs. hollow) categorical differences in environmental variables, and 3) test for point-scale influence of elevation relative to water table on environmental variables.

4.3.4.1 Understory vegetation community

To test our prediction that that hydrology is a strong control on black ash wetland vegetation, we first regressed site-level richness with site-level hydrology metrics using simple linear regression. To incorporate variability and uncertainty in our site level analysis, we used the average of the three plot level measurements for richness and diversity.

To assess categorical differences in vegetation composition among both sites and microsites (i.e., hummock vs. hollow), we first classified understory vegetation in ordination space using nonmetric multi-dimensional scaling (NMDS). NMDS is a common ordination method to determine ecologically meaningful community dissimilarities, which uses a rank order relation that allows for non-linear species responses. Prior to analysis, we removed rare species (<1% presence overall) from the understory community matrix to improve the detection of significant differences in sites and microsites (McCune and Grace 2002). Also prior to NMDS ordination, we categorized each sampling point as either hummock or hollow using previous delineation from TLS analysis of site surface models (see Chapter 3, Stovall et al. [in revision]). However, we note here that for lowland sites with less clear hummock features (see Chapter 3), we identified intermediate elevation or “lawn”-type points as hummocks, with no demonstrable effect on results (*cf.* Eppinga et al. 2008). We then aggregated point-scale measurements to site-level hummock and hollow values by averaging species’ percent cover for hummocks and hollows within each site. We used *metaMDS* function

from the *vegan* package (Oksanen et al. 2018) in the R statistical software (R Core Team 2018) on our site level understory vegetation community matrices to conduct the ordination analyses. We then tested for significant understory community differences (per NMDS analysis) among sites and microsites using a multivariate permutational analysis of variance (PerMANOVA) with the *adonis* function from the same package.

We also evaluated species fidelity and association to particular sites and microsites. To do so, we conducted an indicator species analysis using the function *multipatt* from the *indicspecies* R package (De Caceres and Legendre 2009). This function generates an indicator value index (IV) for each species within each category (e.g., site or microsite). The IV ranges from 0–1, and is the product of two conditional probability values: "specificity" and "sensitivity". Specificity is the conditional probability that the sampling point belongs to a particular group (e.g., hummock or hollow), given the fact that a particular species was found there (Cáceres and Legendre 2009). Sensitivity is the conditional probability of finding a particular species in a sampling point, given that the sampling point belongs to a particular group (Cáceres and Legendre 2009). We used the function standard 1,000 Monte Carlo simulations with permutationally randomized data to test the null hypothesis that the observed species IV is not significantly greater than a value produced with randomized data. To remove the influence of rare species on the indicator analysis, we limited the candidate species to those that were present in more than 10% of its identified microsite or site category. Using this reduced sample, we identified species or species combinations that had a specificity of at least 0.80 and a sensitivity of at least 0.20. We based these thresholds on observations of clear delineations in the indicator species output and from guidance in package materials (Cáceres 2013).

To test categorical differences in richness between hummocks and hollows, we calculated Welch's two sample t-tests on richness between hummocks and hollows for each site. We additionally calculated hummock-hollow Bray-Curtis community dissimilarity indices using the *vegdist* function. This dissimilarity index falls between 0 and 1, where 1 indicates complete dissimilarity and 0 indicates identical communities. The t-test allowed us to test our prediction that hummocks were more diverse than hollows within a site, and the dissimilarity index allowed us to further determine how

different the vegetation communities were. To examine differences in moss and vascular plant communities, we conducted this analysis for both 1) moss and vascular plants separately, and 2) moss and vascular plants combined.

Lastly, we analyzed the relationship between point-scale understory richness and point-scale elevation relative to mean water table (data from Chapter 3) using a generalized linear mixed effect model (GLMM). We conducted all GLMM analysis using the *lme4* R package (Bates et al. 2015) using suggested methods for Poisson distributions from Bolker et al. (2009). We compared the following richness-elevation models and chose the best model based on a combination of the Akaike Information Criterion (AIC) and the Bayesian Information Criterion (BIC): 1) random site-level intercept, 2) random site-level intercept and slope, 3) random site level intercept and slope with plots nested in sites, 4) inclusion of "moss" binary covariate (1 for moss, 0 for not moss) with random site-level intercept, 5) inclusion of "moss" binary covariate with random site-level intercept and slope.

4.3.4.2 Stand structure

To compare site-scale differences in biomass, we used previously measured stand-level basal area, including both midstory (2.5≤DBH≤10 cm) and canopy components at each site. We tested our hypothesis that site-scale hydrology influences tree biomass by regressing site-scale basal area with site-scale hydrology metrics including mean, median, and variance of daily water table, and mean annual hydroperiod (see Chapter 3).

To determine categorical differences in canopy and midstory biomass between hummocks and hollows, we used individual tree DBH data (from the TLS scan data) and conducted simple two-sample t-tests on DBH between hummocks and hollows. We then estimated a fraction of trees at each site that occupied hummocks relative to hollows and related this fraction to measured hydrologic attributes. We used results from this DBH-hummock analysis to infer importance of elevation on tree biomass.

Finally, we analyzed within site relationships between point-scale DBH (from the TLS data) and point-scale elevations relative to water table. To do so, we used a linear mixed effect model to regress within-site individual tree DBH with estimated tree base elevation from digital elevation models derived from TLS point clouds, which serves as a

proxy for tree distance from the mean water table. The linear mixed effect model used allowed for uncorrelated random slopes and intercepts across sites.

4.3.4.3 Soil chemistry

To compare soil chemistry across sites and test our hypothesis that there would be less variation in soil chemistry at drier sites compared to wetter sites (H3), we conducted standard ANOVA and post-hoc Tukey's Honestly Significant Difference t-test on soil extraction chemistry. We first examined differences among hydrogeomorphic categories, and then tested differences among individual sites. To assess soil chemistry variation among groups, we conducted a Levene test on hydrogeomorphic group variances for each analyte.

To then test the overall importance of microsite influence on soil extraction chemistry, we examined differences between hummocks and hollows, averaged across sites. Across-site comparison of hummocks and hollows (as opposed to within-site comparison) increased the power of our inference because, due to our random sampling, some sites did not have equal measurements of hummocks and hollows. Prior to averaging across sites, we scaled soil extraction concentrations to site-level average concentration for each solute. This allowed us to compare relative differences between hummocks and hollows across sites, even when absolute concentrations differed among sites. We then used these scaled concentrations to compare hummocks and hollows across sites using Welch's two-sample t-tests. We also calculated the relative difference between hollows and hummocks with a simple ratio of hollow to hummock scaled concentrations. This ratio allowed us to contextualize differences in scaled concentrations between microsites, regardless of among site variability in absolute concentrations.

Finally, to test our hypothesis that relative elevation variability is a strong control on soil chemistry (as opposed to just microsite category), we regressed point-scale soil analyte concentrations with local elevation relative to water table. We used a similar method to our richness-elevation analysis, where we chose a best-fit linear mixed-effect model (using the *lme4* R package, Bates et al. 2015) based on the following possibilities: 1) random site-level intercept, 2) random site-level intercept and slope, and 3) random site level intercept and slope with uncorrelated random effects for slope and intercept.

4.4 Results

4.4.1 Understory vegetation community

Across all sites (30 plots), we observed 95 distinct understory species: nine moss species, 85 vascular species, and one liverwort species. The most common vascular species were sedges of the *Carex* genus, grasses of the *Glyceria* genus, *Impatiens capensis* Meerb., *Aster lateriflorus* (L.) Britton, and *Caltha palustris* (L.). The most common mosses were *Calliergon cordifolium* (Hedw.) Kindb., *Thuidium delicatulum* (Hedw.) Schimp., and *Rhizomnium magnifolium* (Horik.) T. Kop.

We observed a clear influence of site-scale hydrology on site-scale community composition. Median daily water level was a significant linear predictor of both richness ($p = 0.003$) and diversity ($p<0.001$) for understory vegetation (Figure 4.3). Mean water level, to a lesser extent, was also able to explain similar amounts of site-level variance in richness ($R^2=0.25$) or diversity ($R^2=0.29$). Lowland sites and transition sites tended to clump together in this relationship, but depression sites exhibited far more intra- and across-site variability in richness and hydrology.

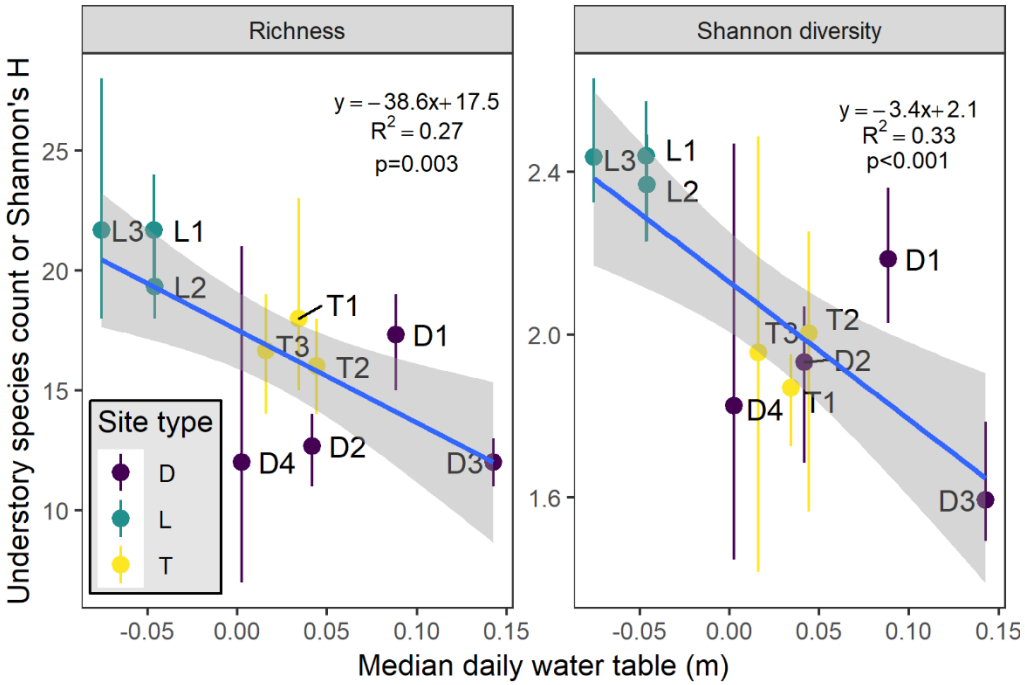

Figure 4.3 Plot level richness or diversity, aggregated by site, as a function of site level median water table relative to the ground surface (negative values indicate belowground). Vertical bars on points indicate bootstrapped 95% confidence intervals calculated from the three plot measurements per site. Linear regression model results presented are also shown.

Our NMDS model demonstrated clear ordinal separation of our understory community matrix between hummocks and hollows within sites (p = 0.001), and also between hummocks and hollows across sites (p=0.002; Figure 4.4). However, we did not observe significant differences in understory community dissimilarities among sites at the site level (p = 0.194). The NMDS procedure converged on a 2-dimensional solution with stress = 0.14, using a Bray-Curtis dissimilarity metric on a centered and rotated dataset, standardized with a Wisconsin double standardization. Hummock and hollow microsites were less clearly separated in NMDS space for lowland sites, particularly L1 and L3, compared to depression and transition sites (Figure 4.4).

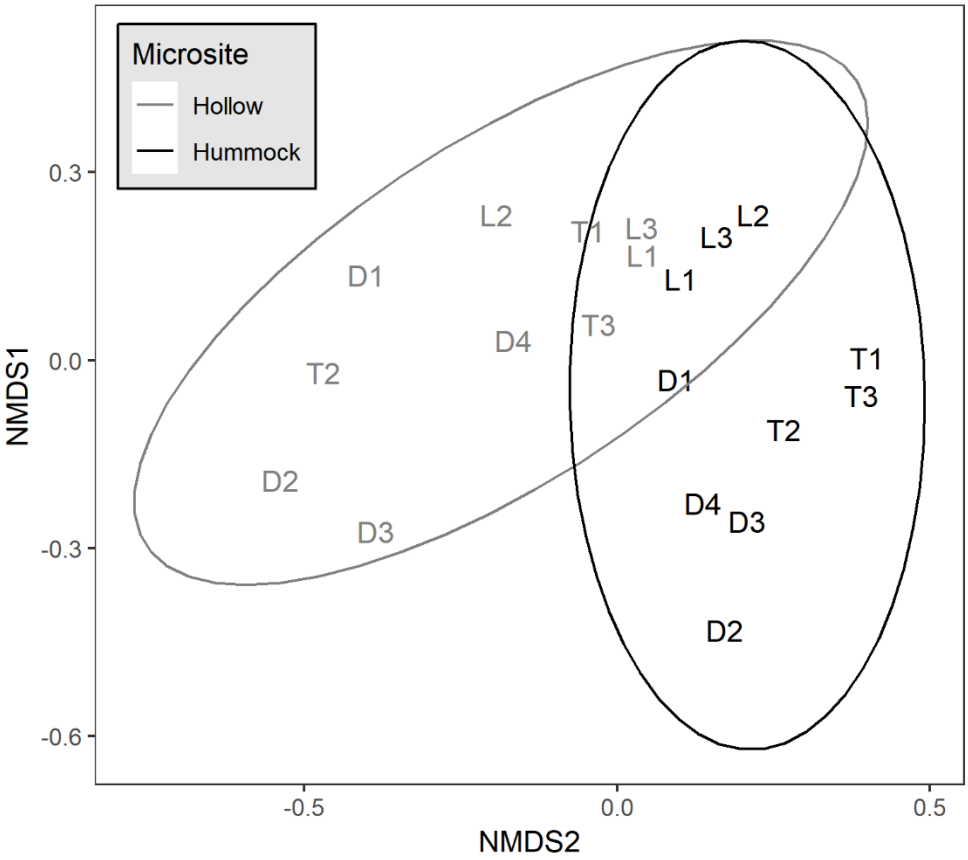

Figure 4.4 NMDS ordination of understory vegetation communities, grouped by sites (text labels) and microsites, with hummocks in black and hollows in grey. Ellipses indicate 95% confidence intervals around the group centroid.

Our indicator species analysis revealed that four moss species (*Climacium dendroides* [Hedw.] F.Weber & D. Mohr, *Funaria hygrometrica* Hedw., *Rhizomnium magnifolium* [Horik.] T.Kop., and *Thuidium delicatulum* [Hedw.] Schimp.) were the most distinguishing species of hummocks across sites (Table 4.2). The best hummock indicator species was *Climacium dendroides* (Hedw.) F.Weber & D. Mohr with it having an 87% chance of indicating that a sampling point is on a hummock, and having a 59% chance that it will be present at a point, given that the point is a hummock. Similarly, for hollows, a moss species (*Calliergon cordifolium* [Hedw.] Kindb.) was the best indicator species, although common duckweed (*Lemna minor* L.) had a nearly perfect (99%) chance of indicating that a sampling point is a hollow. When we removed the criteria for across-site species presence (>10%, see 4.3.4.1), we observed approximately an order of magnitude more candidate indicator species for hummocks than for hollows, with most

species having very high specificity (Table S4.1). We also observed differences in indicator species among sites, with six sites (D1, D2, L2, L3, T1, and T3) showing high specificity for some species, like *Sphagnum sp.* mosses at T1 and T3 (Table S4.2).

Table 4.2 Indicator species analysis for hummocks and hollows across sites. Species indicator values (IV) range from 0–1, and are the product of specificity and sensitivity conditional probabilities. Specificity is the conditional probability that the sampling point belongs to a particular microsite, given the fact that a particular species was found there, and sensitivity is the conditional probability of finding a particular species in a sampling point, given that the sampling point belongs to a particular microsite.

Microsite	Species	Specificity	Sensitivity	IV
Hummock	*Climacium dendroides* (Hedw.) F.Weber & D. Mohr	0.87	0.59	0.51
	Funaria hygrometrica Hedw.+ *Rhizomnium magnifolium* (Horik.) T.Kop.	0.85	0.27	0.23
	Rhizomnium magnifolium (Horik.) T.Kop.+ *Thuidium delicatulum* (Hedw.) Schimp	0.90	0.24	0.21
Hollow	*Calliergon cordifolium* (Hedw.) Kindb.	0.79	0.61	0.48
	Lemna minor L.	0.99	0.27	0.27
	Carex tuckermanii Boott	0.58	0.29	0.17
	Glyceria striata (Lam.) Hitchc.	0.77	0.21	0.16

We also observed distinct differences in richness between hummock and hollow microsites. Hummocks were nearly always locations of both greater moss species richness and greater understory vascular plant species richness (Figure 4.5). This pattern was identical when also combining both moss and vascular plants (Figure S4.1). We found the greatest hummock-hollow differences in understory species richness in depression sites (mean water table = 0.01 m), with less difference in transition sites (mean water table = -0.04 m) and lowland sites (mean water table = -0.32 m). Community dissimilarities for both mosses and understory vascular plants were greatest for depression and transition sites (BC values in Figure 4.5).

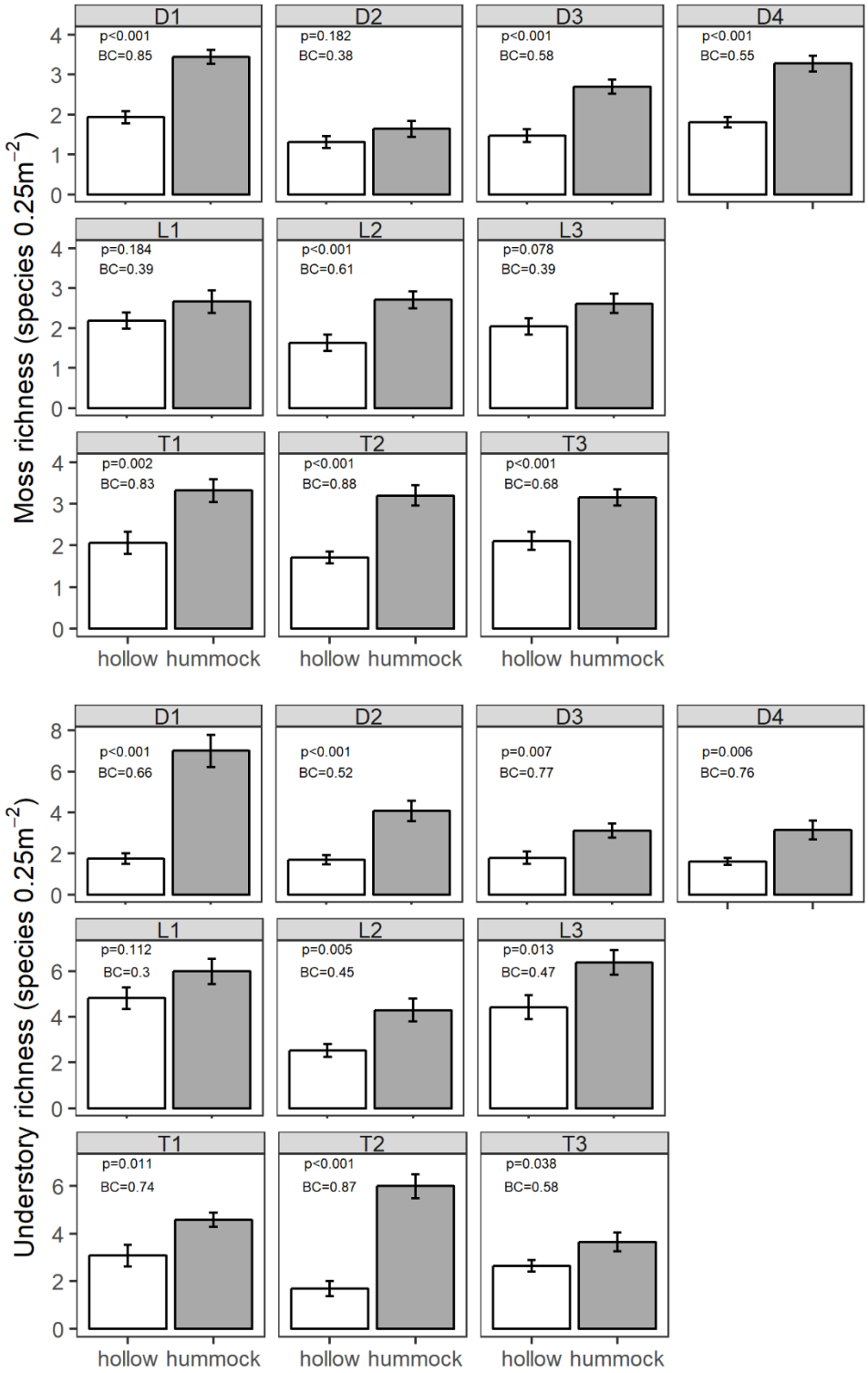

Figure 4.5 Understory species richness on hummocks and hollows for (top) mosses and (bottom) understory vascular plants for each study site. BC text values indicate Bray-Curtis dissimilarity, with a 0–1 range, spanning identical (0) to completely dissimilar (1) vegetation communities. p-values indicate Welch's two sample t-test significances.

At the sampling-point scale, we found that the best-fit GLMM model for richness *versus* elevation relative to mean water table was one with site-level random effects for both intercept and slope, as well as a dummy variable for moss (contrasted with vascular understory vegetation). The model was fit with a maximum likelihood Laplace approximation using a Poisson regression with log-link function and correlated random intercepts and slopes; standardized residuals were normally distributed about zero. Although random site effects modulated the richness-elevation relationship, all site slopes were significantly greater than zero (Table 4.3, and see site-specific fits in Figure S4.2), implying positive association between richness and elevation across sites. Importantly, we found that drier lowland sites had lower overall slopes (i.e., more negative random slope effects) compared to wetter sites (Figure S4.2a), indicating less rapid increases in richness with elevation at dry sites. Overall, we observed that moss richness increased approximately 22% slower than vascular plant richness with increasing elevation. We also observed negative correlation between random effects of intercept and slope (Table 4.3), where site level effects of more rapid increases in richness with elevation were typically offset by lower initial values.

Table 4.3 GLMM model results for species richness versus relative elevation

Effect	Term	Estimate	SE	Z-score	P(Z>|z|)
Fixed	Intercept	1.07	0.09	11.62	<<0.0001
	z	2.04	0.31	6.66	<<0.0001
	moss	-0.45	0.04	-10.17	<<0.0001
Random	SD Intercept	0.26			
	SD z	0.74			
	Cor (z-intercept)	-0.69			

Note: Random effects are presented here as the standard deviation (SD) of all site effects on intercept and slope, with correlation (Cor) between random intercept and slopes. Figure S4.2 has individual site effects.

To visualize more clearly the results from this point-scale analysis, we plotted GLMM-predicted richness values as a function of relative elevation above water table without considering site effects (Figure 4.6). Both moss and vascular plants exhibited only one or two species when at sampling points near or below the mean water table, but species counts increased rapidly beginning near the mean water table, notably for vascular plants.

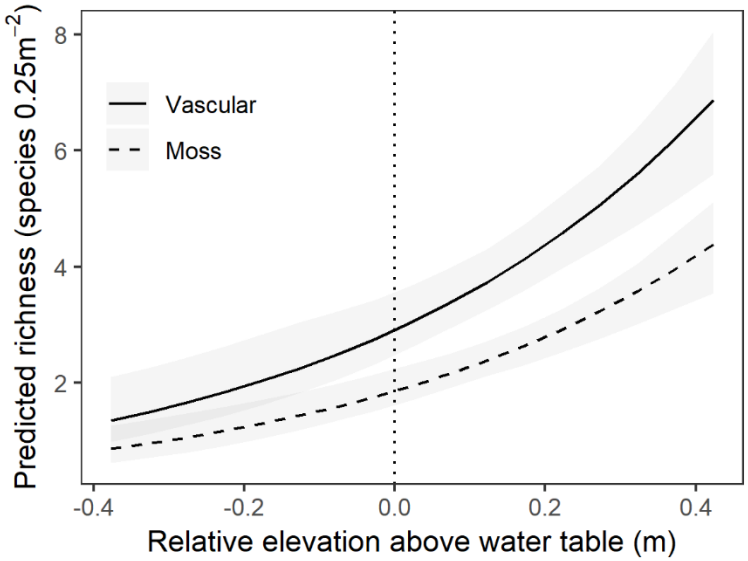

Figure 4.6 Predicted understory species richness as a function of elevation above mean water table, split by moss and vascular species components. Shaded ribbons indicate 95% confidence intervals about the estimate.

4.4.2 Stand structure

We did not observe significant ($p<0.05$) relationships between hydrology and basal area for either the canopy or midstory level, at the site-scale (Figure 4.7). Median water table was the best predictor of basal area out of the hydrology metrics tested (i.e., mean, median, and variance of daily water table, and hydroperiod), but even then, it was not significant. We observed that T1 was a major outlier in the midstory basal area-elevation relationship (Figure 4.7), but its omission did not result in a significant fit ($p = 0.137$).

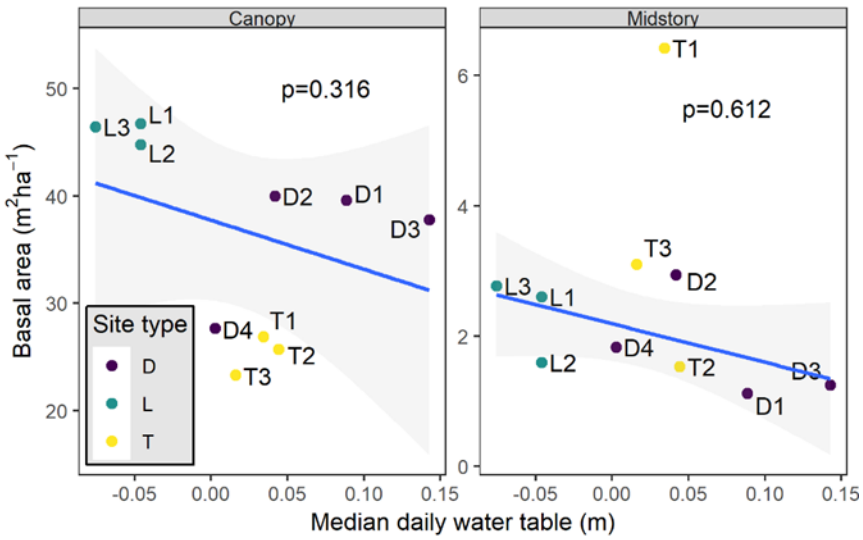

Figure 4.7 Site-scale basal area in the canopy and midstory versus median water table linear regression, with sites labeled and colored by hydrogeomorphic category. p-values indicate p-values for linear regression and shaded region indicates 95% confidence interval about the best-fit line.

Although we did not observe linear relationships between site-scale hydrology and basal area, we noticed a negative trend in canopy basal area that seemed to relate to site hydrogeomorphic category (Figure 4.7, Table S4.3). Hence, we aggregated site types and tested for differences in canopy basal area. ANOVA results indicated significant ($p = 0.001$) differences among sites and post-hoc Tukey's Honestly Significant differences clarified that the drier lowland sites (mean basal area±standard deviation = 46.0±0.9 m^2 ha^{-1}) had approximately 20% more basal area than depression sites ($p = 0.035$) and 45% more basal area than transition sites ($p = 0.001$, Figure 4.8). While depression sites were on average wetter than transition sites by approximately 5 cm, they contained more basal area (36.3±5.0 *versus* 25.3±1.5 m^2 ha^{-1}, $p = 0.020$). Interestingly, while we did not find strong linear association between hydrology and basal area, we did observe a clear site-level negative linear association between confining layer depth (m) and canopy basal area (m^2 ha^{-1}) (R^2=0.83, slope =-29.8, $p<0.001$; data not shown), possibly suggesting an importance of hydrologic storage capacity on growth.

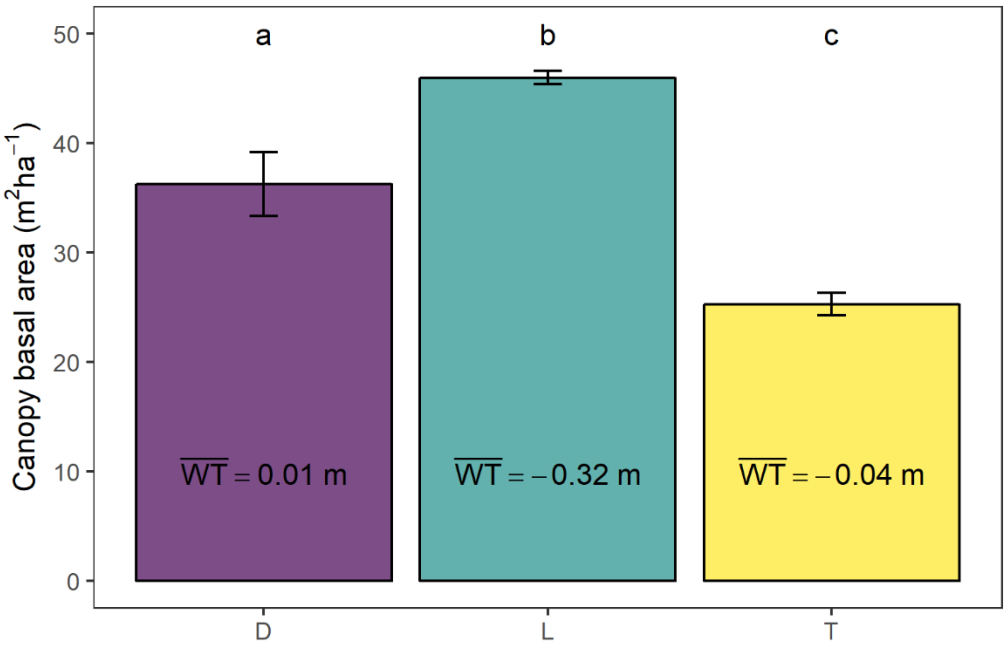

Figure 4.8 Average canopy basal area (±standard error) by site hydrogeomorphic category (depression, lowland, and transition). Letters indicate significant differences at p = 0.05. Text in bars indicates the average daily water table among sites for that hydrogeomorphic category.

Using our TLS-derived DBH data at a subset of sites, we further assessed differences between microsites (hummocks vs. hollows). Trees were significantly ($p<0.05$) larger on hummocks than in hollows at two of six scanned sites, although average DBH on hummocks was always greater than on hollows (Figure 4.9). We found that although trees were not significantly larger on hummocks across sites, they were found nearly exclusively on hummocks at our wettest sites (D and T sites; Figure 4.9). Across all size classes, we found that trees in depression and transition sites occupy hummocks between 83–94% of the time. We also observed size-dependent association with hummocks, especially for sites D1, D3, and T1, where larger trees (i.e., trees with DBH>20 cm) were 2–3x more likely to exist on hummocks compared to hollows (Figure 4.9). This is in contrast to drier lowland sites, where trees do not prefer hummocks to hollows, at least not in our subsampled areas.

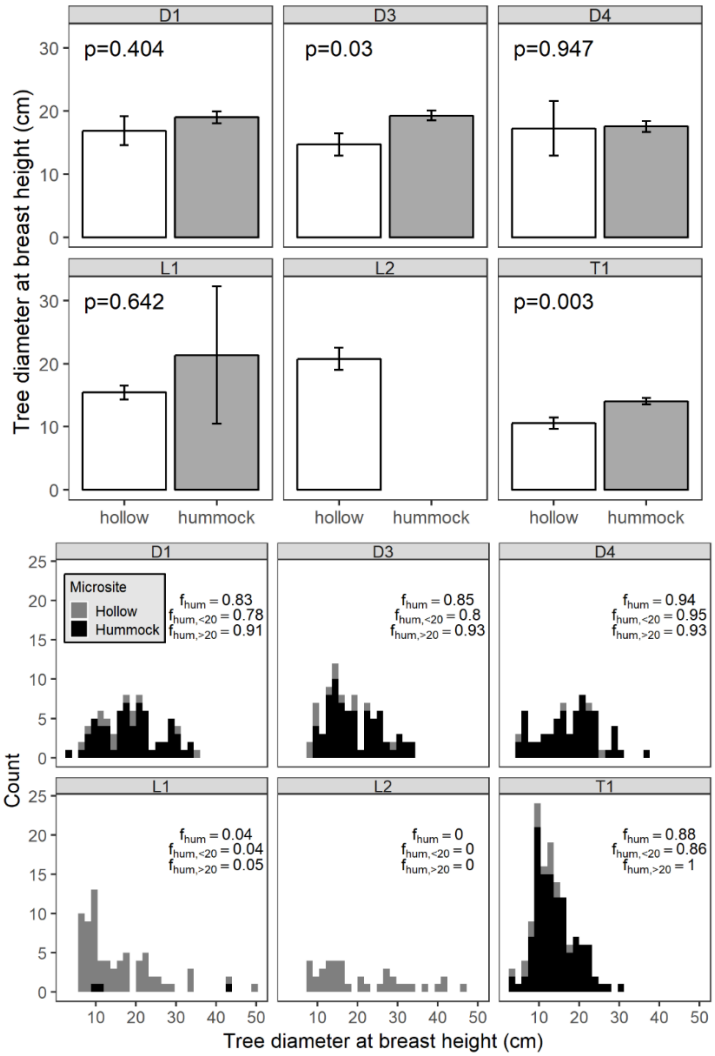

Figure 4.9 (Top) Categorical comparison of average (±standard error) DBH between hummocks and hollows; text indicates p-value for Welch's two sample t-test. We did not observe any trees on hummocks at L2, resulting in possible comparisons. (Bottom) Stacked histograms of DBH size classes across sites. Black bars represent trees on hummocks and grey bars represent the remaining proportion of trees on hollows. Fraction of bars that are black indicate the fraction of trees that are on hummocks in that DBH size bin. Text refers to the fraction of observed trees that occupy hummocks at each sampling area for 1) the total sampling distribution (f_{hum}), 2) the sampling distribution for trees ≤ 20cm DBH ($f_{hum,<20}$), and 3) the sampling distribution for trees >20 cm DBH ($f_{hum,>20}$).

Despite these differences in DBH on hummocks vs. hollows, point-scale linear mixed effect models of DBH *versus* relative elevation did not reveal any significant (p>0.05) trends (and see Figure S4.3). We note here that this is a preliminary analysis, and matching procedures to tie digital elevation models from TLS to tree base height elevations may have high uncertainty.

4.4.3 *Soil chemistry*

There were significant differences in soil chemistry among sites and site hydrogeomorphic groups for all analytes ($p < 0.01$, Figure 4.10). Depression sites had the lowest soil base cation concentrations (Ca^{2+} and Mg^{2+}), followed by lowland, and then transition sites. Depression sites and transition sites had considerably less NO_3^-– N than lowland sites, but somewhat more PO_4^{3-}– P, and clearly higher C:N. However, we observed more variability among sites than among hydrogeomorphic site groupings. We observed some indication that drier lowland sites exhibited less variability in soil chemistry than wetter transition and depression sites, but this trend was not consistent across analytes (Table S4.4). In fact, we observed significantly greater variance in %C, NO_3^-–N, and SO_4^{2-} in drier lowland sites than in wetter sites (Table S4.4).

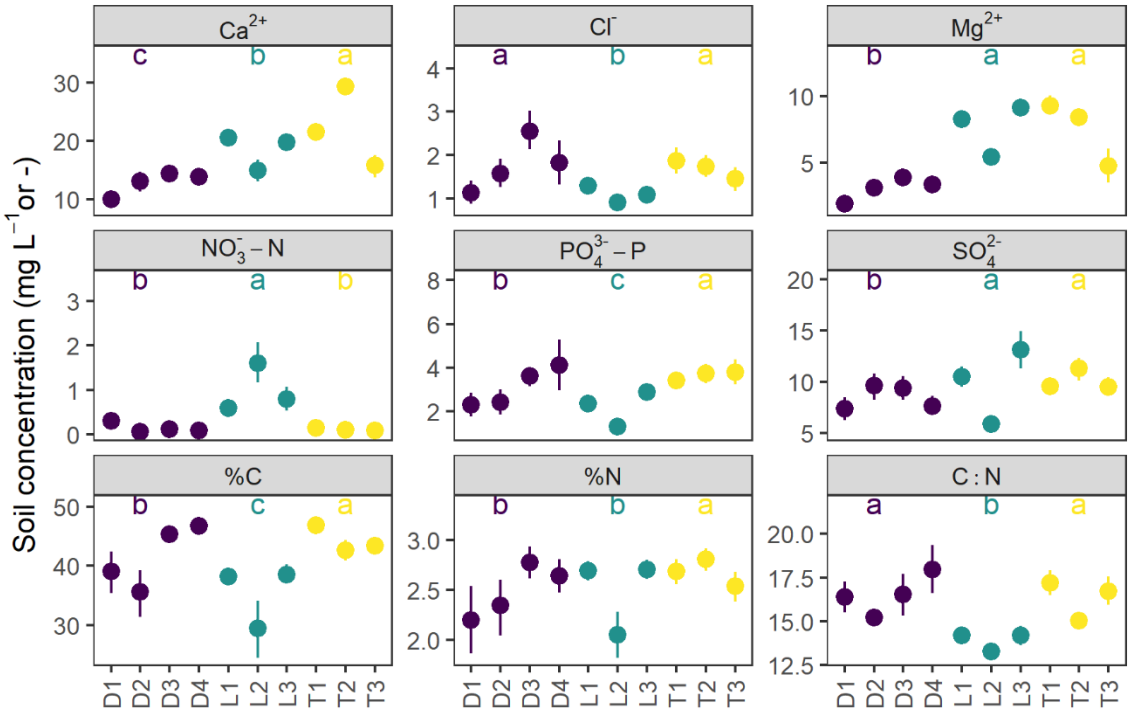

Figure 4.10 Average soil extraction concentrations for every site and solute analyzed. Colors indicate site type, and bars indicate bootstrapped 95% confidence intervals about the mean. If intervals among sites do not overlap, they are significantly different at p = 0.05. Significantly different groups at p=0.05 are labeled with letters. Note: %C, %N, and CN are unitless and are determined from combustion, not soil extraction.

We also found significant ($p<0.05$) differences in soil chemistry between hummocks and hollows for seven out of nine analytes (Figure 4.11). Except for NO_3^-–N, %N, and SO_4^{2-}, hummocks had higher analyte concentrations than hollows. Relative

across-site hummock-hollow differences in mean concentration range from-27% for NO_3^-–N to +23% for Cl^-. Although some sites varied in their relative differences between hummock and hollow analyte concentrations (Table S4.5), broad patterns were still discernible wherein hummocks were generally loci of higher Ca^{2+}, Cl^-, Mg^{2+}, PO_4^{3-}–P, C, and C:N (though only by 4%) relative to hollows.

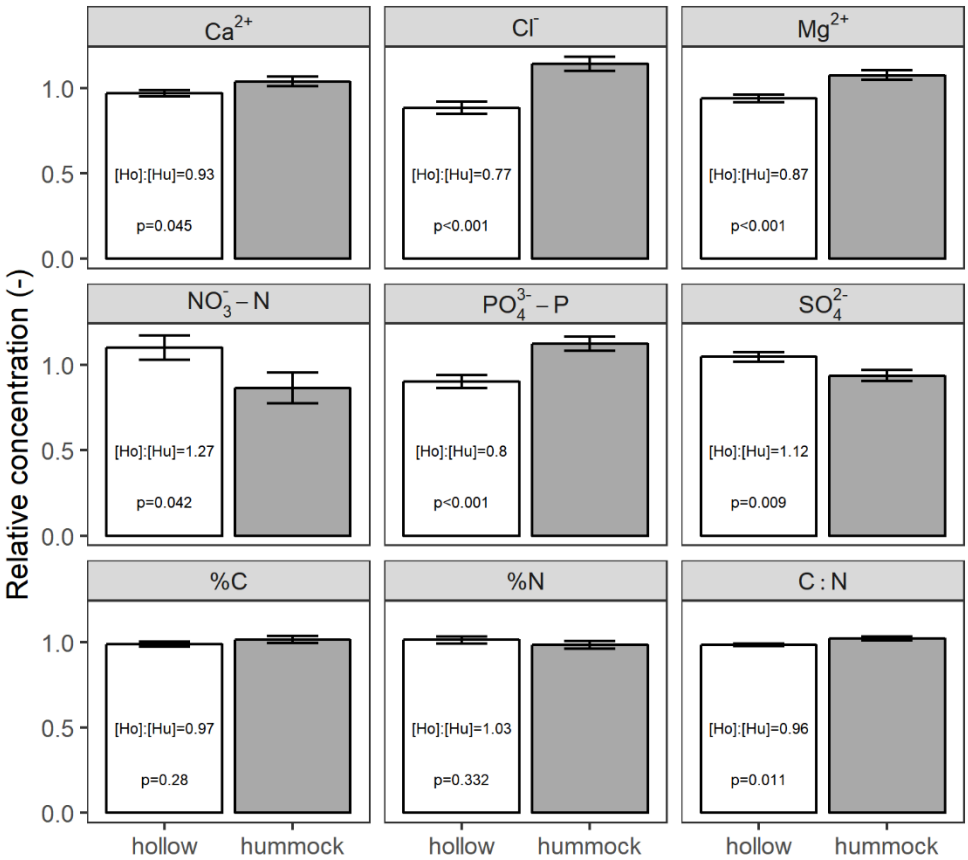

Figure 4.11 Across-site comparison between hummocks and hollows of relative concentrations of soil analytes. Relative concentration for any particular sample is normalized to its site average concentration. Text in each panel refers to the across-site ratio of hollow to hummock relative concentrations and the Welch's two sample t-test of hollow and hummock means.

We found significant ($p<0.05$) linear relationships between concentration and relative elevation above water table at the sample point scale for six out of nine soil chemistry analytes. The linear mixed effect models were fit with a restricted maximum likelihood estimation with uncorrelated random intercepts and slopes; standardized residuals were normally distributed about zero (Table S4.6). Results from this point-scale linear fitting align with categorical results from hummock and hollow analysis (section

4.3.2). To show more clearly results from this analysis, we present the concentration-elevation results using predicted concentrations from the model fit, without taking into account site level random effects (Figure 4.12). Some analytes varied much more among sites in the concentration-elevation relationship than others, leading to large variability in some best-fit lines (e.g., Ca^{2+}, NO^{3-}–N), but most analyte concentrations had clear linear relationships with elevation (Figure 4.12). Random site effects modulated the overall concentration-elevation relationship, implying large variability in responses (direction and magnitude) among sites. We did not observe clear patterns in random effects relating to sites or site hydrogeomorphic groupings (Figure S4.4), indicating no obvious control of hydrology or setting on the strength of these relationships. However, relationships for PO_4^{3-}-P and Cl^- were similar in wetter depression and transition sites in contrast to drier lowland sites, which did not have as steeply positive linear relationships with elevation.

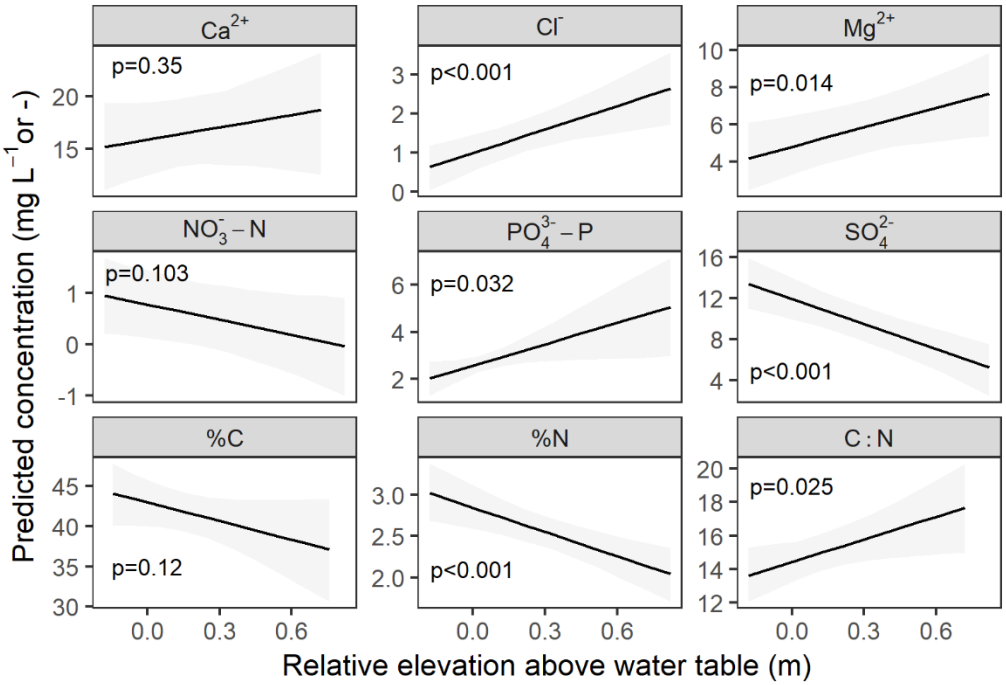

Figure 4.12 Linear mixed effects model-predicted soil extract concentration as a function of elevation above mean water table, split by analyte, without random site effects. Shaded ribbons indicate 95% confidence intervals about the estimate. Text are p-values for linear mixed effects model regressions.

In addition to a clear elevation influence on soil chemistry, we found significant correlation among soil analyte concentrations. Across sites, we observed strong correlations between %C and %N ($r=0.73$, $p<0.001$), Ca^{2+} and Mg^{2+} ($r=0.82$, $p<0.001$),

and PO_4^{3-}–P and Cl^- (r=0.63, p<0.001). We observed several other statistically significant, but weak (r<0.3; ρ<0.3) correlations among analytes, but do not report them here. However, we note that across sites, %C was significantly (p<0.01) positively correlated with all other analytes except for NO_3^-–N (r=-0.3, p <0.001).

4.5 Discussion

In this study, we quantified the influence of vertical relief on vegetation and soils in forested black ash wetlands to assess hypothesized feedbacks that maintain and structure observed hummock and hollow microtopography. Our findings highlight the primacy of elevation and microsite position on controlling vegetation distributions and soil chemistry in black ash wetlands, potentially driven by decreased anaerobic stress on elevated hummocks. Although we did not directly measure evaporation rates, we found support for the hummock evapoconcentration feedback in these systems through concentrated soil chloride and phosphorus on hummocks. Critically, we note that the vegetation and soil chemistry differences between hummocks and hollows were muted in drier sites compared to wetter sites. We posit that this result directly relates to hydrology's influence on the feedbacks that maintain microtopography (see Chapter 3).

4.5.1 Controls on understory composition

To our knowledge, we show for the first time that site-scale hydrologic behavior of black ash wetlands is a major determinant of site-scale understory richness and diversity. We found that even a simple hydrologic metric like mean water table could explain 30% of inter-site understory richness variability (Figure 4.3). For example, our wettest site had half of the species richness as our driest site, and was two-thirds as diverse. Numerous other studies have observed the influence hydrologic regime on site-scale species richness (e.g., van der Valk et al. 1994, Nielsen and Chick 1997, Nielsen et al. 2013), but most have been based on treatment studies of expected hydrologic change or in riparian systems dominated by flood pulses. This study demonstrates that black ash wetlands, which are abundant ecosystems in the Great Lakes region (e.g., they cover approximately 5% of forested land in Minneosta, Michigan, and Wisconsin; USDA Forest Service 2016), may exhibit similar hydrology-richness responses as other studied wetland systems, and further solidifies hydrology as the primary determinant of understory species distributions in wetlands.

Despite clear broad site-scale controls on understory richness, we also observed a dominant microsite-scale influence on richness. Our NMDS analysis suggested that hummocks and hollows clearly separated along community structure, but also that the degree of this separation was highly site dependent. For example, drier lowland sites (especially L1 and L3) had considerably less understory community variation between microsites than the wetter depression or transition sites, further supporting the notion that distinct and stable microsite states arise in response to wet conditions. Interestingly, some hummock communities were more similar to hollow communities at different sites than to hollow communities in their own site (e.g., D1 hummocks and T1, T3, or D4 hollows; Figure 4.4). We surmise that this may result from a combination of local microclimate and edaphic factors, whose analyses were outside the scope of this study.

We further characterized understory communities to assess species fidelity to specific microsites, the results of which lent additional support to the notion that hummocks and hollows are discrete ecosystem states (*cf.* Watts et al. 2010). Using indicator species analysis, we found that mosses were the most discriminative understory lifeform for parsing hummocks from hollows (Table 1.2). This finding garners more evidence for the contention that hummocks provide hydrologic stress relief for vegetation, as moss species are highly sensitive to soil moisture regimes (i.e., they are poikilohydric; Busby et al. 1978, Proctor 1990). Additionally, Bray-Curtis dissimilatory index testing at our wettest sites indicated that understory vegetation communities between hummocks and hollows were highly dissimilar (i.e., BC closer to 1), with little overlap in species. We suggest that the diversity in microsite presence increases overall site richness, because some species show clear affinity for microsite type, a finding supported by similar studies of richness and microsite variability (Vivian-Smith, 1997; Bruland and Richardson, 2005). For example, wetland flora and fauna may occupy distinct hydrologic and biogeochemical niches defined by hummocks or hollows that depend on their specific environmental tolerances and optimal growth conditions (Beatty 1984). Therefore, microtopography greatly expands potential hydrologic and associated habitat niches.

Out of curiosity, we also wanted to determine if measured soil chemistry better explained variability in understory community composition. While our sample size

differences between soil and vegetation precluded full correlation analysis of NMDS ordination and abiotic variables, we did assess soil chemistry influence on understory community structure on a subset of our data. We found that, indeed, relative elevation was a better predictor than soil chemistry of understory community structure in ordination space (Figure S4.5 and Table S4.7). Moreover, two of the three next best predictors (Mg^{2+} and PO_4^{3-}–P) were also highly correlated with elevation.

In addition to different community structure between hummocks and hollows, we found strong evidence for our prediction (H1) that hummocks support a higher number and greater diversity of understory vegetation species than hollows. In our systems, hummocks were loci for approximately 60% of total sampled species per site, with larger richness differences between hummocks and hollows in wetter sites. This finding aligns with field observations of visually distinct breaks between the relatively bare organic surface of hollows and the verdant structure of hummocks. We suggest that greater understory richness on hummocks may imply greater understory GPP vis-à-vis the richness-productivity relationship (Olde Venterink et al. 2003, van Ruijven and Berendse 2005), lending credence to productivity-elevation feedback. Adding further support, our direct modeling demonstrated clear increases in richness with elevation, where the slope of this relationship was greatest in the wettest sites (Figure 4.9). Perhaps these are not surprising results given that distance to water table may be the most important control on wetland community structure (Bubier et al. 2006, Økland et al. 2008, Malhotra et al. 2016). Our results add black ash swamps to a number of wetland ecosystems with similar understory richness structure, including salt marshes (Stribling et al. 2006), alluvial swamps (Bledsoe and Shear 2000), tidal freshwater swamps (Dubertstein and Connor 2009, Courtwright and Findlay 2011), tropical swamps (Koponen et al. 2004), boreal swamps (Økland et al. 2008), and northern sedge meadows (Peach and Zedler 2006). The concordance of similar observations across systems substantiates hypotheses that hummocks play a critical role in supporting wetland plant diversity.

Lastly, we note that while hollows have less species on average than hummocks, they are not devoid of understory productivity. At some sites, we observed large swaths of *Carex spp.* in the hollow understory, whose thick stems and spanning rhizomes would

have contributed to high primary productivity. Follow-up studies could focus on this aspect of hummock-hollow differences in these and other systems.

4.5.2 Controls on canopy productivity

Despite lack of significant direct association between measured hydrology and stand structure, we found indirect evidence that links site-scale hydrology to tree biomass (H2). The driest sites (lowland sites) had the greatest basal area, supporting observations from floodplain wetlands where sites that received less inundation were more productive and had greater basal area than intermediately or regularly inundated sites (Megonigal et al. 1997). Perhaps unexpectedly, even though transition sites were of intermediate wetness between lowland and depression sites, they were the least productive sites. This finding contrasts with similar studies that have focused on the stress-subsidy relationship of inundation and wetland primary productivity in floodplain systems (Odum et al. 1979), where sites of intermediate inundation have the greatest productivity relative to permanently inundated or permanently dry sites (Mitsch et al. 1991, Day and Megonigal 1993). It is possible that our hydrologic record is not long enough to capture wetter conditions in transition sites relative to depression sites thereby assigning a misleading hydrologic gradient to our sites. On the other hand, perhaps transition sites are under additional stresses from close their proximity to spruce bogs, which may increase competition (Looney et al. 2016) and possibly reduce local pH. Although we did not measure soil pH, greater [Ca^{2+}] in transition sites may support this notion, in due in part to displacement from hydronium ions (Sjörs and Gunnarsson 2002) and in part due to increased solubility of calcium precipitates at lower pH. Finally, we acknowledge that basal area may not be an appropriate metric to compare productivity across sites without further knowledge of stand age or basal area change with time.

Our findings also highlight local hydrologic influences and demonstrate that trees at wetter sites almost exclusively occupy raised hummocks and typically with greater basal area than in hollows. In other words, almost the entirety of live basal area corresponded directly to elevated hummock structures in wet black ash systems. A recent study of canopy competition in black ash wetlands acknowledged this importance of microsite variation in explaining lack of predicted competition and subsequent tree size distributions among black ash trees (Looney et al. 2016). In contrast to our findings at the

site level, we did not find support for our prediction that basal area would correlate with tree base elevation within sites. However, this may not be surprising for three primary reasons: 1) black ash trees are extremely slow growing and there can be very little discernible variability in DBH across trees (D'Amato et al. 2018, Looney et al. 2018), 2) hummock heights (and thus tree base elevation), while centered around some site mean, exhibit variation within a site (see Chapter 3), leading to a range of elevations supporting trees with similar DBH, and 3) tree base elevations were extremely difficult to ascertain using our TLS matching method, leading to high uncertainty in elevation measurements. Perhaps in wetter black ash systems, it is merely the fact that trees are alive (and on hummocks) that is important.

4.5.3 Controls on soil chemistry

We observed clear and significant differences in soil chemistry among sites that could broadly be attributed to site-scale hydrology and site hydrogeomorphic category. For example, the drier lowland sites had an order of magnitude greater NO_3^-–N soil concentrations than wetter depression or transition sites (Figure 4.10) despite having nearly equal soil %N (CV = 0.1). We suggest that the water table regimes of our sites correspond directly with expected water-table specific shifts in N-processing. Where water tables are below ground surface by 30 cm or more, net nitrification dominates and where water tables are within 10 cm of the surface, net ammonification dominates (Hefting et al. 2003). Further, observed variability among sites in base cation availability may indicates the primary sources of water to these systems, with depressions likely being primarily rain-fed, and transitions sites likely being primarily groundwater-fed, with lowlands as some combination of the two. Last, and specific to our hypothesis (H3), we found some support that within site variation in analytes (specifically for Cl^-, PO_4^{3-}-P, C:N, %N, and Mg^{2+}) was greater at wetter sites, suggestive of higher within-site allocation due to evapoconcentration-induced transport.

We found some support for our hypothesis that hummocks can act as evapo-concentrators of mobile soil chemical pools. We observed this hummock-hollow soil chemistry separation at all sites, regardless of variability in absolute concentrations among sites. The strongest evidence for this comes from the relatively high level of the conservative tracer, chloride, in hummocks relative to hollows (23% greater on average).

There are few biogeochemical mechanisms, if any, apart from preferential hydraulic flow that would result in such a locally disproportionate concentration of chloride. Chloride is commonly used across scales and systems as a hydrologic tracer to evaluate hydrologic storage and transport processes (Kirchner 2000, Kirchner et al. 2010), and its concentration in terrestrial waters is widely attributed to evaporation effects (e.g., Thorslund et al. 2018). Further, we believe that our chloride values may be a conservative estimate of differences between hummocks and hollows, because our sampling occurred after leaf-off and approximately one week after a series of rainfall events, the combination of which likely flushed solutes from hummocks towards hollows. As a reference, these systems already have on average an order of magnitude higher chloride concentrations than rainfall in the region (<0.1 mg L^{-1}, NADP 2019), indicating that evaporation is major component of their water cycle–a prerequisite for the evapoconcentration hypothesis. In northern bog wetlands, encroachment or presence of woody vascular plants can dramatically increase evapotranspiration losses (Takagi et al. 1999, Frankl and Schmeidl 2000) aligning with results here suggesting presence of black ash trees may be a significant driver of evapotranspiration on hummocks.

The significantly greater amounts of soil phosphorus on hummocks also aligns with the purported evapoconcentration mechanism. However, in addition to evapoconcentration, the mechanisms of increased nutrient availability in hummocks relative to hollows may be also attributed to accumulation of debris and litter (Resler and Stine 2009), and/or higher turnover and cycling rates (Wetzel et al. 2005). Even mycorrhizal activity is greater in hummocks than hollows, which may be important in P acquisition from ferric-bound particles (Cantelmo and Ehrenfeld 1999). Eppinga et al. (2008) were the first to empirically test and provide evidence for hummock evapoconcentration of limiting nutrients, which had previously been suggested as a mechanism inducing greater phosphorus on tree islands in the Everglades, FL (Wetzel et al. 2005, Ross et al. 2006). Although we do not have direct evidence that 1) black ash wetlands are phosphorus limited, or 2) phosphorus is driven into hummocks via evapotranspiration gradients (e.g., as opposed to local resource recycling only), our phosphorus and chloride results comport with modeled hummock-hollow system responses under the evapoconcentration assumption (e.g., Eppinga et al. 2008, Ross et al.

2006). Hence, while we cannot definitively reject other mechanisms of nutrient enhancement on hummocks, this study adds further support for the evapoconcentration hypothesis. Overall, our finding of greater phosphorus on hummocks aligns with numerous studies where hummocks are consistently found to be zones of greater phosphorus concentrations than hollows (Jones et al. 1996, Wetzel et al. 2005, Eppinga et al. 2008).

In contrast to phosphorus, we observed that hummocks were sites of lower nitrate concentrations. These findings are in contrast to most microtopographic studies, where hummocks often have higher nitrate than hollows (e.g., Bruland and Richardson 2005). However, Courtwright and Findlay (2011) also observed hollow nitrate enrichment, which they attributed to biologically mediated effects such as enhanced uptake on hummocks and coupled nitrification-denitrification (Courtwright and Findlay 2011). In this model, high nitrification rates on aerobic hummocks (Noe et al. 2013) may result in diffusive transport of mobile nitrate to hollows, where it is subsequently denitrified under hydrologically induced anaerobic conditions (Wolf et al. 2011). It seems likely that coupled nitrification-denitrification resulting from distinct hummock-hollow microtopography in wetter transition and depression sites limits nitrate buildup in these systems, in contrast to the drier sites with less topographic relief (see Chapter 3). However, the unexpected NO_3^-–N enrichment hollows in this study may simply be due to sampling period, which was after leaf fall that may have transferred NO_3^-–N to hollows. Additionally, lower NO_3^-–N in hummocks at our sites implies relatively greater organic N and NH_4^+–N, as there is very little difference in total soil N between hummocks and hollows (RPD = 4.6%). However, while most of this hummock N is likely organic, we posit that much of inorganic hummock N is likely NH_4^+–N because low C:N ratios in aerobic hummocks (~15:1) indicate a preference for mineralization over immobilization (Reddy et al. 1984) and similar wetlands in the region have a high propensity for N mineralization (Bridgham et al. 1998).

In addition to phosphorus, hummocks were also enriched in base cations compared to hollows. We postulate that this base cation enrichment effect may also be part of the evapoconcentration feedback in black ash wetlands. Black ash trees are known to exhibit considerably higher Ca^{2+} and Mg^{2+} in live tissues than neighboring species at

the same site, or in other nearby ecosystems (Reiners and Reiners 1970), indicating preferential uptake of these nutrients relative to other species. Interestingly, however, despite having nearly identical base-cation exchangeability, Ca^{2+} and Mg^{2+} were not present in similar ratios between hummocks and hollows, where hummocks had lower Ca:Mg than hollows. Karlin and Bliss (1984) also observed reduced Ca:Mg on hummocks relative to hollows in their study of six peatlands in central Alberta, and attributed this consistent loss of cations to filtering by peat as water passed through it. We suggest that relatively lower mobile Ca^{2+} in hummocks is likely due to preferential binding and association with greater phosphorus availability on hummocks relative to hollows.

To our knowledge, this study presents the first measurements of soil SO_4^{2-} in freshwater hummock-hollow systems, but the results are in contrast to what we expected. We surmised that oxidized SO_4^{2-} would be greater in aerobic hummocks than in more anaerobic hollows. However, we observed consistently less soil SO_4^{2-} in hummocks than in hollows, which we tentatively attribute to either diffusive transport from hummocks to hollows to support sulfate reduction or assimilatory sulfate reduction in hummocks. Our results also contrast with observations in saltwater systems, where vegetated zones are areas of increased SO_4^{2-} due to root-zone oxygenation of reduced toxic suflides (Hsieh and Yang 1997, Madureira et al 1997, Ferreira et al. 2007). Clearly, we are missing a piece of the puzzle with respect to sulfur cycling in hummock-hollow systems, because our results are also in stark opposition to expected results from coupled sulfur-hydrology-microtopography modeling exercises for freshwater systems (Frei et al. 2012).

We found some evidence for our hypothesis that relative elevation, as opposed to simply microsite position, was a major control on soil chemical pools in black ash wetlands. Unsurprisingly, all analyte-elevation trends directly corresponded with categorical hummock-hollow trends, both in direction and in strength. We also observed some indication that Cl^- and PO_4^{3-}-P exhibited more similar and more positive relationships with elevation in wetter sites compared to drier sites (Figure S4.4), potentially indicating enhanced evapoconcentration at wetter sites. However we note that the tendency for some sites with hummock-hollow microtopography to exhibit bimodal elevation distributions (see Chapter 3) led to clumping of sampling points at ends of the

elevation distribution, which may not be appropriate for linear modeling. However, we observed that most sampling distributions spanned an approximately 30 cm range. Whereas most other studies examining relative elevation effects on soil chemistry use sample depth to water table as their elevation measurement (e.g., Bubier et al. 2006, Stribling et al. 2006), our study took a combined approach where we measured water table at a point, but measured relative surface elevation in high-resolution at all points. Hence, a major underlying assumption in our approach is that the water table is flat across our study area, and that capillary fringe and/or hydraulic redistribution effects are negligible in comparison to water table fluctuations. We concede that this approach may be inappropriate for other systems with less organic soils or more undulating terrain, but note that it appeared to provide reasonable and practical results in our case.

Our work here provides a strong foundation for viewing microtopography in black ash wetlands as a result of biogeomorphic feedback processes that concentrate biomass and nutrients into hummock structures, but many questions still remain. Future studies could explore differences in evapotranspiration rates between hummocks and hollows for further elucidation of evapoconcentration differences. Inferences along these lines would also be bolstered by leaf tissue measurements on hummocks and hollows to test for limiting nutrients. We also suggest investigating, at the microsite-level, additional species of nitrogen (e.g., ammonium), sulfur (e.g., sulfide), and other important redox compounds (e.g., iron) and biogeochemical processes (e.g., denitrification) that may explain observed trends in soil chemistry. Finally, we note that our methodology for cold-water extractions may result in highly conservative estimates compared to more standard soil extractions.

4.6 Conclusions

This work provides support for ecosystem engineering by vegetation in swamps, where vegetation capitalizes on and amplifies small changes in surface elevation. The result of this engineering is hummock-hollow microtopography, where hummocks and hollows are distinct, self-organized ecosystem states. Here we used the case study of black ash wetlands to illustrate this possibility. Importantly, we found that black ash hummocks are characterized by increased local species richness, biomass, and nutrient availability, all of which are likely due to reduced hydrologic stress. We conclude the following: 1)

hummocks develop as a response to flooding stress in wetlands, 2) trees, and in particular black ash, occupy and reinforce hummock structure, and 3) hummock and hollow microtopography yields predictable patterns of understory richness, biomass, and soil chemistry. Chapter 3 strongly supports (1), and findings in this chapter support (2) and (3). Therefore, we infer that black ash trees fundamentally structure their environment through vertical building of soil and harvesting of nutrients. Finally, we also show that sampling location and strategy in wetlands should be a considered under the context of microtopography (*cf.* Branfireun 2004), as random sampling, or avoiding certain microsites will result in skewed results and interpretation.

Acknowledgments

This project was funded by the Minnesota Environmental and Natural Resources Trust Fund, the USDA Forest Service Northern Research Station, and the Minnesota Forest Resources Council. Additional funding was provided by the Virginia Tech Forest Resources and Environmental Conservation department, the Virginia Tech Institute for Critical Technology and Applied Science, and the Virginia Tech William J. Dann Fellowship. We gratefully acknowledge the fieldwork and data collection assistance provided by Mitch Slater, Alan Toczydlowksi, and Hannah Friesen. We also gratefully acknowledge Breanna Anderson for assistance with soil sample processing, David Mitchem for assistance in sample preparation and analysis, and Kelly Peeler for assistance in soil sample processing.

4.7 References

Bates, D., Maechler, M., Bolker, B., & Walker, S. (2015). Fitting Linear Mixed-Effects Models Using lme4. Journal of Statistical Software, 67(1), 1-48. doi:10.18637/jss.v067.i01.

Beatty, S. W. 1984. Influence of Microtopography and Canopy Species on Spatial Patterns of Forest Understory Plants. Ecology 65:1406-1419.

Belyea, L. R. and R. S. Clymo. 2001. Feedback control of the rate of peat formation. Proceedings of the Royal Society B-Biological Sciences 268:1315-1321.

Bledsoe, B. P., & Shear, T. H. (2000). Vegetation along hydrologic and edaphic gradients in a North Carolina coastal plain creek bottom and implications for restoration. Wetlands, 20(1), 126-147.

Bolker, B. M., Brooks, M. E., Clark, C. J., Geange, S. W., Poulsen, J. R., Stevens, M. H. H., & White, J. S. S. (2009). Generalized linear mixed models: a practical guide for ecology and evolution. Trends in ecology & evolution, 24(3), 127-135.

Branfireun, B. A. (2004). Does microtopography influence subsurface pore-water chemistry? Implications for the study of methylmercury in peatlands. Wetlands, 24(1), 207-211.

Bridgham, S. D., Updegraff, K., & Pastor, J. (1998). Carbon, nitrogen, and phosphorus mineralization in northern wetlands. Ecology, 79(5), 1545-1561.

Bruland, G. L. and C. J. Richardson. 2005. Hydrologic, edaphic, and vegetative responses to microtopographic reestablishment in a restored wetland. Restoration Ecology 13:515-523.

Bubier, J. L., Moore, T. R., & Crosby, G. (2006). Fine-scale vegetation distribution in a cool temperate peatland. Botany, 84(6), 910-923.

Busby, J. R., Bliss, L. C., & Hamilton, C. D. (1978). Microclimate control of growth rates and habitats of the boreal forest mosses, Tomenthypnum nitens and Hylocomium splendens. Ecological Monographs, 48(2), 95-110.

Clarke, K. R., & Ainsworth, M. (1993). A method of linking multivariate community structure to environmental variables. Marine Ecology-Progress Series, 92, 205-205.

Cohen, M. J., Creed, I. F., Alexander, L., Basu, N. B., Calhoun, A. J., Craft, C., ... & Jawitz, J. W. (2016). Do geographically isolated wetlands influence landscape functions?. Proceedings of the National Academy of Sciences, 113(8), 1978-1986.

Courtwright, J., and S.E.G. Findlay. 2011. Effects of microtopography on hydrology, physicochemistry, and vegetation in a tidal swamp of the Hudson River. Wetlands 31:239-249.

Couwenberg, J., & Joosten, H. (2005). Self-organization in raised bog patterning: The origin of microtope zonation and mesotope diversity. Journal of Ecology, 93(6), 1238-1248.

D'Amato, A., Palik, B., Slesak, R., Edge, G., Matula, C., & Bronson, D. (2018). Evaluating Adaptive Management Options for Black Ash Forests in the Face of Emerald Ash Borer Invasion. Forests, 9(6), 348.

Day, F. P., & Megonigal, J. P. (1993). The relationship between variable hydroperiod, production allocation, and belowground organic turnover in forested wetlands. Wetlands, 13(2), 115-121.

Cáceres, M. D., & Legendre, P. (2009). Associations between species and groups of sites: indices and statistical inference. Ecology, 90(12), 3566-3574.

De Cáceres, M. (2013). How to use the indicspecies package (ver. 1.7. 1). R Proj, 29.

Duberstein, J. A., & Conner, W. H. (2009). Use of hummocks and hollows by trees in tidal freshwater forested wetlands along the Savannah River. Forest Ecology and Management, 258(7), 1613-1618.

Duberstein, J. A., Krauss, K. W., Conner, W. H., Bridges, W. C., & Shelburne, V. B. (2013). Do hummocks provide a physiological advantage to even the most flood tolerant of tidal freshwater trees?. Wetlands, 33(3), 399-408.

Eppinga, M. B., Rietkerk, M., Borren, W., Lapshina, E. D., Bleuten, W., & Wassen, M. J. (2008). Regular surface patterning of peatlands: confronting theory with field data. Ecosystems, 11(4), 520-536.

Eppinga, M. B., De Ruiter, P. C., Wassen, M. J., & Rietkerk, M. (2009). Nutrients and hydrology indicate the driving mechanisms of peatland surface patterning. The American Naturalist, 173(6), 803-818.

Ferreira, T. O., Otero, X. L., Vidal-Torrado, P., & Macías, F. (2007). Effects of bioturbation by root and crab activity on iron and sulfur biogeochemistry in mangrove substrate. Geoderma, 142(1-2), 36-46.

Fogel, B. N., Crain, C. M., & Bertness, M. D. (2004). Community level engineering effects of Triglochin maritima (seaside arrowgrass) in a salt marsh in northern New England, USA. Journal of Ecology, 92(4), 589-597.

Frankl, R., & Schmeidl, H. (2000). Vegetation change in a South German raised bog: Ecosystem engineering by plant species, vegetation switch or ecosystem level feedback mechanisms?. Flora, 195(3), 267-276.

Frei, S., Knorr, K. H., Peiffer, S., & Fleckenstein, J. H. (2012). Surface micro-topography causes hot spots of biogeochemical activity in wetland systems: A virtual modeling experiment. Journal of Geophysical Research: Biogeosciences, 117(G4).

Gunnarsson, U., & Rydin, H. (1998). Demography and recruitment of Scots pine on raised bogs in eastern Sweden and relationships to microhabitat differentiation. Wetlands, 18(1), 133-141.

Hackenberg, J., Spiecker, H., Calders, K., Disney, M., & Raumonen, P. (2015). SimpleTree—an efficient open source tool to build tree models from TLS clouds. Forests, 6(11), 4245-4294.

Hefting, M., Clément, J. C., Dowrick, D., Cosandey, A. C., Bernal, S., Cimpian, C., ... & Pinay, G. (2004). Water table elevation controls on soil nitrogen cycling in riparian wetlands along a European climatic gradient. Biogeochemistry, 67(1), 113-134.

Hsieh, Y. P., & Yang, C. H. (1997). Pyrite accumulation and sulfate depletion as affected by root distribution in aJuncus (needle rush) salt marsh. Estuaries, 20(3), 640-645.

Huenneke, L. F. and R. R. Sharitz. 1986. Microsite abundance and distribution of woody seedlings in a South Carolina cypress-tupelo swamp. American Midland Naturalist 115:328-335.

Iremonger, S. F., & Kelly, D. L. (1988). The responses of four Irish wetland tree species to raised soil water levels. New Phytologist, 109(4), 491-497.

Jones, D. L. & Willett, V. B. (2006). Experimental evaluation of methods to quantify dissolved organic nitrogen (DON) and dissolved organic carbon (DOC) in soil. Soil Biology and Biochemistry, 38(5), 991-999.

Karlin, E. F., & Bliss, L. C. (1984). Variation in substrate chemistry along microtopographical and water-chemistry gradients in peatlands. Canadian Journal of Botany, 62(1), 142-153.

Kirchner, J. W., Feng, X., & Neal, C. (2000). Fractal stream chemistry and its implications for contaminant transport in catchments. Nature, 403(6769), 524.

Kirchner, J. W., Tetzlaff, D., & Soulsby, C. (2010). Comparing chloride and water isotopes as hydrological tracers in two Scottish catchments. Hydrological Processes, 24(12), 1631-1645.

Koponen, P., Nygren, P., Sabatier, D., Rousteau, A., & Saur, E. (2004). Tree species diversity and forest structure in relation to microtopography in a tropical freshwater swamp forest in French Guiana. Plant Ecology, 173(1), 17-32.

Larsen, L. G., & Harvey, J. W. (2010). How vegetation and sediment transport feedbacks drive landscape change in the Everglades and wetlands worldwide. The American Naturalist, 176(3), E66-E79.

Looney, C. E., D'Amato, A. W., Fraver, S., Palik, B. J., & Reinikainen, M. R. (2016). Examining the influences of tree-to-tree competition and climate on size-growth relationships in hydric, multi-aged Fraxinus nigra stands. Forest Ecology and Management, 375, 238-248.

Looney, C. E., D'Amato, A. W., Fraver, S., Palik, B. J., & Frelich, L. E. (2018). Interspecific competition limits the realized niche of Fraxinus nigra along a waterlogging gradient. Canadian Journal of Forest Research, 48(11), 1292-1301.

Madureira, M. J., Vale, C., & Gonçalves, M. S. (1997). Effect of plants on sulphur geochemistry in the Tagus salt-marshes sediments. Marine chemistry, 58(1-2), 27-37.

Malhotra, A., Roulet, N. T., Wilson, P., Giroux-Bougard, X., & Harris, L. I. (2016). Ecohydrological feedbacks in peatlands: an empirical test of the relationship among vegetation, microtopography and water table. Ecohydrology, 9(7), 1346-1357.

Malmer, N., Albinsson, C., Svensson, B. M., & Wallén, B. (2003). Interferences between Sphagnum and vascular plants: effects on plant community structure and peat formation. Oikos, 100(3), 469-482.

McCune, B., & Grace, J. B. (2002). Analysis of ecological communities (Vol. 28). Gleneden Beach, OR: MjM software design.

Megonigal, J. P., Conner, W. H., Kroeger, S., & Sharitz, R. R. (1997). Aboveground production in southeastern floodplain forests: a test of the subsidy–stress hypothesis. Ecology, 78(2), 370-384.

Mitsch, W. J., Taylor, J. R., & Benson, K. B. (1991). Estimating primary productivity of forested wetland communities in different hydrologic landscapes. Landscape ecology, 5(2), 75-92.

National Atmospheric Deposition Program (NRSP-3). 2019. NADP Program Office, Wisconsin State Laboratory of Hygiene, 465 Henry Mall, Madison, WI 53706.

Nielsen, D. L., & Chick, A. J. (1997). Flood-mediated changes in aquatic macrophyte community structure. Marine and Freshwater Research, 48(2), 153-157.

Nielsen, D. L., Podnar, K., Watts, R. J., & Wilson, A. L. (2013). Empirical evidence linking increased hydrologic stability with decreased biotic diversity within wetlands. Hydrobiologia, 708(1), 81-96.

Noe, G. B., Krauss, K. W., Lockaby, B. G., Conner, W. H., & Hupp, C. R. 2013. The effect of increasing salinity and forest mortality on soil nitrogen and phosphorus mineralization in tidal freshwater forested wetlands. Biogeochemistry, 114(1-3), 225-244.

Odum, E. P., Finn, J. T., & Franz, E. H. (1979). Perturbation theory and the subsidy-stress gradient. Bioscience, 29(6), 349-352.

Økland, R. H., Rydgren, K., & Ø kland, T. (2008). Species richness in boreal swamp forests of SE Norway: The role of surface microtopography. Journal of Vegetation Science, 19(1), 67-74.

Oksanen, J.F., Blanchet, B., Friendly, M., Kindt, R., Legendre, P., McGlinn, D., Minchin, P.R., O'Hara, R. B., Simpson, G.L., Solymos, P., Stevens, M.H.H., Szoecs E., & Wagner, H. (2018). vegan: Community Ecology Package. R package version 2.5-3. https://CRAN.R-project.org/package=vegan

Olde Venterink, H., Wassen, M. J., Verkroost, A. W. M., & De Ruiter, P. C. (2003). Species richness–productivity patterns differ between N-, P-, and K-limited wetlands. Ecology, 84(8), 2191-2199.

Palik, B. J., Ostry, M. E., Venette, R. C., & Abdela, E. (2012). Tree regeneration in black ash (Fraxinus nigra) stands exhibiting crown dieback in Minnesota. Forest ecology and management, 269, 26-30.

Palmer, M. L., & Mazzotti, F. J. (2004). Structure of Everglades alligator holes. Wetlands, 24(1), 115-122.

Peach, M., & Zedler, J. B. (2006). How tussocks structure sedge meadow vegetation. Wetlands, 26(2), 322-335.

Pouliot, R., Rochefort, L., Karofeld, E., & Mercier, C. (2011). Initiation of Sphagnum moss hummocks in bogs and the presence of vascular plants: Is there a link?. Acta Oecologica, 37(4), 346-354.

Proctor, M. C. F. (1990). The physiological basis of bryophyte production. Botanical Journal of the Linnean Society, 104(1-3), 61-77.

R Core Team (2018). R: A language and environment for statistical computing. R Foundation for Statistical Computing, Vienna, Austria. URL https://www.R-project.org/.

Reddy, K. R., Patrick, W. H., & Broadbent, F. E. (1984). Nitrogen transformations and loss in flooded soils and sediments. Critical Reviews in Environmental Science and Technology, 13(4), 273-309.

Reiners, W. A., & Reiners, N. M. (1970). Energy and nutrient dynamics of forest floors in three Minnesota forests. The Journal of Ecology, 497-519.

Resler, L. M., & Stine, M. B. (2009). Patterns and Processes of Tree Islands in Two Transitional Environments: Alpine Treeline and Bog Forest-Meadow Ecotones. Geography Compass, 3(4), 1305-1330.

Rodríguez-González, P. M., Stella, J. C., Campelo, F., Ferreira, M. T., & Albuquerque, A. (2010). Subsidy or stress? Tree structure and growth in wetland forests along a hydrological gradient in Southern Europe. Forest Ecology and Management, 259(10), 2015-2025.

Ross, M. S., Mitchell-Bruker, S., Sah, J. P., Stothoff, S., Ruiz, P. L., Reed, D. L., Jayachandran, K. & Coultas, C. L. (2006). Interaction of hydrology and nutrient limitation in the Ridge and Slough landscape of the southern Everglades. Hydrobiologia, 569(1), 37-59.

Sjörs, H., & Gunnarsson, U. (2002). Calcium and pH in north and central Swedish mire waters. Journal of Ecology, 90(4), 650-657.

Stribling, J. M., Glahn, O. A., Chen, X. M., & Cornwell, J. C. (2006). Microtopographic variability in plant distribution and biogeochemistry in a brackish-marsh system. Marine Ecology Progress Series, 320, 121-129.

Stribling, J. M., Cornwell, J. C., & Glahn, O. A. (2007). Microtopography in tidal marshes: ecosystem engineering by vegetation?. Estuaries and Coasts, 30(6), 1007-1015.

Takagi, K., Tsuboya, T., Takahashi, H., & Inoue, T. (1999). Effect of the invasion of vascular plants on heat and water balance in the Sarobetsu mire, northern Japan. Wetlands, 19(1), 246-254.

Thorslund, J., Cohen, M.J., Jawitz, J.W., Destouni, G., Creed, I.F., Rains, M.C., Badiou, P., Jarsojo, J. 2018. Solute evidence for hydrological connectivity of geographically isolated wetlands. Land Degradation and Development: doi:10.1002/ldr.3175.

Turetsky, M. R. (2003). The role of bryophytes in carbon and nitrogen cycling. The bryologist, 106(3), 395-410.

USDA Forest Service. (2016). Forests of the Northern Forest Inventory & Analysis Program. Web report. U.S. Department of Agriculture, Forest Service, Northern Research Station, Houghton, MI.

van der Valk, A. G., Squires, L., & Welling, C. H. (1994). Assessing the impacts of an increase in water level on wetland vegetation. Ecological Applications, 4(3), 525-534.

van Ruijven, J., & Berendse, F. (2005). Diversity–productivity relationships: initial effects, long-term patterns, and underlying mechanisms. Proceedings of the National Academy of Sciences, 102(3), 695-700.

Vivian-Smith, G. 1997. Microtopographic Heterogeneity and Floristic Diversity in Experimental Wetland Communities. The Journal of Ecology 85:71-82.

Wallis, E., & Raulings, E. (2011). Relationship between water regime and hummock-building by Melaleuca ericifolia and Phragmites australis in a brackish wetland. Aquatic botany, 95(3), 182-188.

Watts, D. L., Cohen, M. J., Heffernan, J. B., & Osborne, T. Z. (2010). Hydrologic modification and the loss of self-organized patterning in the ridge–slough mosaic of the Everglades. Ecosystems, 13(6), 813-827.

Werner, K. J., & Zedler, J. B. (2002). How sedge meadow soils, microtopography, and vegetation respond to sedimentation. Wetlands, 22(3), 451-466.

Wetzel, P. R., Van Der Valk, A. G., Newman, S., Gawlik, D. E., Troxler Gann, T., Coronado-Molina, C. A., ... & Sklar, F. H. (2005). Maintaining tree islands in the Florida Everglades: nutrient redistribution is the key. Frontiers in Ecology and the Environment, 3(7), 370-376.

Wilson, J. B., & Agnew, A. D. (1992). Positive-feedback switches in plant communities. In Advances in ecological research (Vol. 23, pp. 263-336). Academic Press.

Windham, L. (1999). Microscale spatial distribution of Phragmites australis (common reed) invasion into Spartina patens (salt hay)-dominated communities in brackish tidal marsh. Biological Invasions, 1(2-3), 137-148.

Wolf, K. L., Ahn, C., & Noe, G. B. (2011). Microtopography enhances nitrogen cycling and removal in created mitigation wetlands. Ecological Engineering, 37(9), 1398-1406.

4.8 Supplementary material

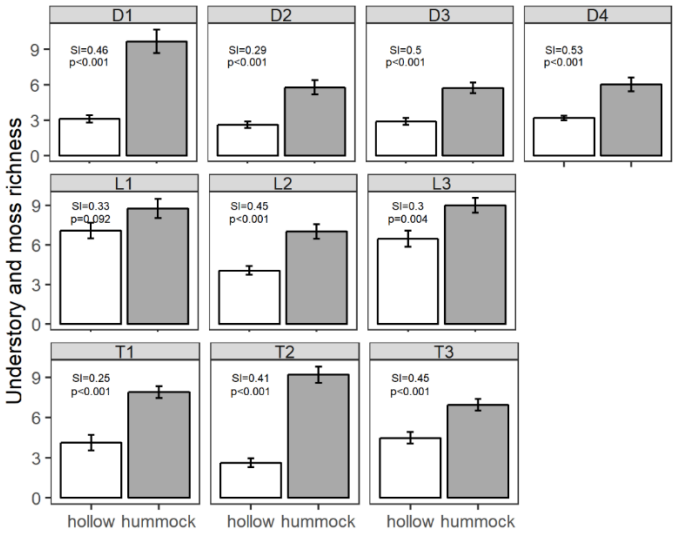

Figure S4.1 Combined vascular and moss richness hummock and hollow comparison. Text values indicate Sorensen dissimilarity indices and Welch's two sample t-test results. Sorensen dissimilarity indices have opposite interpretation of Bray-Curtis dissimilarity indices: the closer to 0, the more dissimilar, and the closer to 1, the more similar.

Table S4.1 Results of indicator species analysis for hummocks and hollows

Microsite	Species	Specificity	Sensitivity	IV	p-val
Hummock	*Climacium dendroides*	0.91	0.59	0.53	0.001
	Rhizomnium magnifolium	0.83	0.60	0.50	0.001
	Rubus pubescens	0.83	0.42	0.35	0.001
	Funaria hygrometrica	0.84	0.40	0.34	0.001
	Carex trisperma	0.86	0.31	0.27	0.001
	Galium triflorum	0.89	0.24	0.22	0.001
	Aster lateriflorus	0.80	0.24	0.20	0.001
	Carex bromoides	0.91	0.16	0.14	0.001
	Acer rubrum	0.93	0.11	0.10	0.001
	Sphagnum angustifolium	0.97	0.11	0.10	0.001
	Maianthemum canadense	1.00	0.09	0.09	0.001
	Calla palustris	0.95	0.09	0.08	0.001
	Dryopteris carthusiana	1.00	0.08	0.08	0.001
	Pleurozium schreberi	0.98	0.08	0.08	0.001
	Carex retorsa	0.94	0.08	0.08	0.003
	Circaea alpina	0.93	0.08	0.07	0.001
	Trientalis borealis	0.89	0.05	0.04	0.005
	Corylus cornuta	0.95	0.04	0.04	0.006
	Rubus idaeus	0.99	0.04	0.04	0.004
Hollow	*Calliergon cordifolium*	0.72	0.61	0.44	0.001
	Lemna minor	0.98	0.27	0.27	0.001

Table S4.2 Results of indicator species analysis for sites

Site	Species	Specificity	Sensitivity	IV	p-val
D1	*Bidens cernua*	0.67	0.23	0.15	0.001
	Carex triflorum	1.00	0.08	0.08	0.007
D2	*Corylus cornuta*	0.94	0.18	0.17	0.001
L2	*Carex intumescens*	0.60	0.18	0.11	0.001
	Rubus idaeus	0.68	0.13	0.09	0.002
L3	*Lycopus uniflorus*	0.74	0.54	0.40	0.001
	Fraxinus nigra	0.67	0.26	0.17	0.001
	Onoclea sensibilis	1.00	0.15	0.15	0.001
T1	*Sphagnum angustifolium*	0.76	0.33	0.26	0.001
	Cornus canadensis	0.75	0.08	0.06	0.028
T3	*Maianthemum canadense*	0.94	0.31	0.29	0.001
	Parthenocissus sp.	1.00	0.10	0.10	0.001
	Sphagnum wulfianum	1.00	0.08	0.08	0.012

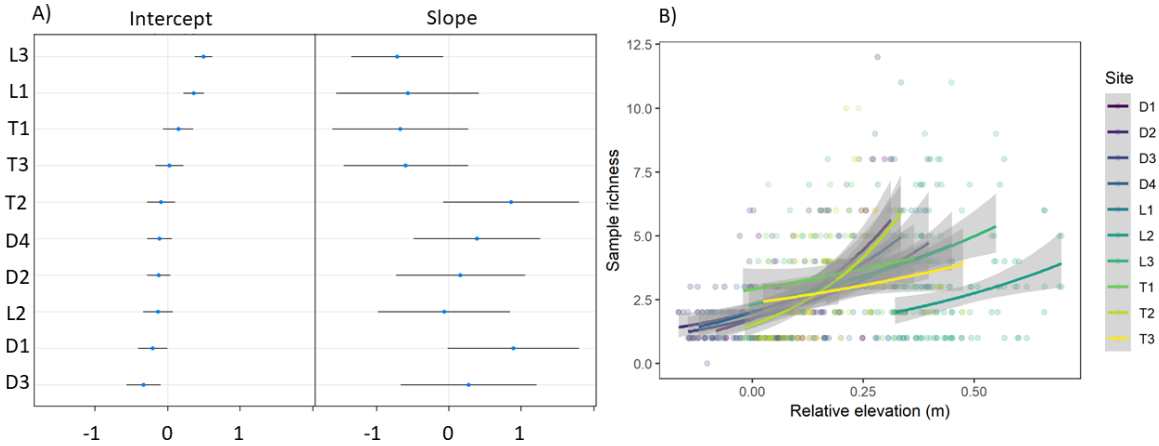

Figure S4.2 a) site-level random effects for intercept and slope for the richness-elevation GLMM , and b) raw data of overall (vascular and moss) richness-elevation relationships for each site with GLMMs fitted.

Table S4.3 Forestry and hydrology metrics for sites

Site	Midstory basal area (m^2 ha^{-1})	Midstory *Fraxinus* fraction	Overstory basal area (m^2 ha^{-1})	Overstory *Fraxinus* fraction	Mean daily water table (m)	Median daily water table (m)	Mean conf. layer depth (cm)	Trees per hectare
L1	2.60	0.70	46.74	0.97	-0.26	-0.05	28.8	729
L2	1.60	0.45	44.79	0.92	-0.35	-0.05	19.6	650
L3	2.77	0.48	46.44	0.98	-0.37	-0.08	24.5	683
D1	1.12	0.4	39.59	0.98	0.01	0.09	28.9	1425
D2	2.94	0.95	39.97	0.97	-0.01	0.04	27.7	1600
D3	1.25	0.25	37.79	0.76	0.05	0.14	69.8	1067
D4	1.83	0.29	27.67	0.76	-0.01	0.00	60.6	700
T1	6.42	0.66	26.87	0.44	0.00	0.03	>150	1038
T2	1.53	0.52	25.69	0.91	-0.05	0.04	80.2	756
T3	3.10	0.48	23.31	0.74	-0.07	0.02	53.6	781

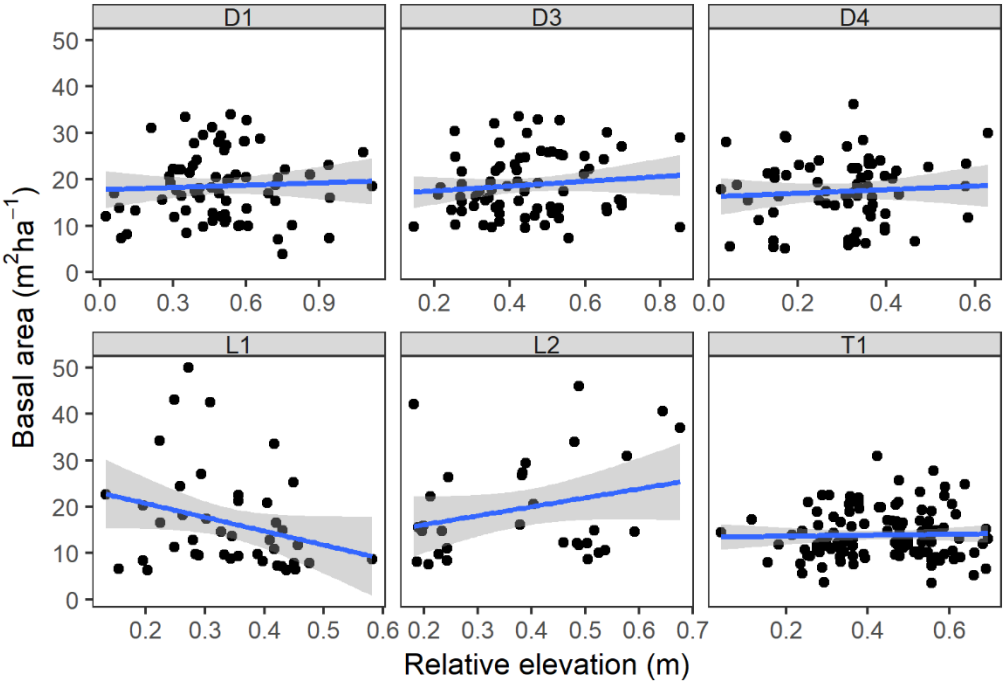

Figure S4.3 Site-scale individual tree base elevation versus individual tree basal area.

Table S4.4 Paired Levene tests for variance in soil chemistry concentrations among hydrogeomorphic categories Bolded values are significant at p=0.05 level. Note that for most analytes, lowland sites (L) have lower variance than D or T sites.

Analyte	Comparison	Estimated differences in variances	Lower 95% confidence interval	Upper 95% confidence interval	Adjusted p-value
Ca^{2+}	L-D	-0.056	-0.931	0.819	0.987
	T-D	-0.182	-1.116	0.751	0.889
	T-L	-0.126	-1.021	0.768	0.941
Cl^{-}	**L-D**	**-0.305**	**-0.473**	**-0.138**	**0.000**
	T-D	-0.032	-0.206	0.141	0.901
	T-L	**0.273**	**0.106**	**0.441**	**0.000**
Mg^{2+}	L-D	0.283	-0.055	0.621	0.120
	T-D	**0.771**	**0.418**	**1.125**	**0.000**
	T-L	**0.488**	**0.147**	**0.829**	**0.002**
NO_3^{-}-N	**L-D**	**0.505**	**0.324**	**0.687**	**0.000**
	T-D	-0.069	-0.262	0.123	0.672
	T-L	**-0.575**	**-0.754**	**-0.396**	**0.000**
PO_4^{3-}-P	**L-D**	**-0.453**	**-0.739**	**-0.167**	**0.001**
	T-D	**-0.309**	**-0.609**	**-0.009**	**0.042**
	T-L	0.144	-0.144	0.432	0.467
SO_4^{2-}	**L-D**	**0.788**	**0.045**	**1.530**	**0.035**
	T-D	0.131	-0.652	0.913	0.918
	T-L	-0.657	-1.409	0.095	0.100
%C	L-D	0.900	-0.981	2.782	0.497
	T-D	**-2.266**	**-4.240**	**-0.292**	**0.020**
	T-L	**-3.166**	**-5.039**	**-1.293**	**0.000**
%N	**L-D**	**-0.163**	**-0.300**	**-0.026**	**0.015**
	T-D	**-0.232**	**-0.374**	**-0.089**	**0.000**
	T-L	-0.069	-0.206	0.068	0.464
C:N	**L-D**	**-0.846**	**-1.266**	**-0.426**	**0.000**
	T-D	**-0.548**	**-0.985**	**-0.112**	**0.009**
	T-L	0.298	-0.127	0.722	0.224

Table S4.5 Average (±standard deviation) soil extraction concentrations for hummocks and hollows across sites. Values are in mg L^{-1} except for %C, %N, and C:N, which are unitless.

Site	Microsite	%C	Ca^{2+}	Cl^-	C:N	Mg^{2+}	%N	NO_3^--N	PO_4^{3-}-P	SO_4^{2-}
D1	hol (18)	39.4±7.7	9.8±3.8	1±0.6	16.7±2.1	1.9±0.9	2.2±0.9	0.3±0.27	2.13±1.38	7.3±3.1
D1	hum (8)	38.2±11.2	10.2±5	1.3±0.7	15.8±2.4	2.2±0.8	2.3±1	0.33±0.59	2.69±1.58	7.4±3.3
D2	hol (7)	33.2±8.2	12.8±2.7	1.3±0.6	15±0.5	3.1±0.7	2.2±0.5	0.06±0.03	1.96±1.05	9.7±3.2
D2	hum (7)	38±8.1	13.2±4	1.8±0.8	15.4±1	3.2±0.8	2.5±0.6	0.06±0.05	2.9±1.03	9.6±2
D3	hol (3)	45±0.5	13.7±0.9	2.7±1.4	14.1±0.9	3.3±0.7	3.2±0.2	0.18±0.08	2.97±0.6	9.5±1.6
D3	hum (10)	45.4±2.1	14.6±2.8	2.5±0.8	17±2	4.1±1.1	2.7±0.2	0.1±0.12	3.82±0.76	9.4±2.4
D4	hol (7)	45.4±2.4	14.7±2	1.1±0.5	16.9±2.6	2.8±0.6	2.7±0.4	0.15±0.11	2.67±1.61	7.9±0.9
D4	hum (6)	48.2±1.2	12.9±3	2.5±0.7	19.2±2.2	4±0.5	2.5±0.3	0.03±0.01	5.83±1.33	7.3±2.2
L1	hol (18)	38±3.8	19.2±2.6	1.3±0.5	14.2±0.6	8±0.9	2.7±0.3	0.63±0.52	2.24±0.83	10.8±2.7
L1	hum (8)	38.7±3.1	23.4±2.6	1.3±0.3	14.1±0.5	8.9±0.7	2.7±0.2	0.53±0.25	2.62±0.83	9.8±2.4
L2	hol (12)	26.1±9.7	14.7±2.7	0.8±0.3	13.3±0.7	5.4±1	2±0.7	1.71±1.06	1.25±0.66	6.3±1.7
L2	hum (13)	32.5±12.8	15.1±6.4	1±0.4	13.3±1.1	5.5±2.1	2.1±0.6	1.51±1.33	1.33±0.82	5.4±2.6
L3	hol (17)	37.8±3.5	19.2±1.4	1.1±0.4	13.9±1	9±0.8	2.7±0.3	0.97±0.72	2.76±0.9	14.5±4.1
L3	hum (9)	39.9±5.6	20.8±2.4	1±0.3	14.8±2.2	9.4±0.9	2.7±0.2	0.5±0.54	3.09±0.82	10.5±5
T1	hol (14)	47.2±0.9	20.6±3	1.3±0.3	16.5±0.9	8.7±1.7	2.9±0.2	0.15±0.06	3.21±0.65	10.3±2.5
T1	hum (12)	46.4±1	22.6±2.5	2.6±0.6	18.2±2.4	10±2	2.5±0.4	0.15±0.13	3.65±0.93	8.6±2.1
T2	hol (15)	44.9±3.3	27.8±3.4	1.4±0.5	14.9±0.9	7.9±1.2	3±0.2	0.11±0.05	3.15±0.78	11.7±2.9
T2	hum (11)	39.4±4.5	31.7±2	2.3±0.6	15.2±0.8	9.2±1.2	2.6±0.3	0.1±0.04	4.63±1.03	10.8±2.9
T3	hol (6)	43.2±1	15.5±4.6	1.4±0.7	16±1.1	3.5±2	2.7±0.1	0.12±0.04	3.54±1.54	10.6±1.9
T3	hum (7)	43.5±1.7	16.1±1.6	1.5±0.3	17.4±1.6	5.9±2.2	2.4±0.3	0.09±0.07	3.99±0.84	9.1±1.1

Table S4.6 Linear mixed effect model results for soil chemistry analytes versus relative elevation above water table with site as a random effect.

Solute	Effect	Term	Estimate	SE	Z-score	P(Z>z)
%C	Fixed	Intercept	42.9	1.51	28.45	<0.001
		z	-7.7	4.93	-1.56	0.120
	Random	SD Intercept	2.9			
		SD z	9.6			
Ca^{2+}	Fixed	Intercept	15.9	1.73	9.19	<0.001
		z	3.9	4.19	0.94	0.350
	Random	SD Intercept	4.8			
		SD z	10.4			
Cl^-	Fixed	Intercept	1	0.23	4.27	<0.001
		z	2	0.6	3.36	0.001
	Random	SD Intercept	0.6			
		SD z	1.3			
C:N	Fixed	Intercept	14.4	0.61	23.72	<0.001
		z	4.5	1.99	2.27	0.025
	Random	SD Intercept	1.5			
		SD z	5.2			
Mg^{2+}	Fixed	Intercept	4.8	0.79	6.12	<0.001
		z	3.5	1.4	2.48	0.014
	Random	SD Intercept	2.3			
		SD z	3.2			
%N	Fixed	Intercept	2.8	0.13	21.71	<0.001
		z	-1.0	0.28	-3.54	0.001
	Random	SD Intercept	0.3			
		SD z	0.0			
NO_3^--N	Fixed	Intercept	0.8	0.34	2.25	<0.001
		z	-1	0.6	-1.64	0.103
	Random	SD Intercept	1			
		SD z	1.4			
PO_4^{3-}-P	Fixed	Intercept	2.6	0.18	14.39	<0.001
		z	3	1.41	2.16	0.032
	Random	SD Intercept	0.2			
		SD z	4			
SO_4^{2-}	Fixed	Intercept	11.9	1.04	11.45	<0.001
		z	-8.1	1.77	-4.57	<0.001
	Random	SD Intercept	2.7			
		SD z	0			

Figure S4.4 Scaled soil extract concentrations versus relative elevation above water table for all sites and analytes. Concentrations were scaled and centered to allow easy comparison across sites and geomorphic categories. Best-fit linear regressions with 95% confidence shading are shown. Site are split by geomorphic category in columns and by analyte in rows.

Environmental fitting to understory NMDS ordination

To fit measured environmental variables to understory community structure, we first subset our community matrix data to sample points where we had coincident soil

chemistry data. We then used the function *envfit* in the *vegan* package to find the optimal subset of environmental variables that explained the community structure; a sensible method for many ecological studies (Clark and Ainsworth 1993). This function compares the dissimilarity structures between biotic and abiotic variables with rank correlation and finds the best correlation between environmental variables and the community matrix; this best fit combination is then further subjected to a permutation test to determine statistical significance of each environmental variable (Okansen et al. 2018). After fitting, we only interpreted and plotted environmental variables that were significant at the $p < 0.01$ level. On NMDS plots fit with environmental variables, plotted arrows refer to the environmental variables that were significant predictors of community structure. The direction of arrows indicates the direction of most rapid change in the environmental variable, and the length of the arrow is proportional to the correlation between community structure and the environmental variable. Using our understory community data subset to sampling points with measured soil chemistry, we observed ordination-space separation of sites and microsites consistent with our aggregated analysis (see section 4.3.1, Figure S4.5). Hummocks and hollows generally separated along the NMDS axis-1 ordination space, and geomorphic site types (i.e., depressions, transitional sites, and lowlands) generally separated along NMDS axis-2 space (Figure S4.5). Overall, the point-scale understory vegetation NMDS procedure required four dimensions to converge. Prior to ordination, the automated NMDS procedure centered, rotated, and used a Wisconsin double standardization on the data. The NMDS achieved a stress of 0.13 using a Bray-Curtis dissimilarity.

Our environmental fitting procedure yielded five environmental variables that correlated significantly ($p<0.01$) with vegetation community structure: relative elevation above water table (z [m]), Ca^{2+}, Mg^{2+}, PO_4^{3-}–P, and %C (Table S4.7). Relative elevation above water table was the strongest covariate with community structure (R^2=0.35) followed by Mg^{2+} (R^2=0.31). Although Ca^{2+} was also a significant environmental predictor of understory vegetation community, we do not plot it in ordination space as it has behavior identical to Mg^{2+}.

Table S4.7 Environmental fitting results for understory vegetation ordination

Environmental variable	NMDS1	NMDS2	R^2	P(R>r)
C	0.46	0.89	0.05	**0.004**
C:N	0.86	0.50	0.04	0.013
Ca^{2+}	0.11	0.99	0.14	**0.001**
Cl^-	0.81	-0.59	0.03	0.036
Mg^{2+}	0.13	0.99	0.31	**0.001**
N	-0.08	1.00	0.02	0.206
NO_3^-–N	-0.87	-0.49	0.01	0.233
PO_4^{3-}–P	0.91	0.42	0.12	**0.001**
SO_4^{2-}	-0.63	0.77	0.02	0.123
z	1.00	0.08	0.35	**0.001**

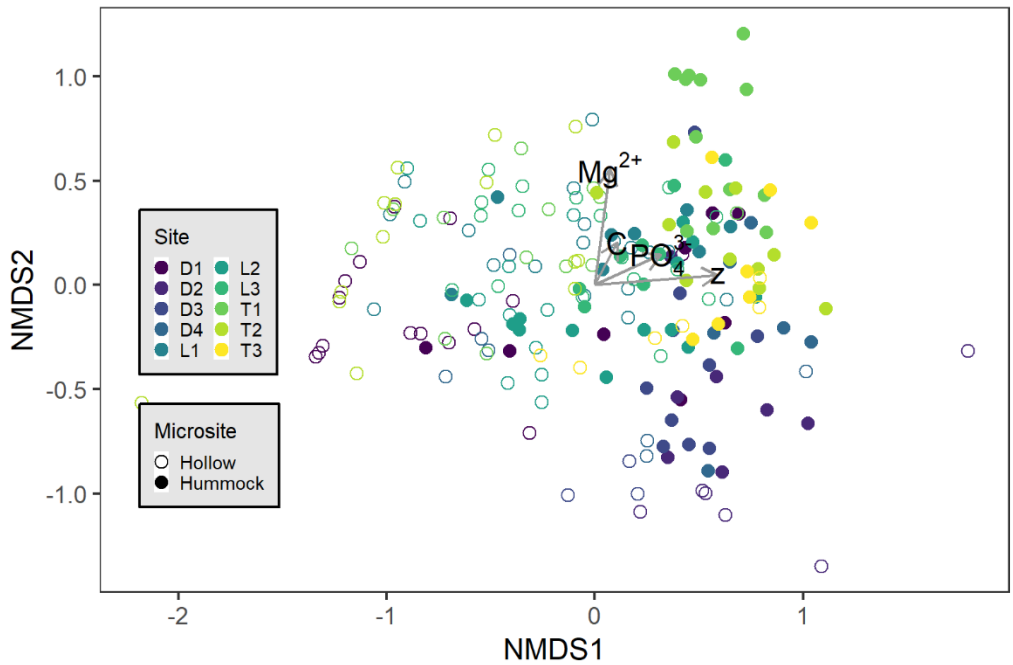

Figure S4.5 Point-scale NMDS ordination of understory vegetation communities with significantly (p<0.01) correlated environmental variables plotted as vectors. Points are colored by their site and are filled by the microsite. Length of environmental variable vectors indicates strength of correlation, and angle indicates the direction of greatest gradient.

CHAPTER 5: CONCLUSION

Although the field of ecohydrology seeks to understand relationships between biota and the water cycle, quantifying these feedbacks remains difficult and elusive. Management of natural resources relies on understanding these feedbacks, so that we are not constantly playing a game of "catch-up" with ecosystem behavior (Zalewski 2000, Krause et al. 2015). It is important to pay more than just lip service to some notion of broad interdisciplinary coupling between ecology and hydrology; process-based understanding of ecohydrology is vital (Hannah et al. 2004). However, the preponderance of ecohydrology research is observational, lacking the rigor of manipulative experimentation and hypothesis testing (King and Caylor 2011). Additionally, most ecohydrology studies rest heavily on the hydrology side of the science, using models to infer processes, leading to decoupling of ecological and hydrological approaches (King and Caylor 2011). This gap in integrated understanding has led to calls for more process-based quantification of ecosystem self-organization (Jennerette et al. 2012), with a particular focus on dynamic transition zones and boundaries between adjacent ecosystems (Krause et al. 2017). Hence, many opportunities remain to connect ecological and hydrological approaches to deepen our insights and further improve management of our natural resources.

In line with these opportunities, this dissertation details some of the many complex ecohydrological dynamics in wetland ecosystems, and explains how these dynamics lead to self-organization of observed patterns in vegetation, hydrology, and microtopographic structure. To do so, I used a combination of experimental hypothesis testing, observational studies, and process-based analysis with methods borrowed from both ecology and hydrology. Across the work presented here, I focused on black ash (*Fraxinus nigra*) wetland systems of northern Minnesota, U.S.A. due to their threatened ecosystem status from the invasive emerald ash borer (EAB; *Agrilus planipennis*). Hence, I sought to explore ecohydrological interactions at the boundaries of our current knowledge in these systems with a high priority for natural resource management.

In Chapter 2, I analyzed results from a large-scale manipulative study to assess the ecohydrologic response of black ash wetlands to three alternative management strategies for EAB. I showed that a do-nothing approach to EAB infestation will likely

lead persistent changes in hydrologic regime defined by shallower water tables and lower ET rates coupled with increased herbaceous vegetation growth, indicating ecosystem state shifts driven by vegetation-water table interactions. However, I showed a strong potential for managed introduction of replacement canopy species to prevent loss of forested conditions. Hence, this work used a process-based, experimental approach to provide informed strategies for forest managers to address the threat of EAB to ecological functions in black ash wetlands. Future work could expand this process understanding through direct partitioning of evaporation and transpiration among plant types to better predict changes to ecosystem water balance and consequent vegetation community shifts after disturbance.

In Chapter 3, I assessed the hypothesis that plants, in response to hydrologically stressful conditions, autogenically maintain microtopography (10^{-1}–10^{0} m variation in surface elevation) in black ash wetlands. Using a novel terrestrial laser scanning (TLS) dataset, I quantified the sizing and spatial distribution of hummocks (local microtopographic high points) in 10 black ash (*Fraxinus nigra*) wetlands in northern Minnesota, U.S.A. I showed that the weight of evidence suggests strong vegetation-water feedbacks in the maintenance of microtopogrpahy. For example, I observed that wetter sites exhibited elevation bimodality and divergence into stable hummock and hollow microsites, whereas drier sites were characterized by more unimodal elevation distributions. I also showed that mean water table depth was a strong control on hummock height, and that hummocks in wetter sites exhibit regular spatial patterning in contrast to hummocks in drier sites, which exhibit random spatial arrangements. Finally, I showed that hummocks may be responsible for increased surface area in black ash wetlands by up to 32%, and may have feedback effects to surface water dynamics through modulation of specific yield by up to 30%. Together, these results implicate hummocks in black ash wetlands as self-organized features. We suggest that vegetation develops and maintains hummocks in response to anaerobic stresses from saturated soils, leading to a microtopographic signature of life. This work, while observational in nature, used direct hypothesis testing to expand both our understanding of plant-water feedbacks in a mechanistic way, and our understanding of how boundaries and dynamic transition zones develop within (not just among) ecosystems. Future efforts could include modeling

exercises based on first principles to determine if wetland microtopography can be recreated from our purported mechanisms.

In Chapter 4, I show the importance of wetland microtopography to biogeochemical state variables at both microsite and site scales. I found a strong influence of microtopography across sites, where hummocks were loci of greater understory species richness, greater canopy biomass, and higher soil concentrations of chloride, phosphorus, and base cations. I also found that microtopography's influence on vegetation and soils was greater at wetter sites than at drier sites, suggesting that distance to mean water table is a primary determinant of wetland biogeochemistry. I suggest that the considerably higher soil concentrations of chloride and phosphorus on hummocks are indicators of evapoconcentration of mobile solutes from hollows towards hummocks, lending support for the evapoconcentration feedback hypothesis of hummock maintanenace. Overall, this chapter provides strong support for the notion that microtopography is a fundamental organizing structure in black ash wetlands. It further demonstrates the important role that wetland microtopography plays in supporting habitat heterogeneity, and how this heterogeneity should be a major component of wetland management, restoration, and mitigation. Future research could focus on the importance of hummock-hollow transitions for organism gestation, movement, and resource use in wetlands. Importantly, future work should investigate how observed microsite differences in state variables aggregate to influence ecosystem functioning (e.g., through aerobic-anaerobic coupling at hummock interfaces), especially greenhouse gas emissions, at larger, landscape scales.

The findings presented in this dissertation demonstrate clear coupling of plants and their environment at both local- and wetland-scales. Through numerous lines of evidence, I show that black ash trees are ecosystem engineers, controlling hydrology through unique evapotranspiration regimes and through building of elevated soil structures, which also support distinct biogeochemical regimes. While not definitive, these results indicate that plants have some agency over their life, and that they are not merely actors on a stage set by greater forces. Moreover, work here suggests that the actions that plants take result in fundamental changes to environmental structure that feeds back to their behavior, providing evidence for plant-landscape co-evolution. Results

here also indicate that microtopography in wetlands precludes the usefulness of "average" conditions that are commonly used in ecosystem modeling applications. Still lacking is a comprehensive process-based understanding of the emergent outcomes for observed plant-water-soil feedbacks, meaning that we cannot include their effects in ecosystem models and management decisions. However, I believe that future process-based work on wetland microtopography will lead to valuable insights into how plants structure their environment, and therefore why landscapes look the way they do.

The earth-sciences research community is heeding the call to achieve a more complete understanding of the underlying feedbacks that structure the world around us. No longer satisfied with directional, deterministic models of ecosystem structure and process, the global research focus is now towards understanding biota-environment co-evolution so that we may more deeply comprehend and predict the consequences of global change. This dissertation represents a small step in this noble direction.

5.1 References

Hannah, D. M., Wood, P. J., & Sadler, J. P. (2004). Ecohydrology and hydroecology: a 'new paradigm'?. Hydrological processes, 18(17), 3439-3445.

Jenerette, G. D., Barron-Gafford, G. A., Guswa, A. J., McDonnell, J. J., & Villegas, J. C. (2012). Organization of complexity in water limited ecohydrology. Ecohydrology, 5(2), 184-199.

King, E. G., & Caylor, K. K. (2011). Ecohydrology in practice: strengths, conveniences, and opportunities. Ecohydrology, 4(4), 608-612.

Krause, S., Lewandowski, J., Dahm, C. N., & Tockner, K. (2015). Frontiers in real-time ecohydrology–a paradigm shift in understanding complex environmental systems. Ecohydrology, 8(4), 529-537.

Krause, S., Lewandowski, J., Grimm, N. B., Hannah, D. M., Pinay, G., McDonald, K., ... & Battin, T. (2017). Ecohydrological interfaces as hot spots of ecosystem processes. Water Resources Research, 53(8), 6359-6376.

Zalewski, M. (2000). Ecohydrology-the scientific background to use ecosystem properties as management tools toward sustainability of water resources. Ecological engineering, 16(1), 1-8.